

**Performance and Emissions of Diesel Engines Fueled by  
Expanded Polystyrene-infused Biodiesel with Additives**

by:  
Sogeesh Mulampath Raman

Supervised by:  
Dr. Murari Mohon Roy, Associate Professor  
Department of Mechanical Engineering

October 2018

A Thesis Submitted in Partial Fulfillment of the Requirement for the Degree of

Master's in Science (MSc.)

in

Mechanical Engineering

Faculty of Engineering

Lakehead University, Thunder Bay, Ontario, Canada P7B 5E1

## **Abstract**

Environmental issues and conventional fossil resource depletion has directed the attention of researchers to seek clean or alternative fuels. Biodiesel was introduced as an answer to day-to-day increases in diesel consumption from heavy machinery to locomotives. The availability from a wide variety of feedstocks (more than 350 crops) and the reduction in emissions such as carbon monoxide (CO), unburnt hydrocarbons (HC) and smoke opacity has made biodiesel attractive among other fuel alternatives. Some of its disadvantages include inferior cold flow properties and slightly higher NO<sub>x</sub> emissions. Expanded polystyrene (EPS) counts for 22% of total plastic waste globally. Proper recycling of EPS at remote locations is practically not feasible. Canola biodiesel is an effective solvent for EPS. This work aims in dissolving EPS at varied concentrations in canola oil biodiesel, and fueled on two modern diesel engines (a light-duty and a heavy-duty) and their performance, emissions are analyzed at different loads and engine speeds. The improvements that resulted after adding the additives (i.e., acetone, tetrahydrofuran, di ethyl ether, xylene and toluene) to EPS-infused biodiesel are also noted on the same engines at various speed and load conditions. The Cummins heavy-duty engine was powered by fuels at two idling conditions (700 rpm and 1700 rpm). The HATZ light-duty engine was powered by fuels at low, medium and high speeds at 1000 rpm, 2100 rpm and 3000 rpm. The fuel properties such as calorific value, density, and viscosity of each fuel are also investigated. The microscopic structure and the particle size distribution of each fuel sample were evaluated to monitor the changes when adding EPS, and any improvements when adding additives were noted.

## **Acknowledgements**

I would like to express my sincere & heartfelt appreciation to my supervisor, Dr. Murari Mohon Roy, for his persistent effort and direction since day one of my Master's Program at Lakehead University. The door to Dr. Roy's office was always open whenever I needed guidance, or whenever I ran into a trouble spot. Much appreciation is extended to Dr. Birbal Singh and Dr. Sudip Rakshit for participating in the committee and editing process. Thanks also given to Debbie Pumala, Technician in the Chemistry Department at Lakehead University, for her support and assistance throughout this project. I also wish to acknowledge Greg Kepka, Technician in the instrumentation lab at Lakehead University, for his assistance.

# Table of Contents

Abstract.....	i
Acknowledgements.....	ii
Table of Contents.....	iii
Caption for Figures.....	vii
Caption for Tables.....	xi
List of Abbreviations.....	xii
Nomenclature.....	xv
1. Introduction.....	1
2. Literature Review.....	3
2.1. Compression Ignition (CI) Engine.....	3
2.2. Regulated Emissions in Diesel Combustion.....	5
2.2.1. Carbon Monoxide (CO) Emissions.....	5
2.2.2. Unburned Hydrocarbon (HC) Emissions.....	6
2.2.3. Particulate Matter (PM) Emissions.....	6
2.2.4. Nitrogen Oxides (NO <sub>x</sub> ) Emissions.....	6
2.3. Biodiesel .....	7
2.4. Biodiesel Feedstock.....	10

2.5 Styrofoam (EPS).....	11
2.6. Biodiesel in Canada.....	12
2.6.1. Provincial Biofuel Policies.....	13
2.7. Biodiesel Produced from Canola Oil.....	13
2.8. Biodiesel Additives.....	14
2.9 Thesis Objective.....	17
3. Materials and Methods.....	18
3.1. Materials.....	18
3.2. Equipment.....	18
3.3. Biodiesel Production from Canola Oil and Mixing of Styrofoam.....	21
3.4. Measurement of Fuel Properties.....	26
3.4.1. Viscosity.....	26
3.4.2. Density.....	28
3.4.3. Heating Value.....	28
3.4.4. Particle Size Distribution.....	30
3.4.5. Microscopic Fuel Structure.....	31
3.4.6. Pitot Tube and Manometer.....	32
3.4.7. Cummins Heavy-Duty Engine.....	33

3.4.8 Hatz 2G40 Light-Duty Engine.....	34
4. Results and Discussions.....	39
4.1 Microscopic fuel structure .....	49
4.2 Particle size distribution.....	49
4.3 Light-duty Engine Performance.....	60
4.3.1 Brake Thermal Efficiency (BTE).....	60
4.3.2 Brake Specific Fuel Consumption (BSFC).....	63
4.4 Light-duty Engine Emissions.....	67
4.4.1 Carbon Monoxide CO Emissions.....	67
4.4.2. NO <sub>x</sub> Emissions.....	69
4.4.3 HC Emissions.....	74
4.4.4 Smoke Opacity.....	77
4.5 Heavy-duty Engine Performance.....	80
4.6 Heavy-duty Engine Emissions.....	81
5. Conclusions.....	85
6. Future Work.....	87
References.....	88
Appendices.....	98

I. Sample Calculations.....	98
II. Photographs of Equipment Used.....	104
III. Tables.....	108

## Caption for Figures

---

Fig. 1: Stepwise transesterification reaction.

Fig. 2: Transesterification by methanol & ethanol.

Fig. 3: EPS

Fig. 4: Styrofoam (EPS) structure

Fig. 5: Transesterification reaction

Fig. 6: Flowchart for biodiesel production

Fig. 7: Viscometer.

Fig. 8: Viscosity measuring setup.

Fig. 9: Precision weighing scale

Fig. 10: Bomb Calorimeter set up.

Fig. 11: Bomb

Fig. 12: Particle size measuring system.

Fig. 13: Polaris Microscope.

Fig. 14: Pitot tube and manometer

Fig. 15: Cummins Heavy duty diesel engine

Fig. 16: Hatz 2G40 light duty engine

Fig. 17: Experimental Setup

Fig.17 (a) Heavy-duty engine (Cummins QSB4.5)

Fig.17 (b): Light-duty engine (Hatz 2G40 2 cylinder)

Fig. 18: Disadvantages of adding EPS to biodiesel.

Fig. 19: Selection criteria for additives.

Fig. 20: Pictures of fuel solution,

Fig.20 (a) B 100 W/EPS 10 g/L @ 25°C

Fig.20 (b) EPS concentrations 13 g/L @ 25°C

Fig.20 (c) Styrofoam concentration of 15g/L @ 90°C

Fig.20 (d) Styrofoam concentration of 10g/L @ 0°C

Fig. 21: Kinematic Viscosity of fuels at various temperature

Fig. 22: Kinematic viscosity of fuels

Fig. 23: Calorific value of different fuels

Fig. 24: Microscopic structure and particle size distribution of B100

Fig.24 (a) microscopic structure

Fig.24 (b) particle size distribution.

Fig. 25: Microscopic structure and particle size distribution of B100 W/ EPS (2g/L)

Fig. 25 (a) microscopic structure

Fig. 25 (b) particle size distribution.

Fig. 26: Microscopic structure and particle size distribution of B100 W/ EPS (6g/L)

Fig. 26 (a) microscopic structure

Fig. 26 (b) particle size distribution.

Fig. 27: Microscopic structure and particle size distribution of B100 W/ EPS (10g/L)

Fig. 27 (a) microscopic structure

Fig. 27 (b) particle size distribution.

Fig. 28: Microscopic structure and particle size distribution of B100 W/EPS (10g/L) + diethyl ether 10%

Fig. 28 (a) microscopic structure

Fig. 28 (b) particle size distribution.

Fig. 29: Microscopic structure and particle size distribution of B100 W/ EPS (10g/L) + Tetrahydrofuran 10%

Fig. 29 (a) microscopic structure

Fig. 29 (b) particle size distribution.

Fig. 30: Microscopic structure and particle size distribution of B100 W/ EPS (10g/L) + Acetone 10%

Fig. 30 (a) microscopic structure

Fig. 30 (b) particle size distribution.

Fig. 31: Microscopic structure and particle size distribution of B100 W/ EPS (10g/L) + Xylene 10%

Fig. 31 (a) microscopic structure

Fig. 31 (b) particle size distribution.

Fig. 32: Microscopic structure and particle size distribution of B100 W/ EPS (10g/L) + Toluene 10%

Fig. 32 (a) microscopic structure

Fig. 32 (b) particle size distribution.

Fig. 33: Brake thermal efficiency (BTE) of fuels at different engine conditions

Fig. 33 (a) BTE @ 1000 rpm

Fig. 33 (b) BTE @ 2100 rpm

Fig. 33 (c) BTE @ 3000 rpm

Fig. 34: Brake specific fuel consumption (BSFC) of fuels at different engine conditions

Fig. 34 (a) BSFC @ 1000 rpm

Fig. 34 (b) BSFC @ 2100 rpm

Fig. 34 (c) BSFC @ 3000 rpm.

Fig. 35: Carbon Monoxide (CO) emissions of fuels at different engine conditions

Fig. 35 (a) CO @ 1000 rpm

Fig. 35 (b) CO @ 2100 rpm

Fig. 35 (c) CO @ 3000 rpm.

Fig. 36: NO emissions of fuels at different engine conditions

Fig. 36 (a) NO @ 1000 rpm

Fig. 36 (b) NO @ 2100 rpm

Fig. 36 (c) NO @ 3000 rpm.

Fig. 37: NO<sub>2</sub> emissions of fuels at different engine conditions

Fig. 37 (a) NO<sub>2</sub> @ 1000 rpm

Fig. 37 (b) NO<sub>2</sub> @ 2100 rpm

Fig. 37 (c) NO<sub>2</sub> @ 3000 rpm.

Fig. 38: Nitrogen oxides (NO<sub>x</sub>) emissions of fuels at different engine conditions

Fig. 38 (a) NO<sub>x</sub> @ 1000 rpm

Fig. 38 (b) NO<sub>x</sub> @ 2100 rpm

Fig. 38 (c) NO<sub>x</sub> @ 3000 rpm.

Fig. 39: Hydrocarbon (HC) emissions of fuels at different engine conditions

Fig. 39 (a) HC @ 1000 rpm

Fig. 39 (b) HC @ 2100 rpm

Fig. 39 (c) HC @ 3000 rpm.

Fig. 40: Smoke opacity emissions of fuels at different engine conditions

Fig. 40 (a) Smoke @1000 rpm

Fig. 40 (b) Smoke @ 2100 rpm

Fig. 40 (c) Smoke @ 3000 rpm.

Fig. 41: Fuel consumption of fuels at (a)700 rpm and (b) 1700 rpm

Fig. 42: Carbon monoxide emissions of fuels at (a)700 rpm and (b) 1700 rpm

Fig. 43: Hydrocarbon emissions of fuels at (a)700 rpm and (b) 1700 rpm

Fig. 44: NO<sub>x</sub> emissions of fuels at (a)700 rpm and (b) 1700 rpm

## Caption for Tables

---

Table 1: Biodiesel feedstock

Table 2: Provincial biofuel policy

Table 3: Properties of fuel additives

Table 4: Specifications of emissions measurement systems

Table 5: Test Results of Canola biodiesel per ASTM 6751

Table 6: HATZ 2G40 engine specifications

Table 7: Cummins QSB4.5 engine specifications

Table 8: Fuel properties of different Biodiesel-Styrofoam blends with various additives

Table 9: Kinematic viscosity of fuels at various temperatures

Table 10: Solubility and Kinematic viscosity of fuel at various temperatures

## List of Abbreviations

---

Ace	Acetone
ASTM	American society for testing and materials
BSFC	Brake specific fuel consumption
BTE	Brake thermal efficiency
B0	Petroleum diesel
B100	Pure canola oil biodiesel.
CC	Cubic centimetres
CI	Compression ignition
CN	Cetane number.
CO	Carbon monoxide
CR	Compression ratio
CO <sub>2</sub>	Carbon dioxide
cSt	Centistoke
DEE	Diethyl ether
EPA	Environmental protection agency (U.S)
EPS	Expanded polystyrene
g/kg	Gram per kilogram

g/kWh	Gram per kilowatt hour
g/L	Gram per litre.
HC, UHC	Unburned hydrocarbons
HL	High load
IC	Internal combustion
kg/m <sup>3</sup>	Kilogram per cubic meter
KW	Kilowatt
LL	Low load
MJ/kg	Mega joule per kilogram
ml	Millilitre
ML	Medium load
NaOH	Sodium hydroxide
NO	Nitrogen oxide
NO <sub>2</sub>	Nitrogen dioxide
NO <sub>x</sub>	Nitrogen oxides
OH	Hydroxide
O <sub>2</sub>	Oxygen
PM	Particulate matter

PS	Polystyrene
RPM	Revolutions per minute
SO <sub>2</sub>	Sulfur dioxide
THF	Tetrahydrofuran
TOL	Toluene
vol.%	Volume percentage
Xyl	Xylene
°C	Degree Celsius

# Nomenclature

---

## Biodiesel, Biodiesel - Expanded polystyrene series

---

Fuel	Biodiesel Content (Vol.%)	EPS Content (g/L)
B100	100	0
B 100 W/ EPS (2g/L)	100	2
B 100 W/ EPS (6g/L)	100	5
B 100 W/ EPS (10g/L)	100	10
B 100 W/ EPS (15g/L)	100	15

## Biodiesel – Expanded polystyrene (EPS) and Additives series

---

Fuels	Composition
B100	Pure canola oil biodiesel
B 100 W/ EPS (2g/L)	Biodiesel + Styrofoam 2g/L
B 100 W/ EPS (6g/L)	Biodiesel + Styrofoam 6g/L
B 100 W/ EPS (10g/L)	Biodiesel + Styrofoam 10g/L
B 100 W/ EPS (10g/L) + Ace 10 %	Biodiesel + Styrofoam 10g/L+ Acetone 10 %
B 100 W/ EPS (10g/L) + DEE 10 %	Biodiesel + Styrofoam 10g/L+ Di-ethyl ether 10 %
B 100 W/ EPS (10g/L) + THF 10 %	Biodiesel + Styrofoam 10g/L + Tetrahydrofuran 10 %
B 100 W/ EPS (10g/L) + Tol 10 %	Biodiesel + Styrofoam 10g/L + Toluene 10 %
B 100 W/ EPS (10g/L) + Xyl 10 %	Biodiesel + Styrofoam 10g/L + Xylene 10 %

\*Volume percentage is used for additives

# 1. Introduction

Population explosion and industrialization has led to an abrupt increase in fossil fuel demand and consumption. Among fossil fuels, petroleum fuels generate a vast variety of chemicals, having a broad range of applications. Apart from its use as fuel to power vehicles, its usage varies from detergent industries to jet propulsion. It can be stated without hesitation that fossil fuels play a vital role in everyone's day-to-day life. However, fossil fuels are confined to limited quantity, and their reserves belong to a small group of countries. Over-exploitation of these reserves powered by increased consumption levels may result in scarcity in future generations. The production and consumption patterns seem to be unsustainable in the long run. Moreover, burning fossil fuels leads to global warming, as well as other environmental and socio-economic concerns.

Among fossil fuels, petroleum fuels (mainly gasoline and diesel) are widely used in a variety of purposes, especially in the transportation and industrial sectors. Urbanization has a strong effect on gasoline and diesel consumption. Gasoline is used mainly in small engines and light transport vehicles, whereas diesel is used for a variety of purposes such as in heavy machinery, power generation, locomotives, and marine engines. Diesel engines have high energy conversion and economic power source over gasoline engines, especially for the same power output. High operational efficiency makes diesel more attractive in these types of machinery [1]. High thermal efficiency, engine durability and reliability, less fuel consumption, and fewer CO<sub>2</sub> emissions are only some among their other tempting qualities. Improvements in performance and emissions have been a key interest for researchers around the globe. Moreover, renewable energy content was introduced to reduce the heavy reliance on fossil fuels. Biofuels, such as alcohols and biodiesel, have been introduced as alternatives for internal combustion engines [2].

Biodiesel is introduced as a renewable energy alternative to petroleum diesel. Biodiesel is eco-friendly, bio-degradable, and non-toxic, and makes exhaust gas free of sulphur or other aromatic compounds [3]. Biodiesel can be used in CI engines with few or no modifications [3]. Pure biodiesel has the capability of reducing HC by as much as 70%, and reducing PM and CO by up to 50% [4]. Biodiesel feedstock can be derived from almost 350 oil-producing crops globally, as well as from animal by-products, waste grease, waste cooking oil, and other sources [5]. Many nations have implemented strict regulations and policies for introducing renewable energy sources such as biodiesel, and other fuel additives in CI engines. Acceptable manufacturing standards for biodiesel content in diesel engines are increasing daily, which makes the field of research more attractive.

Expanded polystyrene (EPS) is a common packaging material used in a variety of purposes such as ceilings, appliances, construction equipment, space insulation, etc. Recycling is not possible in remote locations such as hill stations, waterfronts, or desert camps. EPS can be dissolved in biodiesel and can be used as a fuel additive. This study investigates the effects of adding expanded polystyrene (EPS) in biodiesel at various concentrations, and the improvements achieved when using additives. The additives used in this study include acetone, di ethyl ether, tetrahydrofuran, toluene, and xylene. Engine performance and regulated emissions are also discussed in this study.

The literature review covers topics on diesel combustion and emissions, biodiesel production, combustion and emissions, as well as various information on the additives used. This study also covers methods and materials, details of testing methods, testing equipment, and productions of fuels, followed by results and discussions in detail.

## 2. Literature Review

### 2.1 Compression Ignition (CI) Engine

The internal combustion engine from its invention by Rudolf diesel in the 1890s, was fueled by fossil fuels. In the early decades, it was operated at low speeds. But in the century that followed, it underwent substantial alterations. Initially, compression ignition (CI) engines were used in transportation sectors, primarily in commercial vehicle applications. Currently, CI engines are used in a variety of purposes such as in heavy machinery, power generation, locomotives, and marine engines. High operational efficiency, high thermal efficiency, engine durability and reliability, less fuel consumption, and fewer CO<sub>2</sub> emissions are some of their other tempting qualities [1] Another indirect advantage of diesel engines is that the higher density of diesel fuel results in about 14% more energy per gallon than gasoline [5]. Diesel engines doesn't involve throttle to control airflow into the engine or a spark plug to initiate ignition of fuel as in gasoline engines. Instead the load is controlled by the amount of fuel injected [6]. The heterogenous combustion process of a diesel also allows much leaner air/fuel ratios than pre-mixed gasoline combustion, thereby reducing the average in cylinder temperatures and improve thermal efficiency by reducing heat loss to cooling system and exhaust [7]. They can also operate at higher compression ratios without knocking for increased efficiency [8]. Compression ignition engines have more flexibility for fuels [9]. Diesel is commonly used as fuel for compression ignition (CI) engines because of its high energy conversion and economic power source over gasoline engines, especially for the same power output. Diesel is less expensive in most developing and under-developed countries, which makes it appealing to use in small automobiles. In addition, the absence of an ignition or carburetor system makes CI engines low-maintenance machines. The

benefits of the CI engine have led to its intensive applications on both passenger and heavy-duty diesel vehicles.

Even though diesel has lower emissions, extensive research is taking place to cut down emissions and to enhance performance, mainly due to stringent rules put forward by regulatory bodies. In terms of emissions reduction, widespread techniques include reducing the in-cylinder temperature and after-treatment of exhaust gases. High combustion temperature increases  $\text{NO}_x$ , whereas HC, CO and PM emissions are reduced. In-cylinder temperature is lowered to cut down  $\text{NO}_x$  emissions. Exhaust gas recirculation reduces in-cylinder temperature by reducing the amount of oxygen that is available for combustion by re-circulating a portion of the exhaust gas back into combustion chamber [10,11]. Diesel oxidation catalyst (DOC) to reduce CO and HC emissions, diesel particulate filter (DPF) to remove particulate matter and soot emissions, and selective catalytic reduction (SCR) to reduce  $\text{NO}_x$  emissions are some of the popular after-treatment techniques [12,13]. However, increased fuel and operational costs make after-treatment techniques less attractive [12,13]. Fuel blends with a variety of chemicals (additives) are also used as a common technique to reduce emissions. Diesel exhaust fluid (DEF) used in commercial trucks is an example of additives.

Engine variables such as injection pressure, injection timing, and compression ratio (CR) have a considerable impact on emissions. Increasing these parameters usually results in a reduction of CO, HC and PM emissions [14,15]. Advanced injection time results in higher ignition delay. Moreover, fuel properties like cetane number (CN), latent heat of vaporization, oxygen content, kinematic viscosity, and density also have a significant influence. Cetane number represents the auto ignition and combustion quality of the fuel. It is the key that affects cold start ability, combustion stability and noise [15]. CN can be defined as the inverse of ignition delay, which

means the higher the cetane number, the lower the ignition delay. A higher CN generally decreases the engine cranking time [16], whereas a very high CN leads to overheating of the injectors, which could possibly lead to engine damage [15]. Increasing the injection pressure results in greater surface volume ratio, thereby leading to shorter ignition delay [16]. Fuel-rich mixtures tend to increase operating temperature and hence, ignition delay decreases [17]. Increasing fuel temperature also decreases ignition delay [17]. High CN also tends to improve combustion efficiency, thereby reducing NO<sub>x</sub> emissions [17].

## **2.2 Regulated Emissions in Diesel Combustion**

The main regulated pollutants specified by the United States Environmental Protection Agency, as well as other regulatory agencies, include CO, HC, NO, NO<sub>2</sub>, and PM [18-20]. These regulations were implemented in USA and Canada, and must be abided by all North American car manufacturers.

### **2.2.1 Carbon monoxide (CO) emissions**

Carbon monoxide is formed by incomplete combustion of fuels. This can be summarized in the following equation [17] where R stands for hydrocarbon radical:



Theoretically, CO will be higher in fuel-rich mixtures. CO is commonly formed due to oxygen-deficient combustion, in which not all carbon can be converted to carbon dioxide, which leads to the formation of CO [17]. Carbon monoxide is dangerous to cell tissues because it forms carboxy haemoglobin, which is approximately 100 times more stable than oxy-haemoglobin.

### 2.2.2 Unburnt hydrocarbon (HC) emissions

Another product of incomplete combustion is unburnt hydrocarbon. Higher oxygen content favours complete combustion, and high CN favours less ignition delay, which in turn tends to reduce unburnt hydrocarbons [17, 21].

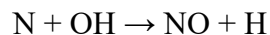
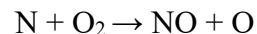
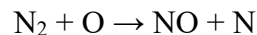
### 2.2.3 Particulate matter (PM) emissions

Particulate matter (PM) emissions involve a complex mixture of solid and liquid particles suspended in a gas. Total particulate matter, or diesel particulate matter, are also synonyms of particulate matter in CI engines [22]. Particulate matter, which is formed by incomplete combustion of hydrocarbon, causes inflammation, innate and acquired immunity, and oxidative stress [22,23].

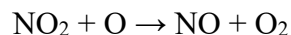
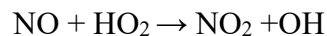
### 2.2.4 Nitrogen oxides (NO<sub>x</sub>) emissions

NO<sub>x</sub> is formed in the combustion chamber due to high combustion temperature, which tends to the oxidation reaction of nitrogen present in the atmospheric air. The series of chemical reactions are listed below [21]:

Kinematics of NO formation (Zeldowich Mechanism)



Kinematics of NO<sub>2</sub> formation



High CN [17,21], and adding volatile additives (which posses high latent heat of vaporization), exhaust gas recirculation (EGR), and fuel emulsions are some of the major techniques used to

reduce NO<sub>x</sub> [24,25]. Among them, exhaust gas recirculation has been proven to be the most efficient and widely-used method [26].

### **2.3 Biodiesel**

Biodiesel is the mono alkyl esters of long-chain fatty acids derived from renewable feedstocks, such as vegetable oil or animal fats, for use in compression ignition engines. Biodiesel is commonly composed of fatty acid (m)ethyl esters that can be prepared from triglycerides in vegetable oils by transesterification with (m)ethanol. The resulting biodiesel is quite similar to conventional diesel fuel in its main characteristics. The flash point of biodiesel is higher, which makes it safer to store and transport. Vegetable oils are not used directly as a fuel due to their high viscosity and poor fuel characteristics, which makes them unsuitable for combustion. Although the density and viscosity difference are within the safe limits, the low cloud point makes them undesirable in cold conditions. The desirability of biodiesel is that it can be used in diesel engines with few modifications [27]. Additionally, it is comparatively less complicated to manufacture, store and transport. Availability of the feedstock is one of the main attractions of biodiesel. Biodiesel feedstock can be derived from nearly 350 oil-producing crops globally, as well as from animal by-products, waste grease, waste cooking oil, and other sources [7]. Even though biodiesel has a low heating value, it possesses a high CN and oxygen content when compared to petroleum diesel. The higher CN of biodiesel is due to its long-chain hydrocarbon groups, which results in higher combustion efficiency and better ignition [28]. Knothe G. [29] stated that biodiesel's viscosity is heavily dependent on molecular structure, chain length, position, and the number and nature of double bonds. In terms of emissions, biodiesel is more appealing due to its low HC, CO, CO<sub>2</sub> and PM emissions [3,30]. The US Environmental Protection Agency (EPA) studies show that biodiesel reduces HC by 32%, and reduces PM and CO emissions by 50% [31]. Biodiesel is well-

known for its low sulphur content, aromatic content, flash point, and lubrication-improving properties [30,10], although it has slightly higher NO<sub>x</sub> emissions due to its high oxygen content and elevated combustion temperatures [4,32,33]. Biodiesel usually possesses heavier molecules, which leads to high viscosity and the slowing down of the combustion process [33]. Biodiesel is sulfur-free, therefore the chances of forming harmful sulphur emissions are eliminated [34,35]. The high lubricity of biodiesel makes it attractive to blend with petroleum diesel in order to enhance diesel's lubricity [36].

Fig. 1 and 2 indicates the stepwise chemical reaction of biodiesel production. Fig. 1 indicates the general explanation of the series of chemical reactions leading to production of biodiesel. Fig.2 indicates the detailed chemical reaction of triglyceride with methanol or ethanol to yield biodiesel. The catalyst generally used is KOH or NaoH. But in this study, we are using NaoH.

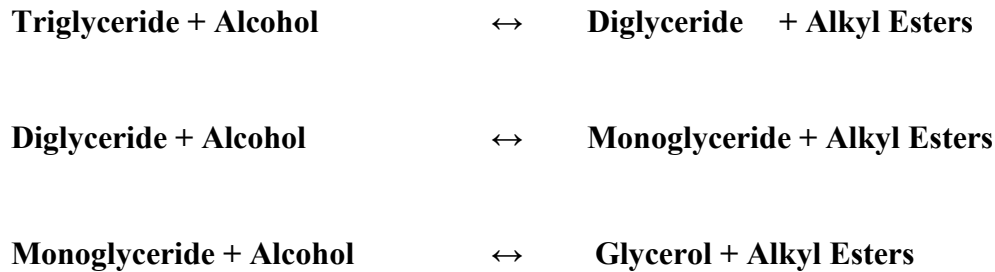


Fig. 1: Stepwise transesterification reaction [37]

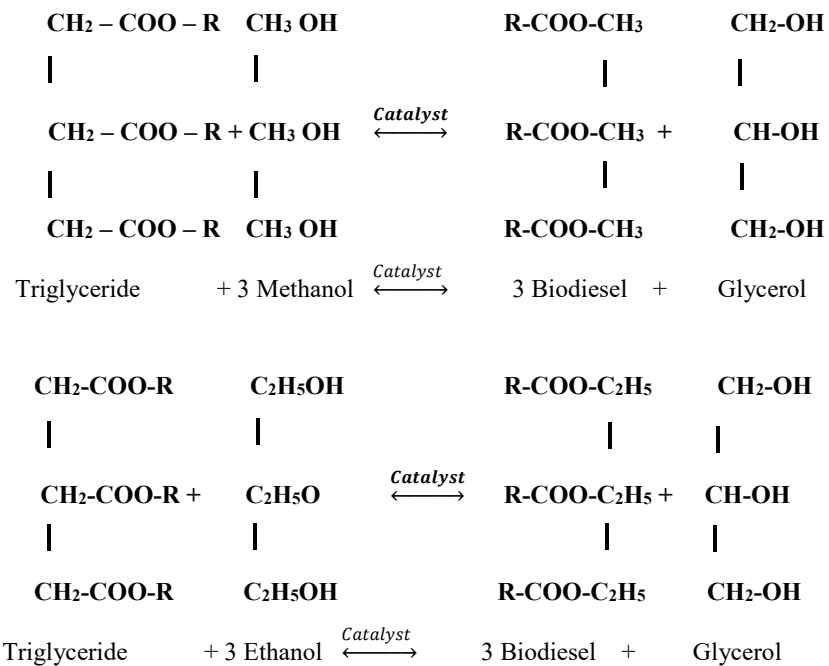


Fig. 2: Transesterification by methanol & ethanol [38]

## 2.4 Biodiesel Feedstock [2,8,14,15,19,22,23,39-47,18,30-38,43-55]

There are more than 350 feedstocks available for biodiesel production, some of which are as follows: [Table 1].

Table 1: Biodiesel feedstock

<b>Edible</b>	<b>Non-edible</b>	<b>Other sources</b>
Babassu	Abutilon muticum	Algae
Barley	Aleurites moluccana	Bacteria
Canola	Almond	Chicken fat
Coconut	Andiroba	Fish oil
Copra	Brassica carinata	Fungi
Corn	Camelina	Latexes
Groundnut	Castor	Microalgae
Laurel	Coffee ground	Miscanthus
Linseed	Cotton seed	Poplar
Oat	Croton megalocarpus	Pork lard
Olive	Cumuru	Poultry fat
Palm	Cynara cardunculus	Switchgrass
Peanut	Jatropha curcas	Tarpenes
Piqui	Jatropha nana	Used cooking oil
Rapeseed	Jojoba	
Rice bran oil	Karanja	
Safflower	Mahua	
Sesame	Moringa	
Sorghum	Nagachampa	
Soybeans	Neem	
Sunflower	Pachira glabra	
Wheat	Passion seed	
	Pongamia	
	Rubber seed tree	
	Salmon oil	
	Tall	
	Terminalia belerica	
	Tobacco seed	
	Tung	

## 2.5 Styrofoam (EPS)

Fig. 3 shows the EPS used in the study collected from a local grocery store.



Fig. 3: EPS

Expanded polystyrene (EPS) is an amorphous and linear polystyrene with a density of  $17 \text{ kg/m}^3$ , a molecular weight between 160,000 to 260,000g/mol, and contains 4-7% blowing agent (usually pentane or butane), which makes it soluble in biodiesel through physical and chemical treatments [31,56]. EPS is a very stable foam with 98% air-in-volume, with a heating value of 8000J/g when combusted [31]. Polystyrene dissolves in a vast variety of aromatic compounds [57], but cannot be burned in a diesel engine in its original form. It can, however, be dissolved into biodiesel to make a fuel mixture, which can in turn be burned in the engine. The chemical structure of biodiesel contains a lengthy hydrocarbon chain of 16-20 carbons with oxygen at the end. The oxygen content is approximately 10% by weight [32,41,58]. However, studies showed that increasing the hydrocarbon chain does not increase styrofoam's solubility in biodiesel [31]. EPS, when mixed with biodiesel, does not interact with methyl esters to decompose it, nor does it form bonds with fatty acids. However, it potentially increases viscosity and may reduce the CN of the fuel blend due to its complex structure [59]. Kuzhiyil and Kong evaluated energy recovery from

polystyrene waste in biodiesel, and found it to be a viable fuel [60]. The styrofoam dissolves in biodiesel and other organic compounds such as acetone, tetrahydrofuran, toluene, etc. due to the molecular interaction between them. This interaction depends on cohesive energy densities (CED), which is related to the polarity of molecules. Another parameter is named the Hildebrand solubility parameter (HSP) [61]. Polymer chemistry texts suggest that the solvent should have a HSP value closer to polymer in order to dissolve it. The solubility of polystyrene is heavily-dependent on temperature; it changes from glassy to rubbery at around 100-110°C, and becomes soft with a drop in viscosity at above 200°C.

Fig. 4 shows the polymerisation reaction used for the production of polystyrene

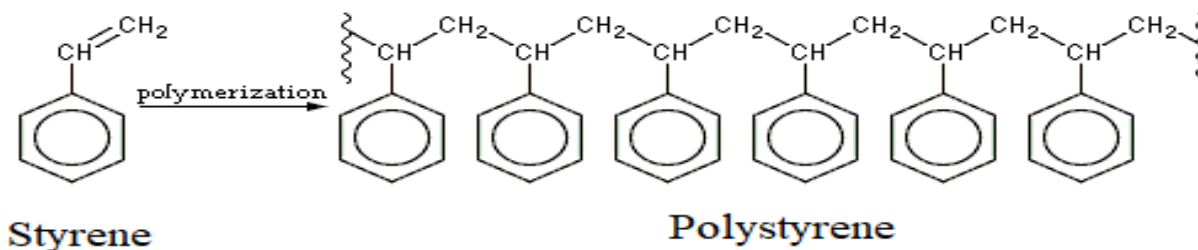


Fig. 4: Styrofoam (EPS) structure [32]

## 2.6 Biodiesel in Canada

The Canadian government introduced a new biofuel strategy (2% use of biodiesel-in-diesel for ground transportation and heating fuel by 2012, and 5% use by 2015) [19]. Canola oil is the prime feedstock for producing biodiesel in Canada. Comparatively lower feedstock cost and economical operating costs make canola oil biodiesel a promising alternative [62]. In 2010, the Canadian Environmental Protection Act (Bill C-33) mandated 5% renewable content in gasoline by 2020, and 2% renewable content in diesel fuel and heating fuel by 2012 [35,36,64]. The lion's share of renewable fuel in Canada comes from the production of ethanol from corn and wheat

[34,53]. The Times Canada model, which predicts the energy consumption, is expected to increase by 42 % by 2050 [35,54]. Canadian Renewable Fuels Association (the lobby group that represents the Canadian biofuels industry at the federal level), is lobbying for an increase of the renewable content in diesel blend mandate to a 5% inclusion rate by 2020, believing that this will encourage an increase in domestic production [63]. Regulations under the Canadian Environmental Protection Act (1999) require a 5% renewable content in the Canadian gasoline pool, and a 2% renewable content in the distillate pool, excluding heating oil [63].

### 2.6.1 Provincial Biofuel Policies [63]

Canada’s provinces, including Ontario, have blend mandates in place [Table 2].

Table 2: Provincial biofuel policy

<b>Province</b>	<b>Ethanol Blend Mandate for Gasoline</b>	<b>Renewable Fuel Blend mandate for Diesel</b>
British Columbia	5%	4%
Alberta	5%	2%
Saskatchewan	7.5%	2%
Manitoba	8.5%	2%
Ontario	5%	2-4%
Quebec	5%	none

### 2.7 Biodiesel Produced from Canola Oil

Rapeseed (*brassica napus*) and its varieties, specifically canola oil (*brassica napus* L.), stand out with mainly high oleic acid (~65%) and low amount of saturates (~6) [48]. The fatty acid composition of canola oil feedstocks varies from seed type to growing environments [48]. These high oleic acid varieties of canola oil are more suitable for oxidative stability of biodiesel fuel. Low oxidation stability may result in lower engine performance due to the decrease in lower heating value and high NO<sub>x</sub> emissions with shorter ignition delay period [600,49,52,64-66]. The calorific value of canola biodiesel is approximately 9.6% less than that of diesel due to its

oxygenated nature [54,55,64-68]. The low oxidation stability of fuel may lead to a decrease in heating value, thereby causing lower engine performance and high NO<sub>x</sub> emissions with short ignition delay period [52,65,66,69,70]. It is reported that lubrication of diesel fuel can be enhanced by 60% with the addition of 1%vol canola-derived methyl ester [70]. The high viscous nature & lubricity of canola biodiesel is because of the additional ester linkage. The increase in the viscosity is also attributed to the intramolecular hydrogen bonding of ester linkages [71]. Comparatively lower feedstock cost and economical operating costs make canola oil biodiesel a promising alternative. Canola oil biodiesel and its blends are known to reduce CO and HC emissions, whereas NO<sub>x</sub> increased slightly [4,49]. High oxygen content, high degree of unsaturation, advancement of ignition timing, and an increase in ignition delay may be the causes of NO<sub>x</sub> increase [44,48,50]. Combustion of canola oil biodiesel results in shorter ignition delay periods with an earlier onset of combustion due to a slightly higher CN and lower aromatic content [33]. Canola biodiesel addition results in reductions of CO by 32%, HC by 30.3%, and smoke by 53.5%, whereas NO<sub>x</sub> slightly increased by 8.9% [33]. The BSFC values increased by 4.4%, whereas the BTE reduced by 2.9%. The increase in BSFC may be due to increased viscosity and density, with a reduction in BTE due to its lower heating value [33,60].

## **2.8 Biodiesel Additives**

The additives used in this study, other than EPS, include acetone, di-ethyl ether (DEE), tetrahydrofuran, toluene and xylene. The additives are used in 10% (vol.) for uniformity, as well as for a few other reasons discussed in detail. DEE has an advantage over additives used in the experiment due to its non-corrosive nature [46]. The additives used in this experiment are highly volatile, which enhanced spray atomization, thereby leading to better mixing of the air-fuel mixture. They also possess high latent heat of vaporization. Among the other additives, xylene

exhibited superior properties than tetrahydrofuran, xylene and toluene. The properties of the additives are mentioned in the table below: [Table 3]

**Table 3: Properties of fuel additives**

Properties	Diesel	Biodiesel	Acetone	DEE	THF	Xylene	Toluene
Formula	C <sub>12</sub> H <sub>24</sub>		C <sub>3</sub> H <sub>6</sub> O	(C <sub>2</sub> H <sub>5</sub> ) <sub>2</sub> O	(C <sub>4</sub> H <sub>8</sub> )O	(C <sub>8</sub> H <sub>10</sub> )	(C <sub>7</sub> H <sub>8</sub> )
Molar Mass (g/Mol)	168.13		58.08	74.12	72.107	106.16	92.141
Density (kg/m <sup>3</sup> )	823	881	791	713	890	864	867
Calorific Value (MJ/kg)	45.573	40.296	31.862	36.892	34.866	43.3822	43.03326
Viscosity (Cst)	3.9	4.72	.27	0.23	0.53	0.62	0.38
Cetane No	48	42-48	-	125	-	-	-
Auto Ignition Temperature (°C)	315	-	465	160	321	530	480
Oxygen content	0	11	27.54	21.6	22.18	0	0
Flash Point (°C)	56	140	-18	-40	-14.5	30	4.0
Boiling Point (°C)	188	-	56	34	66	139	110.6
Latent heat of Vaporization (kJ/kg)	600	-	520	350	420	341	351
Reference	[46,55]	[15,50,51]	[58,72,73]	[16,75-77]	[78,79]	[80,81]	[82,83]

## **Thesis Objective**

Alternative sources of energy were in the limelight of researchers from time immemorial. Biodiesel is among one of the most prominent sources of energy for CI engines. Biodiesel is mixable, and acts as a good solvent with a wide variety of chemicals including styrofoam, or expanded polystyrene. EPS accounts for 22% of the total weight of plastics used worldwide. Previous researchers conducted many studies on dissolving EPS in biodiesel. This study particularly aims on biodiesel produced from canola oil, and dissolving EPS on the same. The maximum concentration of EPS that can be dissolved in biodiesel within the limits of kinematic viscosity, measured with and without additives. The correlation between the addition of biodiesel and its impacts on kinematic viscosity, heating value, density, etc., are investigated. The microscopic fuel structure is examined to have a closer look into the changes made on fuel structure by the addition of EPS, and the improvements made using various additives. Particle size distribution is measured to ensure the changes in the fuel particles' shape and its changes with the addition of EPS, as well as additives. The additives are used in 10% (volume %) for uniformity, as well as other reasons such as miscibility issues, reduction in heating value, etc. The emissions and performance of each fuel are examined at various loads and engine speeds.

## **3. Materials and Methods**

### **3.1 Materials**

1. Biodiesel produced from canola oil purchased from a retail grocery store;
2. Styrofoam purchased from a construction warehouse;
3. Methanol, Sodium Hydroxide, Acetone, Di ethyl Ether, Tetrahydrofuran, Toluene, and Xylene obtained from Lakehead University's Science Lab.

### **3.2 Equipment**

The CI engine in the experiment was a light-duty HATZ 2G40 engine (2 cylinders) for load tests, with the assistance of Dyno 2010 software at three engine speeds (1000, 2100 and 3000 rpm), at three different engine loads (LL, ML and HL), respectively. The data acquisition system was connected to a computer via a USB port. The Dyno 2010 software installed on the engine measures important parameters such as torque, brake power and speed, and has a capacity of 15-800 kW, torque of between 2 lb/ft and over 5000 lb/ft, and rpm ranging from 1000 to over 10000. Water brake loads control the engine load. The DYNO-MAX software, which runs on a Microsoft Windows platform, can generate real-time trace graphs. It is equipped with special features such as adjustable limits and variable voice, colour warnings, push-button controls, user-configurable analog, digital gauge ranges, etc. The engine load may be adjusted either through the software, or by manually turning the knob. The engine load condition was also recorded and controlled with the data system via a servo controller connected to the water load knob. Several parameters can be obtained from the software, including engine rpm, exhaust gas temperature, ambient temperature, engine load, engine torque, and operation time in various units according to our requirements. Data was recorded and analyzed using the DYNO-MAX software at a rate of 20 MHz; it records up to 1000 readings per second. The fuel in the removable tank was then measured to determine fuel

consumption. Equipment assigned to detect the regulated emissions (CO, NO<sub>x</sub>, CO<sub>2</sub> and HC) include a Nova Gas 7466K analyzer and a Dwyer 1205A (special analyzer for CO emissions). A thermo couple was also inserted into the exhaust pipe to measure the exhaust gas temperature, using an Extech EasyView 10, with a resolution of 0.1°C, with an accuracy of ±0.3%. CO emissions were measured using the Dwyer 1205A handheld CO analyzer with a resolution of 10 ppm. Smoke opacity was measured with a Smart 2000 smoke opacimeter connected to a PC, with software that works on a Microsoft Windows platform. The smoke opacimeter software also displays the ambient temperature and exhaust gas temperature on a different unit according to the requirements, and plots real-time graphs that can be critically analyzed for further clarification. The specifications of the emission measurement devices are outlined in Table 4.

**Table 4: Specifications of emissions measurement systems**

Method of Detection	Species	Measured Unit	Range	Resolution	Accuracy
Nova Gas 7466 PK					
Infrared Detector	CO	%	0-10%	0.01%	±1%
Infrared Detector	CO <sub>2</sub>	%	0-20%	0.10%	±1%
Electro Chemical	NO	ppm	0-5000 ppm	1 ppm	±1%
Electro Chemical	NO <sub>2</sub>	ppm	0-800 ppm	1 ppm	±1%
Electro Chemical	O <sub>2</sub>	%	0-25%	0.10%	±1%
Infrared Detector	HC	ppm x 10	0-20000 ppm	10 ppm	±1%
Dwyer 1205A Electro chemical	CO	ppm	0-2000 ppm	1 ppm	±5%
Smart 2000	Opacity Soot Density	% mg/m <sup>3</sup>	0-100% 0-10 mg/m <sup>3</sup>	0.10% 0.00001	±0.5% ±0.5%
Ex Tech EA10	Temperature	0.1 °C	(-)200 °C- 1360 °C	0.1 °C	±0.3%

### Fuel Blends used

The following are the fuel blends used in the study.

1. Biodiesel + Styrofoam 2g/L
2. Biodiesel + Styrofoam 6g/L
3. Biodiesel + Styrofoam 10g/L
4. Biodiesel + Styrofoam 10g/L+ Acetone 10%
5. Biodiesel + Styrofoam 10g/L+ tetrahydrofuran 10%
6. Biodiesel + Styrofoam 10g/L + Di-ethyl ether 10%
7. Biodiesel + Styrofoam 10g/L + Toluene 10%
8. Biodiesel + Styrofoam 10g/L + Xylene 10%

### 3.3 Biodiesel Production from Canola Oil and Mixing of Styrofoam

Fig. 5 shows the stepwise transesterification reaction in which the reaction of glyceride with alcohol

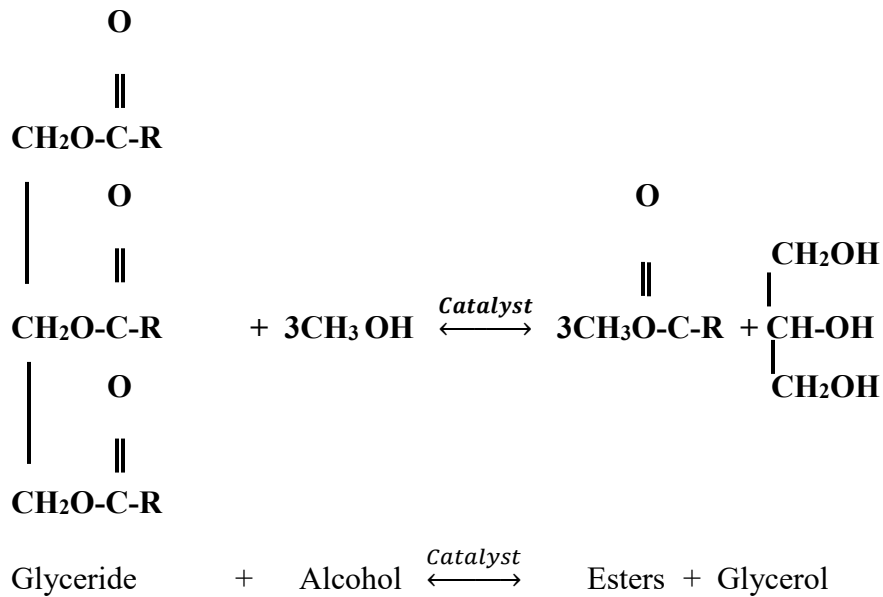


Fig.5: Transesterification reaction

Transesterification is the process used to convert canola oil to biodiesel [39,40]. This process is very popular due to its simplicity, cost-effectiveness, and yield. During transesterification, alcoholysis of canola oil (triglycerides) reacted with methanol in the presence of a catalyst, producing biodiesel, with glycerol as a by-product [4]. Methanol was used as alcohol for transesterification. It was observed to be 80% efficient, and obtained from its manufacturing location (i.e., laboratory at Lakehead University). Biodiesel was produced through a sequential process in the lab. Firstly, to avoid problems due to viscosity, 2L of canola oil was heated until it reached 65°C and stirred slightly using a magnetic stirrer. At the same time, sodium hydroxide (NaOH) (7gm) and methanol (CH<sub>3</sub>OH) (400ml) were mixed and stirred thoroughly until dissolved in a closed glass beaker by means of a magnetic stirrer. Secondly, the heated canola oil was mixed with the above-mentioned solution and blended fiercely for approximately 45 minutes. After these steps, the biodiesel was left to settle for 24 hours, after which time impurities such as fatty acids and glycerin were separated. This was followed by sequential water washes (vigorous shaking or mixing in a closed bottle) with 500ml and 300ml, respectively, at 24-hour intervals between each wash. The final step consisted of heating the biodiesel after washing to 105°C to remove any remaining water and impurities. Canola oil biodiesel was produced according to ASTM 6751 standards [Table 3]. The weighed styrofoam was added to pure biodiesel at room temperature (25°C) and stirred constantly by means of a magnetic stirrer. The above mixture was left for 24 hours for complete mixing. The solubility of styrofoam could be increased by applying heat. However, the temperature treatment tended to form polymer once again after the solution cooled down to ambient temperature, which in turn may have adversely affected the quality of the generated fuel blend [59]. The kinematic viscosity could be reduced by including the additive (i.e., DEE, THF etc.), which, in this study, was at 10% (vol.) to the biodiesel styrofoam solution.

Canola oil biodiesel was measured (1 L) in a container, EPS was measured in a measuring scale and added in increments of specific amounts. The maximum concentration was found using the same method, and the kinematic viscosity was measured to ensure it complied to ASTM standards. The solution was kept for 24 hours for complete dissolution. Heating value of the fuel was also performed.

The additives were mainly alcohols (i.e., acetone, di ethyl ether, tetrahydrofuran, toluene, and xylene) were mixed in 10% (vol.) to avoid complications such as:

1. Low calorific value
2. Miscibility issues
3. High flammability
4. Engine lubricity
5. May lead to leakage of fuel from the injection pump due to the decrease in viscosity

### **Steps in biodiesel production**

1. Canola oil biodiesel was measured (2L) and heated to 60°C.
2. Methanol (200 ml) and sodium hydroxide (7 gm) was mixed in an air-tight container and stirred with the help of a magnetic stirrer.
3. The above mixture was placed in an air-tight blender and blended vigorously for 60 minutes.
4. The mixture was kept in the container for 24 hours, and the yellow viscous liquid was separated (glycerin) and washed with water (500 ml); the impurities and viscous waste fats were also separated.
5. The solution was kept for another 24 hours, and washed a second time with water (300 ml) through the same procedure as above.
6. The biodiesel was heated up to 105°C to remove impurities (e.g., traces of methanol, water, etc.).

Table 5 depicts the qualitative values of the biodiesel thus manufactured in the laboratory.

**Table 5: Test Results of Canola biodiesel per ASTM 6751 [5]**

<b>Test name</b>	<b>Test Method</b>	<b>ASTM limits</b>	<b>Results</b>
Free glycerin (mass %)	ASTM D6584	Max 0.020	0.000
Total Glycerin (mass %)	ASTM D6584	Max 0.24	0.112
Flash Point, Closed cup (°C)	ASTM D93	Min. 130	169
Water & sediment (vol.%)	ASTM D2709	Max. 0.050	0.000
TAN (mg KOH/g)	ASTM D664	Max. 0.50	0.14
Sim. Dist., 50% recovery (°C)	ASTM D2887	N/A	359.8
Cetane Index	ASTM D976 (2 variable formula)	N/A	50
Copper corrosion 3h @50°C	ASTM D130	Max. 3a	1a

Fig.6 illustrates the summarized steps in the production of biodiesel, which can be classified in five steps

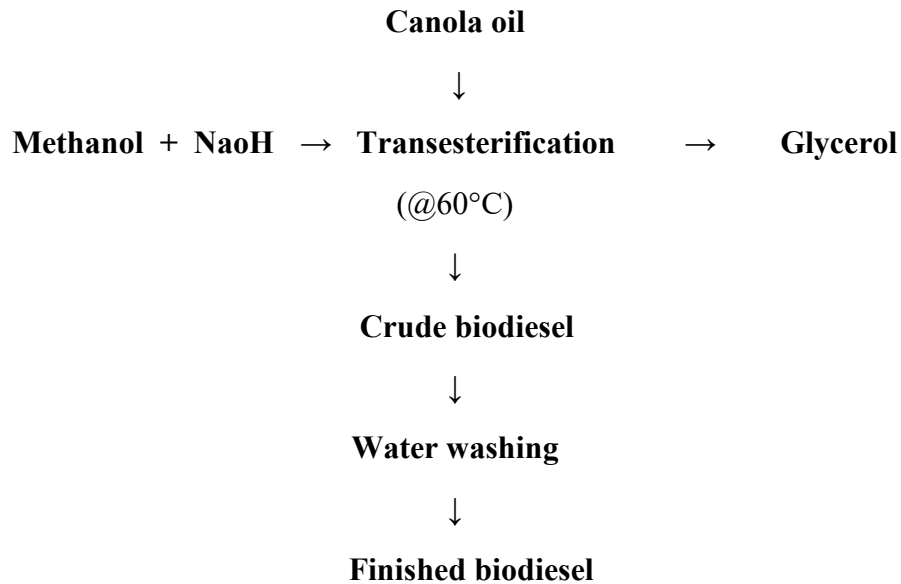


Fig. 6: Flowchart for biodiesel production

Some of the by-products of biodiesel production are crude glycerine, fatty acids, methanol, salt, chemical impurities, etc. Approximately 1/10<sup>th</sup> of the total biodiesel production leaves crude glycerin. Since the purification of crude glycerine is not cost-effective, it is used in anaerobic digestion, preparation of animal feeds, composting, etc. Burning of crude glycerin leads to production of a carcinogen called acrolein [80-82]. Glycerine has low auto ignition quality, low heating value, and high ignition temperature limits, and is used as a fuel in combustion. Studies are in progress with respect to the emulsification of pure glycerine in diesel and biodiesel.

### 3.4 Measurement of fuel properties

#### 3.4.1 Viscosity

Viscosity is the resistance to the flow of liquid. Viscosity measurement was performed using an Ostwald viscometer. Kinematic viscosity (cSt) was measured using the viscometer inside a water bath at the required temperature. Viscosity of fuels was calculated according to ASTM D 445 standards, and measured at 40°C. Kinematic viscosity measurement is of key importance as solving EPS in biodiesel, which increases kinematic viscosity, as observed in our studies. The requirements include the Ostwald apparatus, fuel at the required temperature, a foot pump, a stopwatch, and a temperature gauge. Fig. 7 shows the picture of viscometer used in the study.



Fig. 7: Viscometer

#### Steps for measuring viscosity

1. Pour the fuel at the required temperature into the viscometer and placed in a water bath on the viscometer holder at the required temperature of measurement (usually 40°C).
2. Ensure that the water in the tank and the fuel are at the required temperature -- adjust the temperature accordingly. The viscometer should be submerged in water up to 80-85%.
3. By means of a foot pump, pressurize the fuel until its crosses the red line mark on the viscometer.

4. When removing the foot pump after the fluid level drops, hit the stopwatch once it reaches the red line.
5. Record the time the droplet took to reach the red line below. Repeat the experiment three times to reduce the chance of error.
6. Calculate the kinematic viscosity using the readings, as per the calculations discussed in the sample calculations section.

Note: Major sources of error include taking the measurement before the fluid / water reaching the required temperature.

Fig. 8 illustrates the viscosity measuring setup at lakehead university laboratoty.

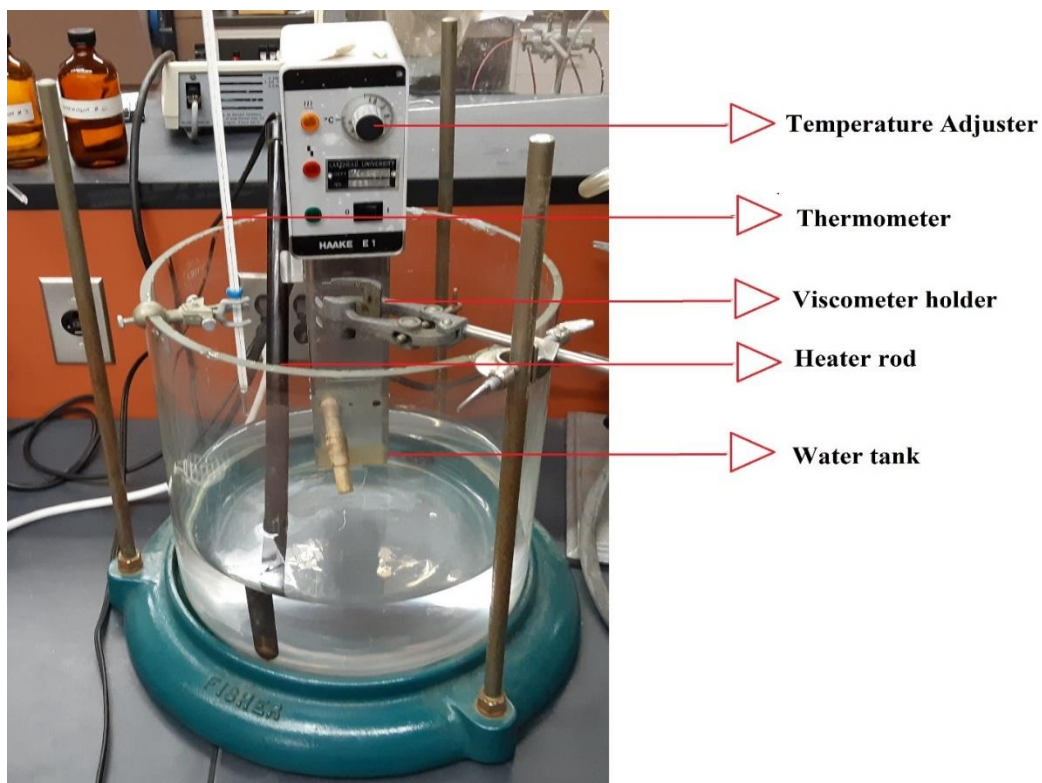


Fig. 8: Viscosity measuring setup.

### 3.4.2 Density

A calculated quantity (100 ml) fuel was weighed using a precision weighing device (Mettler Toledo AL 204). The weight was recorded, and the density was determined using the following equation:

$$\text{Density} = \frac{\text{mass}}{\text{volume}} \frac{(g)}{(cm^3)}$$

Fig. 9 depicts the picture of the precision measuring device used in the study



Fig. 9: Precision weighing scale

### 3.4.3 Heating Value

The amount of heat released by total combustion of unit mass of fuel. The Parr instruments (1341 plain jacket bomb calorimeter) was used to measure the heating value in the lab. The measurements were taken in compliance to ASTM standards for measuring heating value.

$$H_g = \frac{\Delta t * W - (L * 2.3)}{m} \left( \frac{cal}{g} \right)$$

$H_g$  = heat of combustion in calories per gram.

$W$  = energy equivalent of the calorimeters in calories per cm.

$L$  = length of burned ignition wire.

2.3 = calories per cm of nickel-chromium wire.

$M$  = mass of hydrocarbon tested.

Fig. 10 depicts the heating value measurement setup in the lab and fig.11 shows the bomb used in the bomb calorimeter.



Fig. 10: Bomb Calorimeter set up



Fig. 11: Bomb

### **Steps for measuring heating value**

1. Place 2 L of distilled water in the bucket, without spilling.
2. Fill combustion capsule with approximately 0.6 g of fuel sample, and place in the holder.
3. Place 10 cm of fuse wire in the slack to dip the wire into the sample fuel.
4. Drop 1 ml of water at the bottom of the bomb.
5. Tighten the bomb head firmly, and attach oxygen inlet filled with oxygen for 30 seconds before closing the purge valve. Close oxygen inlet once the pressure reaches 35 atm.
6. Place the bomb in the bucket, connect the wires, and close the calorimeter lid.
7. Turn on stirrer motor after connecting the pulley, using the drive belt.
8. Run the unit for 5 minutes before switching on the thermocouple; record the initial temperature.
9. Press the ignite button for 5 seconds; the red light will blink.
10. Record the temperature every minute until it reaches its peaks and levels out.
11. Turn off the device and dismantle the setup. Measure the left-over wire and subtract it from the initial length to determine the length of wire used in the equation.

The calculations are described in the sample calculations section.

#### **3.4.4 Particle size distribution**

The particle size distribution experiment is conducted using a Malvern Mastersizer 2000 instrument. The fuel sample was mixed with distilled water and poured into a glass container (900 ml). The medium with appropriate refractive index should be selected for the experiment. The mixture was then stirred and pumped into the particle size measurement equipment by means of the Hydro 2000 S. The measurement, interpretation and representation were calculated using the

software provided by the equipment firm. The obscuration level before measurement should be around 15%. The refractive index used in the measurement was 1.4565. The Mastersizer software creates particle size distribution graphs. Fig. 12 depicts the picture of particle size measuring setup.

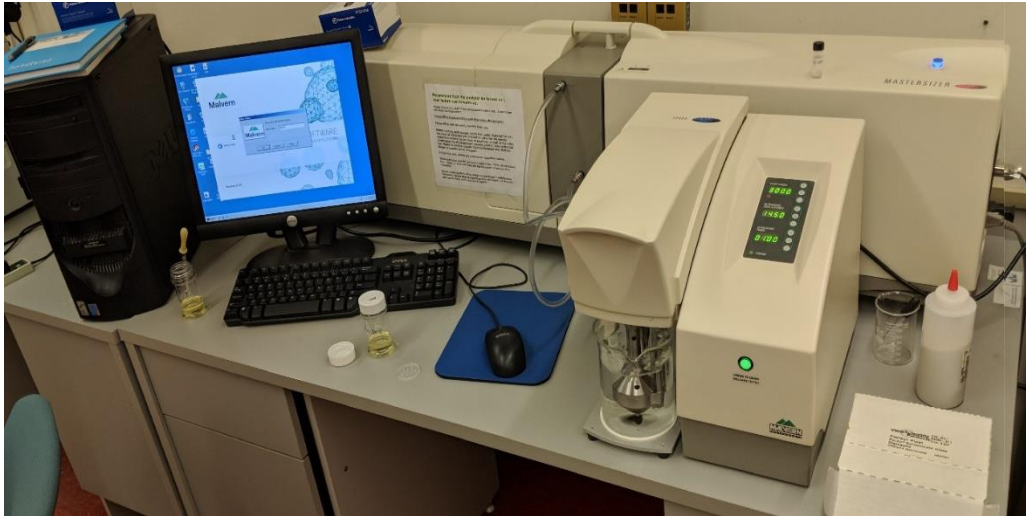


Fig. 12: Particle size measuring system.

### 3.4.5 Microscopic fuel structure

Fuel structure of each fuel was measured at 10X resolution using a Polaris IX 51 inverted microscope [Fig.13], and a digital picture was captured using the software. The microscopic structure revealed the changes to the fuel structure with the amount of EPS in the fuel, as well as the improvements to the fuel structure achieved by the addition of additives at the microscopic level.



Fig. 13: Polaris Microscope

### 3.4.6 Pitot tube and manometer

Fig. 14 illustrates the pitot tube and manometer setup used in the study for measuring air flow.



Fig. 14: Pitot tube and manometer

A pitot tube manometer was used to measure the fluid flow velocities using the pressure difference. From the difference between total pressure and static pressure, the air velocity is calculated. Detailed are described in the sample calculations section.

### 3.4.7 Cummins heavy-duty engine

A Cummins 4-cylinder, air-cooled, turbocharged diesel engine [Fig. 15], designed with a high pressure common rail injection system was used (see Table 7 for engine specifications). This type of engine is used mainly in agricultural, construction and mining industries, as well as for irrigational purposes. The engine was considered heavy-duty because of its use in heavy load applications. Testing was conducted at idling conditions under cold start conditions at two different speeds (i.e., 700 rpm and 1700 rpm). Following each test, a time gap of 5-6 hours was allowed in order to ensure cold start conditions. The engine was tested outdoors, where the atmospheric temperature was at times below 20°C. The experimental setup is shown in Fig. 17(a). The time span of the experiments was 30 minutes. Probes for emissions measurement were inserted into the exhaust pipe. Peak results for each component were read after every test, and emissions were recorded at the required time intervals (i.e., at 60 seconds, 120 seconds, 240 seconds, 360 seconds, 480 seconds, 600 seconds, 900 seconds, 1200 seconds and 1800 seconds) after the beginning of the experiment. After each 30-minute mark, the removable fuel tank was drained and measured to calculate the fuel consumption. When changing the fuel type, the engine was run on petroleum diesel (B 0) for a short duration after which time a new fuel type was tested.



Fig. 15: Cummins Heavy duty diesel engine

### 3.4.8 Hatz 2G40 light duty Engine

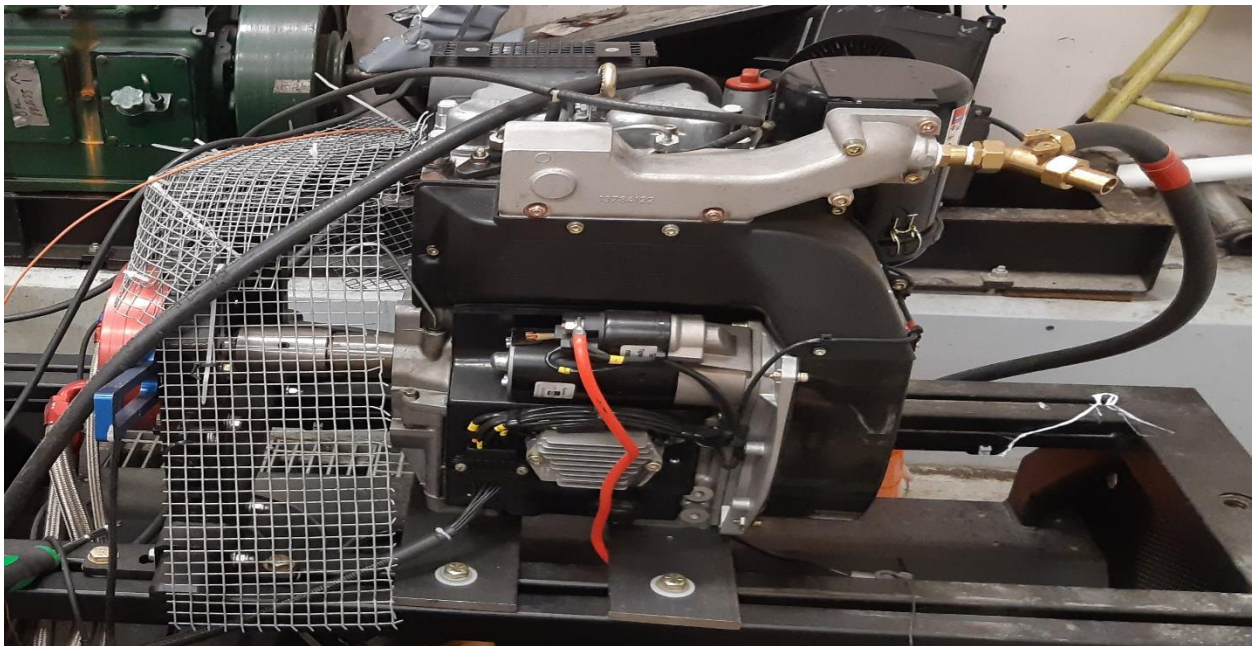
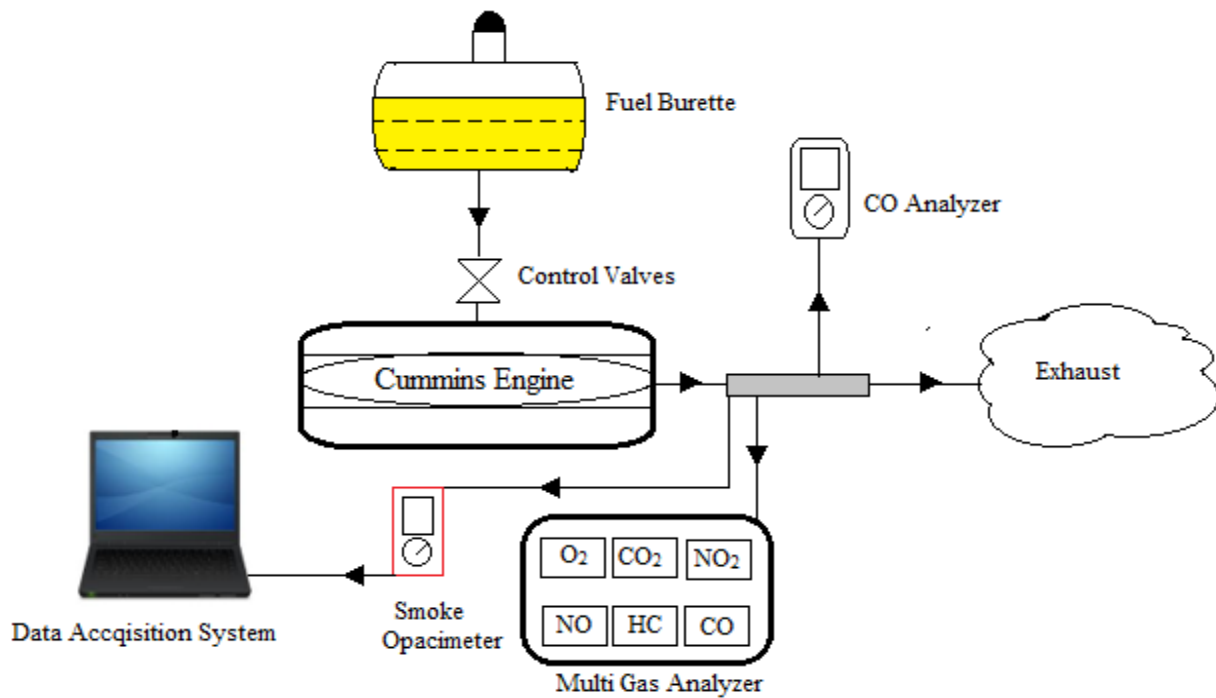
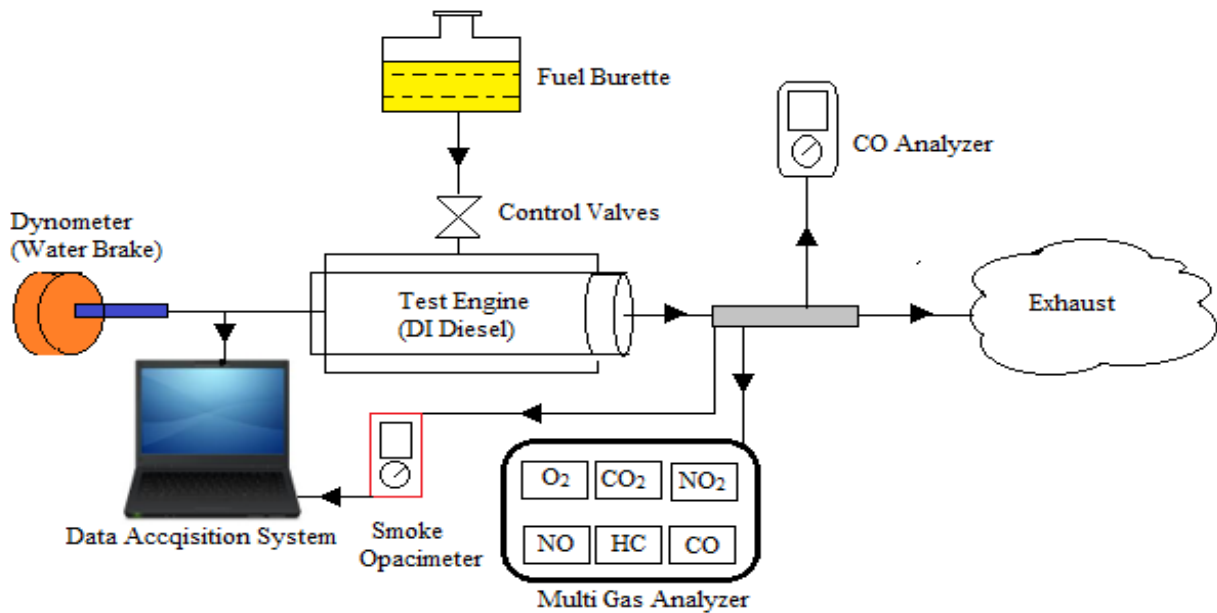


Fig. 16: Hatz 2G40 light duty engine

A HATZ 2G40 air-cooled, 2-cylinder, 4-stroke engine was used for testing at 1000, 2100 and 3000 rpm, each with low, medium, and high loads, respectively (specifications are detailed in Table 6). Loading was determined using a land and sea dynamometer, and the interface was measured using DYNO-MAX software provided by the dynamometer supplier. The data acquisition system was connected to the computer via a USB port. The fuel used in the HATZ 2G40 was measured in a graduated cylinder. The experimental setup is shown in Fig. 17(b). Holes were punched in the exhaust system through which three gas measurement systems (namely a Nova gas 7466K multi gas analyzer, a Dwyer 1205A CO analyzer, and a Smart 2000 opacimeter) were inserted. A thermo couple was also inserted into the exhaust system to measure exhaust gas temperature.



17 (a) Heavy-duty engine (Cummins QSB4.5)



17 (b) Light-duty engine (Hatz 2G40 2 cylinder)

Fig. 17: Experimental setup

Table 6 shows the specifications of HATZ 2G40 light-duty engine.

**Table 6: HATZ 2G40 engine specifications**

Engine make & model	HATZ 2G40
Engine type	4 stroke air-cooled
No of cylinders	2
Bore × Stroke	92 mm×75 mm
Swept Volume	997 cc
Compression Ratio	20.5:1
Fuel injection pressure	26 MPa
Fuel injection timing	8° BTDC ( $\leq 2250$ rpm); 10° BTDC ( $\leq 2300$ rpm)
Continuous Max. rated power	13.7kW @3000 rpm

Table 7 shows the specifications of Cummins heavy-duty engine.

**Table 7: Cummins QSB4.5 engine specifications**

---

Engine make & model	Cummins QSB 4.5 T4I
Engine type	Inline 4-cylinder
No of cylinders	4
Bore × Stroke	102 mm × 138 mm
Swept Volume	4.5 L
Compression Ratio	17.3:1
Rated power	97kW @ 2300 rpm

## 4. Results and Discussions

Adding styrofoam to biodiesel increases viscosity. The maximum concentration of styrofoam in canola oil biodiesel is 10g/L. The sticky texture on the walls of the container is noted at concentrations above 12g/L. In concentrations above 15g/L, tiny styrofoam particles can be observed in the solution, as well as on the walls of the container. The solubility of styrofoam can be altered through heat supply. However, temperature treatment is not preferred, as it may lead to re-formation of the polymer when the solution cools down to ambient temperature, which may adversely affect the quality of the fuel blend that is generated [59]. In the experiment, it was verified that the viscosity of the fuel blend increased with the increase in polystyrene concentration [Table 2] and that the density of the blends up to 15g/L remained nearly similar [Table 2] [22]. The main drawback of dissolving high concentrations of polystyrene was increased viscosity. High viscosity may cause bigger droplet sizes, poorer fuel atomization and vaporization, a narrower injection spray angle, and greater in-cylinder penetration of the fuel spray [32]. High viscosity may also reduce fuel flow rates, resulting in inadequate fuel supply. Elevated viscosity may result in pump distortion [60,32]. The temperature dependence EPS solubility is dictated in table 10. The kinematic viscosity of Maximum soluble EPS below 6 cSt is investigated. The experiment also revealed the cold flow properties are little inferior as the temperatures below 15°C dissolved only trace amounts of polystyrene. Previous studies reveal that adding EPS to canola biodiesel causes reduction in cetane number and increase in kinematic viscosity [60,61,32,74,59]. Higher EPS concentrations tend to reduce the cetane number considerably and tends to reduce the combustion quality [60,61,74,59]. The cetane number can be considered as one among the main factors affecting the combustion quality [46]. Fig. 18 shows the cons of adding EPS to biodiesel.

### Cons OF Adding EPS to Biodiesel

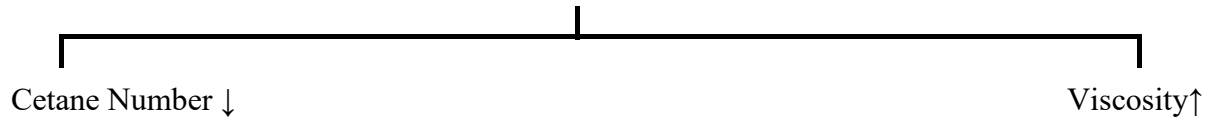


Fig. 18: Disadvantages of adding EPS to biodiesel

Additives were selected to overcome the disadvantages associated with adding EPS to canola biodiesel. The strategy for selecting the additives was based on these two factors. Many studies prove the ability of DEE to improve the performance and emissions of CI engine fuels [16, 75-77]. Diethyl ether was selected because of its capability of improving the cetane number and kinematic viscosity, along with its other fuel properties, whereas EPS-soluble additives (acetone, tetrahydrofuran, toluene, xylene) were selected based on their ability to make EPS soluble, their reduction of kinematic viscosity, and their other fuel properties. Their reactivity to a rubber hose was examined prior to testing the fuel in order to ensure that the fuel does not result in damage to the fuel lines. Fig. 19 illustrates the strategy used in the selection of additives for EPS-infused biodiesel.

### Selection of Additives

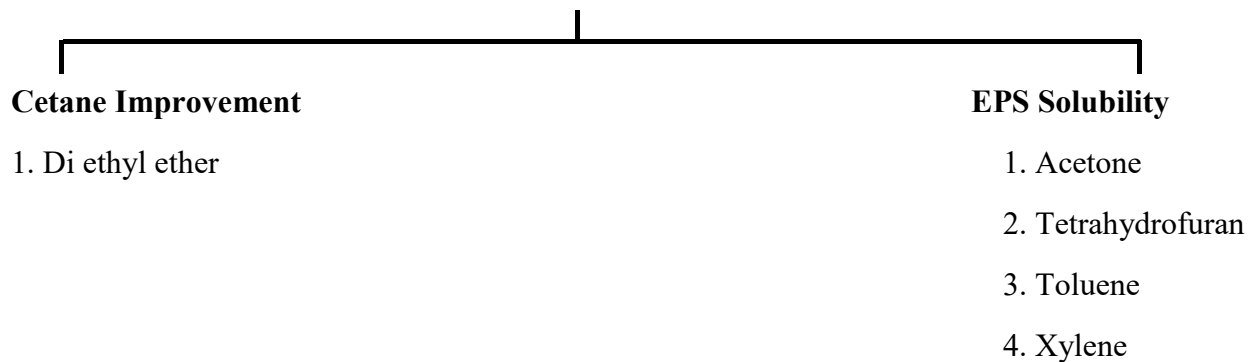


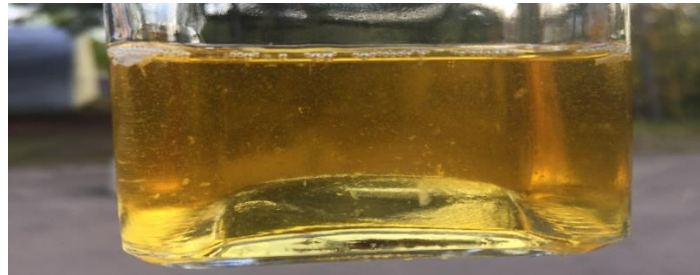
Fig. 19: Selection criteria for additives

Styrofoam dissolution in biodiesel and other organic compounds such as acetone, tetrahydrofuran, toluene, etc., is due mainly to the molecular interaction between them, which is explained by its cohesive energy densities (CED). This is related to the polarity of molecules, as well as to the Hildebrand solubility parameter (HSP) [61]. Polymer chemistry texts suggest that the solvent should have a HSP value closer to polymer in order to dissolve it. The solubility of polystyrene is heavily-dependent on temperature. The figure below reveals the temperature dependency of EPS in its dissolution, its viscosity, and the change in its physical appearance. Fig. 20 shows the EPS-infused canola biodiesel at various concentrations and temperatures.

(a) B 100 W/EPS (10 g/L) @ 25°C



(b) Styrofoam concentrations 13 g/L @ 25°C



(c) Styrofoam concentration of 15g/L @ 90°C



(d) Styrofoam concentration of 10g/L @ 5°C



Fig. 20: Pictures of fuel solution, (a) B 100 W/EPS (10 g/L), (b) EPS concentrations 13 g/L, (c) Styrofoam concentration of 15g/L @ 90°C, (d) Styrofoam concentration of 10g/L @ 0°C

The above figures explain the temperature dependency of EPS solubility in canola oil biodiesel. Fig. 20(a) shows the maximum solubility at an ambient temperature of 25°C (i.e., EPS 10 g/L) in canola biodiesel. Styrofoam concentrations beyond this concentration leave traces of EPS in the fuel sample, which is displayed in Fig. 20(b). As per the studies, 6 g/L is the recommended amount of EPS in canola biodiesel. The experiment revealed that temperature has a huge impact on the solubility and stability of EPS-infused canola biodiesel. Fig. 20(c) and Fig. 19(d) reveal the stability and temperature dependency of EPS-infused biodiesel. As the temperature increased, the stability of the EPS-infused biodiesel was higher. The figures also reveal that more EPS can be mixed at elevated temperatures, as seen in Fig. 20(d), and that the solution remained clear without any visible traces of EPS. At 90°C, we could increase the EPS concentration to 1.5 times without compromising kinematic viscosity standards. The temperature dependency on solubility and kinematic viscosity is further explained in Table 9. On the other hand, Fig. 20(d) shows that the cold flow properties of EPS-infused canola biodiesel were poor. The viscosity increased abruptly with the temperature increase, which is outlined in Table 9. Below 10°C, the ability of the canola oil biodiesel to dissolve EPS was considerably reduced, even at EPS concentrations of 10 g/L. When excess polystyrene was melted with the application of temperature, it led to polymer re-formation when cooled to low temperatures, especially below 10°C. At low temperatures, it formed a gel structure at the bottom of the container, as seen in Fig. 20(d). The recommended maximum EPS concentration is 10 g/L in order to avoid re-formation of polymers, thus avoiding the gel-like structure formation. All these factors make EPS-infused biodiesel more attractive in tropical climatic conditions, especially in stationary power plants.

Table 8 depicts the values of viscosity, density and heating vales of different fuels.

**Table 8: Fuel properties of different Biodiesel-Styrofoam blends with various additives**

<b>Fuels</b>	<b>Composition</b>	<b>Viscosity (cSt)</b>	<b>Density (kg/m<sup>3</sup>)</b>	<b>Heating value (MJ/kg)</b>
B100	Pure canola oil biodiesel	4.74	883.6	40.196
B 100 W/EPS (2g/L)	Biodiesel + styrofoam 2g/L	4.92	883	39.588
B 100 W/EPS (6g/L)	Biodiesel + styrofoam 6g/L	5.34	882	37.974
B 100 W/ EPS (10g/L)	Biodiesel + styrofoam 10g/L	5.81	882	36.548
B 100 W/ EPS (10g/L) +Ace 10%	Biodiesel + Styrofoam 10g/L+ Acetone 10%	5.25	871.4	39.324
B 100 W/ EPS (10g/L) +DEE 10%	Biodiesel + styrofoam 10g/L + Di-ethyl ether 10%	5.25	863.3	39.933
B 100 W/ EPS (10g/L) +THF 10%	Biodiesel + Styrofoam 10g/L+ tetrahydrofuran 10%	5.28	881.3	39.037
B 100 W/ EPS (10g/L) + Tol 10%	Biodiesel + Styrofoam 10g/L + Toluene 10%	5.26	879.7	40.321
B 100 W/ EPS (10g/L) + Xyl 10%	Biodiesel + Styrofoam 10g/L + Xylene 10%	5.29	879.3	40.683

Table 8 illustrates that styrofoam in biodiesel led to an increase in kinematic viscosity, whereas the density remained nearly identical. The use of EPS infused in biodiesel at higher concentrations (greater than 10 g/L) could have a detrimental effect on an engine, as it could lead to early ignition, possibly resulting in reduced power output and clogging of the fuel lines. It may also lead to elevated injection pressure if the fuel flow is choked by the fuel's high viscosity. Polystyrene in biodiesel reduced the fuel's CN due to its complex structure. Mixing EPS in biodiesel increased HC and CO emissions. Table 8 also discloses the improvements to the heating value and kinematic viscosity by including the additives to the maximum concentration of EPS at 25°C (i.e., 10 g/L). Even at low EPS concentrations, NO<sub>x</sub> slightly increased at high polystyrene concentrations, leading to a reduction in NO<sub>x</sub>. The experimental investigation concluded that adding EPS led to an increase in kinematic viscosity, abruptly after concentrations in excess of 10 g/L. The data supporting this fact is reported in Table 8. The kinematic viscosity of the fuels (B 0, B 100, B 100 W/ EPS 10g/L) at various temperatures were investigated, and are listed in Table 9. The fuel's calorific value (or heating value) diminished considerably with the addition of EPS. Many studies concluded that adding EPS to biodiesel may lead to a decrease in CN, thereby reducing combustion quality. In addition, EPS has low heating value. These contributing factors might be the reason for the reduction in heating value [59-61, 32]. A considerable reduction in kinematic viscosity was noted, and the heating value increased, which are both admirable qualities. From the table, the maximum value among the additives was for the Xylene blend (i.e., Biodiesel + Styrofoam 10g/L + Xylene 10%). The heating value of the Toluene blend was comparable to the Xylene blend. The minimum heating value among the EPS-infused biodiesel with the additives was for acetone (Biodiesel + Styrofoam 10 g/L+ Acetone 10%). The minimum value for kinematic viscosity was for diethyl ether (Biodiesel + Styrofoam 10g/L + Diethyl ether 10%), and acetone

(Biodiesel + Styrofoam 10 g/L+ Acetone 10%). The reduction in kinematic viscosity may have been helped by the capability of the additives to melt EPS (i.e., EPS dissolves in acetone). The density values with the addition of EPS in canola biodiesel followed a similar trend.

**Table 9: Kinematic viscosity of fuels at various temperatures**

Temperature (°C)	Kinematic Viscosity (cSt) <b>Diesel</b>	Kinematic Viscosity (cSt) <b>Biodiesel</b>	Kinematic Viscosity (cSt) <b>Biodiesel + Styrofoam 10 g/L</b>
25°C	3.26	6.74	7.12
40°C	1.87	4.23	5.81
65°C	1.42	2.94	3.93
90°C	1.19	2.09	2.78

Table 9 elucidates the temperature dependency on kinematic viscosity over various temperature range, especially from 0°C to 100°C and the comparison to Canola biodiesel and petroleum diesel.

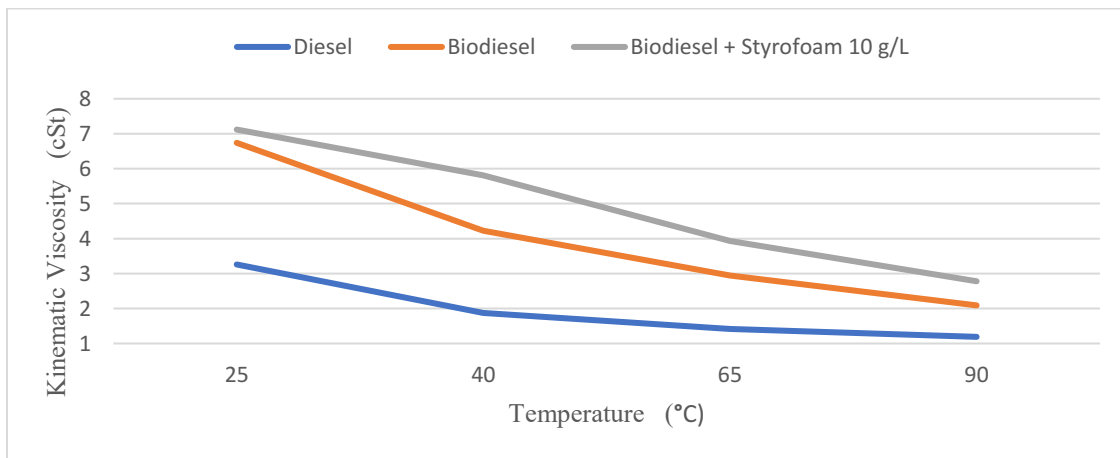


**Fig. 21: Kinematic Viscosity of fuels at various temperature**

Fig. 21 depicts the variation of kinematic viscosity of different types of fuel over various temperature ranges, especially from 0°C to 100°C. As expected, the kinematic viscosity reduced with an increase in temperature. The data is graphically illustrated in Fig. 22 for better interpretation. The values exhibit a steeper decrease in kinematic viscosity, with temperature, for canola oil biodiesel. The canola biodiesel properties and composition, which was explained in the earlier sections, may be responsible for this variation. EPS-infused biodiesel also followed the same trend (i.e., reduction of kinematic viscosity with temperature). Even though the temperature increase led to a decrease in kinematic viscosity, it was less desirable in EPS-infused canola biodiesel due to re-formation of polymers when cooled, whereas the stability of the petroleum diesel remained unaffected when cooled, even after continuous heating.

**Table 10: Solubility and Kinematic viscosity of various fuels at various temperatures**

Temperature (°C)	Kinematic Viscosity (cSt)	EPS Solubility (g/L)
25°C	5.91	8
40°C	5.76	10
65°C	5.79	15
90°C	5.97	19

The results in Table 10 are outlined more explicitly in Fig. 21, which illustrates photos of the temperature dependency of EPS solubility in canola biodiesel at various temperatures and EPS concentrations. Although increasing the temperature increased EPS solubility and kinematic viscosity to a great extent (1.5 times @ 90°C), cooling it caused more harm due to the formation

of a gel-like structure on the bottom of container, which is termed polymer re-formation. The recommended concentration is 10 g/L, according STM standards.

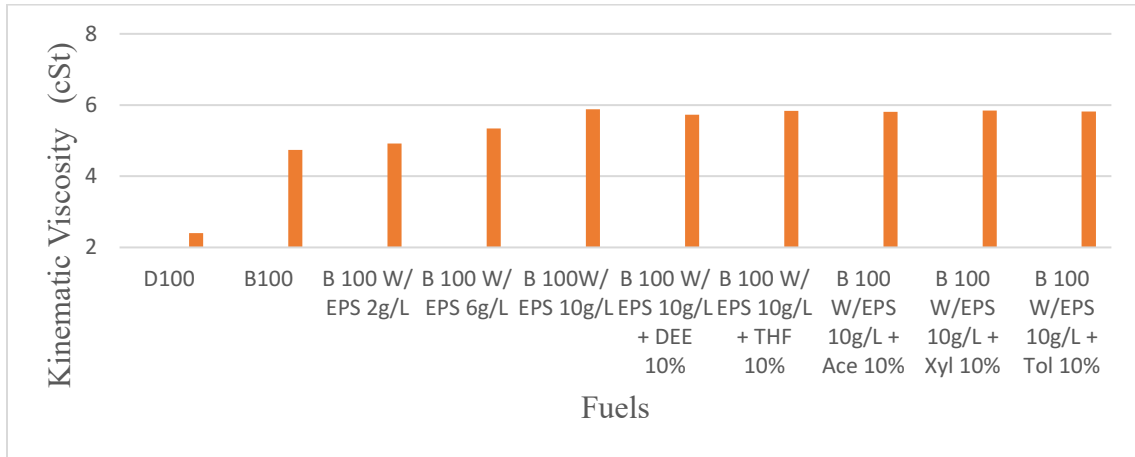


Fig. 22: Kinematic viscosity of fuels

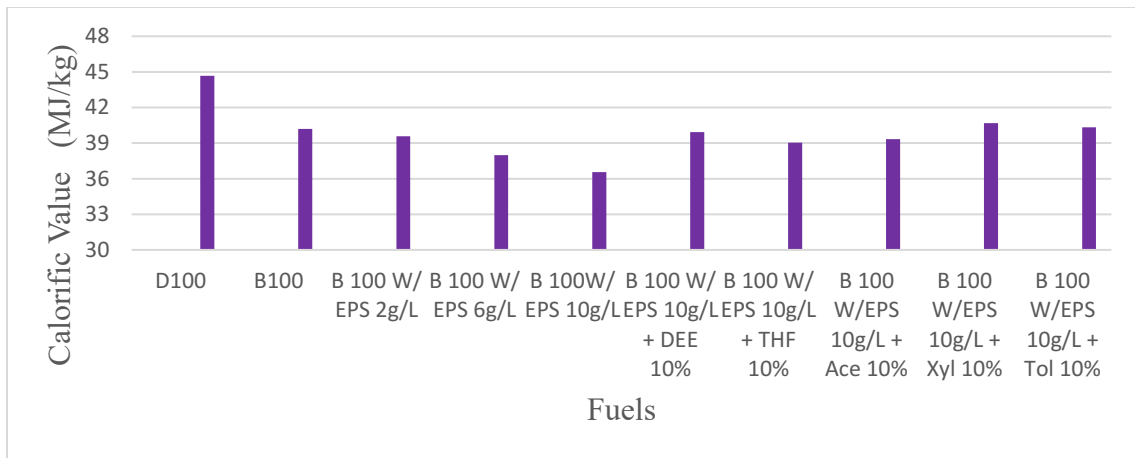


Fig. 23: Calorific value of different fuels

The heating values and kinematic viscosity of EPS fuel blends, as well as with additives, is depicted in Fig. 22 and Fig. 23, and are explained in Table 8. As the graph trend shows, the kinematic viscosity increased with EPS concentrations in canola biodiesel, with the best among additives such as acetone and diethyl ether having the least kinematic viscosity value. The heating value decreased with EPS concentrations, which was improved by adding the additives, with Xylene having the best heating value.

#### **4.1 Microscopic fuel structure**

Microscopic fuel structure is used in the study to get a closed picture of the fuel molecules, the changes by addition of EPS as well as additives can be investigated. The microscopic fuel structure of the sample was viewed at 10X resolution. The microscopic fuel structure of pure canola oil biodiesel was clear, and contained no particles [fig. 24(a)]. The further addition of EPS showed their presence in the fuel structure. The microscopic structure of EPS concentration (2g/L) was like pure canola oil biodiesel [fig. 25(a)]. Until the concentration of EPS (6g/L), EPS particles tended to appear [fig. 26(a)]. As per the microscopic structure, the concentrations of EPS on or over 10g/L revealed a high population of EPS particles in the structure [fig. 27(a)]. The improvement of adding DEE as well as other additives was clearly seen under the microscope, as the EPS particles are seen far apart or in trace amounts [fig. 28,29,30,31,32 (a)]. The clogging due EPS particles in 10g EPS concentration is resolved. This can be backed by the reduction in kinematic viscosity with the addition of diethyl ether as well as with other additives. EPS soluble additives (acetone, THF, xylene, toluene) may have enhanced the dissolution of EPS adding gravity to disappearance of EPS molecules. Among EPS soluble additives (acetone, THF, xylene, toluene), Xylene and THF shows more vigorous dissolution property [fig. 29,31 (a)].

#### **4.2 Particle size distribution.**

The particle size distribution reveals the average particle size distribution of a given sample. The particle size distribution of pure canola oil biodiesel and EPS concentrations until 6g/L appeared similar with a single peak [fig.26 (b)]. The single particle size distribution peak is due to the presence of nearly similar-sized particles. The EPS concentrations of 10g/L and higher led to the formation of a second peak, which may be due to particles left by overcrowding of EPS particles

[fig.27 (b)]. The EPS concentration 10g/L was evaluated for particle size distribution after the addition of 10% (vol.%) additives showed favorable results. The addition of diethyl ether and other additives removed the curve completely, which in turn was a desirable fuel quality. This may be due to the enhancement of the EPS dissolution in biodiesel with diethyl ether as well as other additives [fig.28,29,30,31,32 (b)]. It also resulted in the reduction of kinematic viscosity.

(a) Microscopic structure



(b) Particle size distribution.

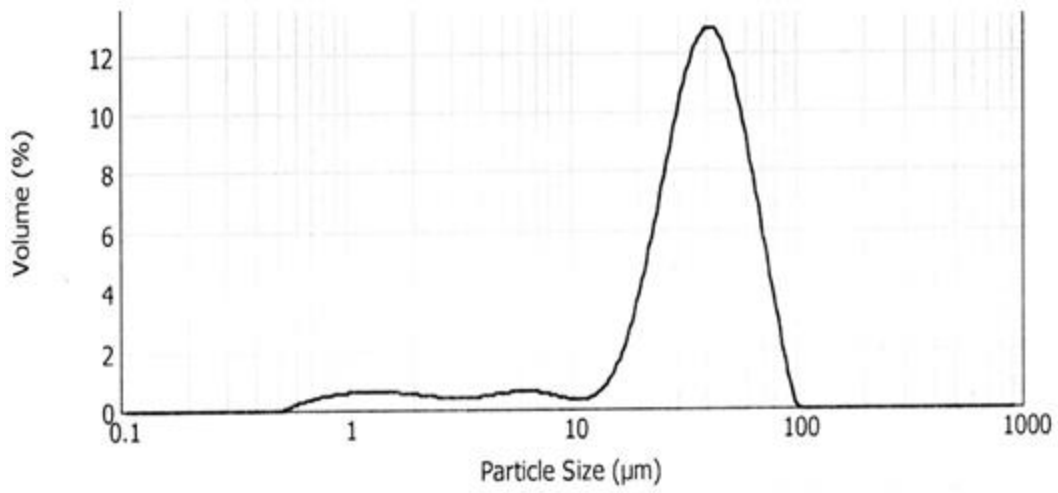
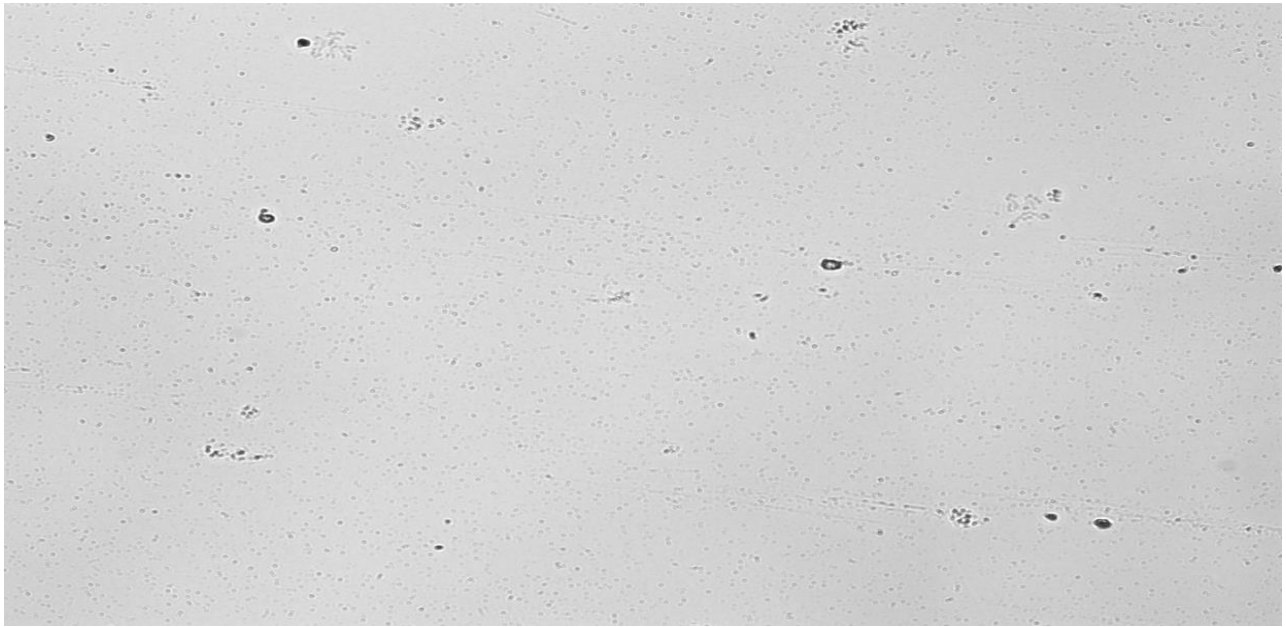


Fig. 24: Microscopic structure (a) and particle size distribution (b) of B100

(a) Microscopic structure



(b) Particle size distribution.

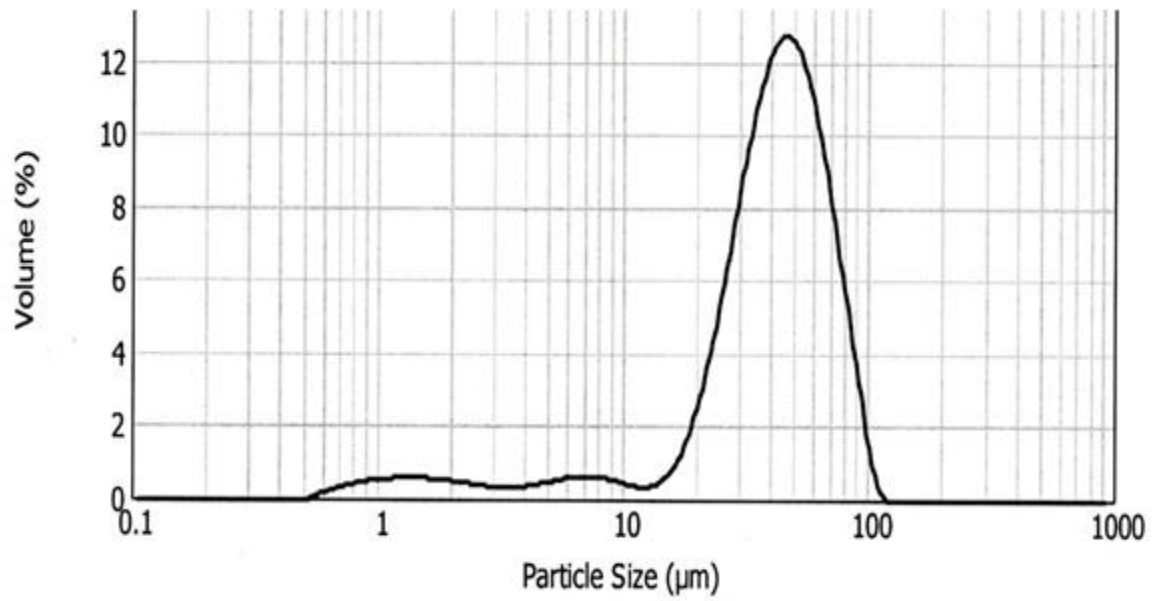
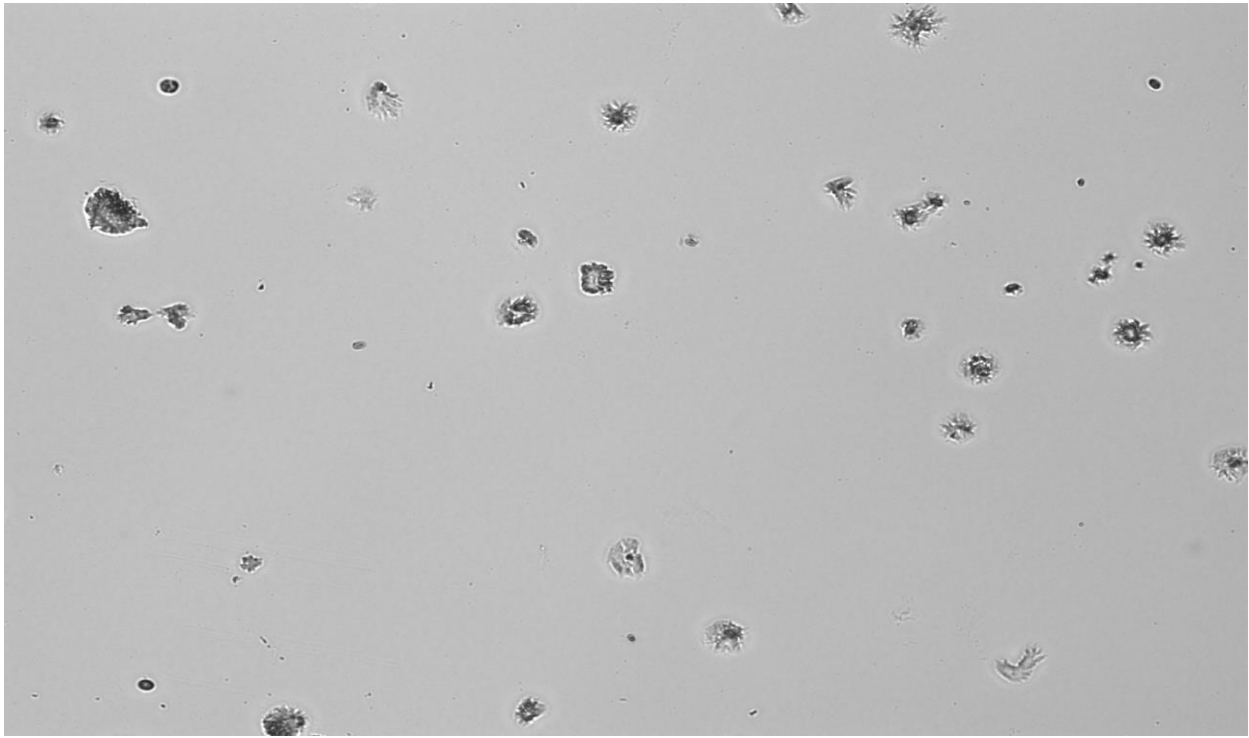


Fig. 25: Microscopic structure (a) and particle size distribution (b) of B100 W/ EPS (2g/L)

(a) Microscopic structure



(b) Particle size distribution.

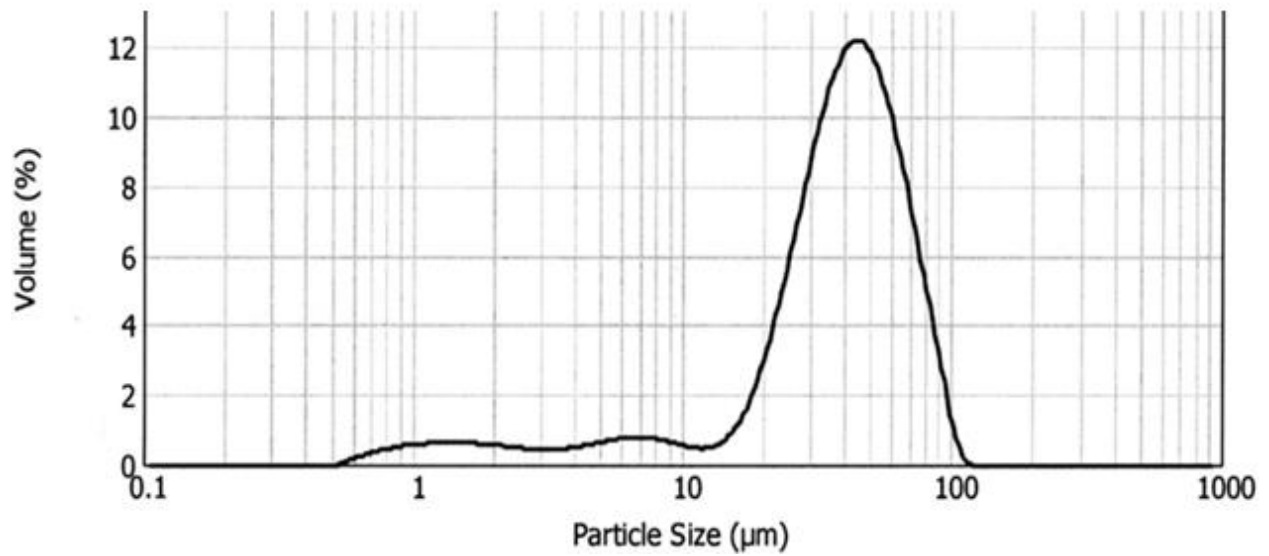
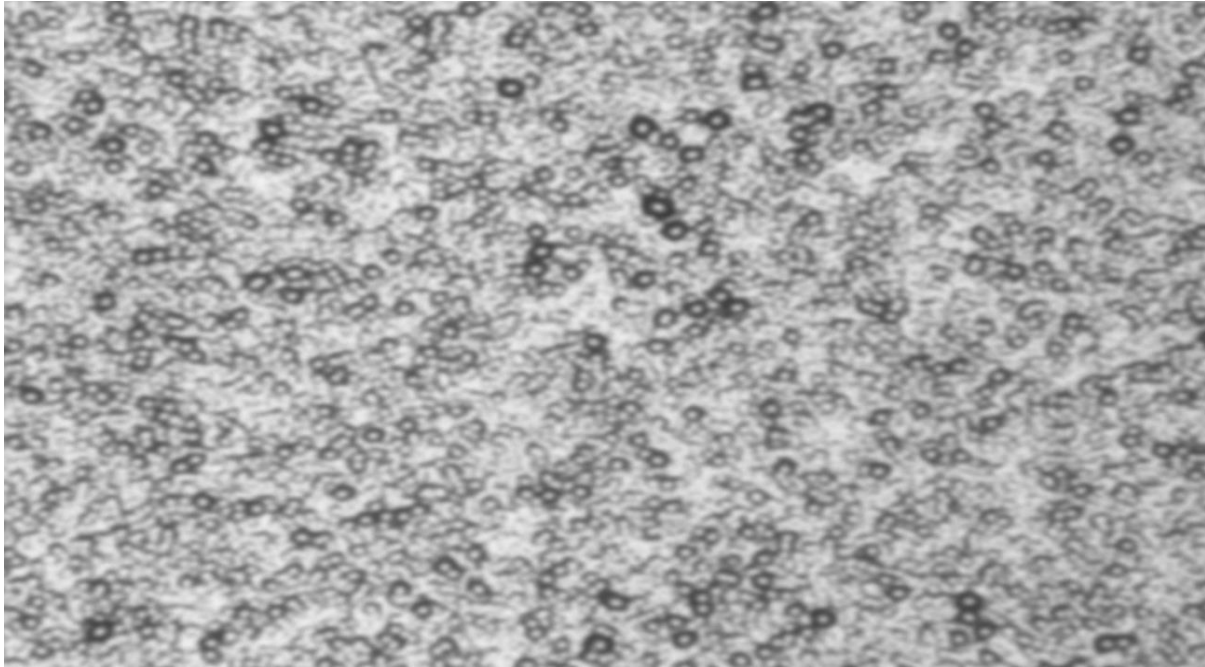


Fig. 26: Microscopic structure (a) and particle size distribution (b) of B100 W/ EPS (6g/L)

(a) Microscopic structure



(b) Particle size distribution

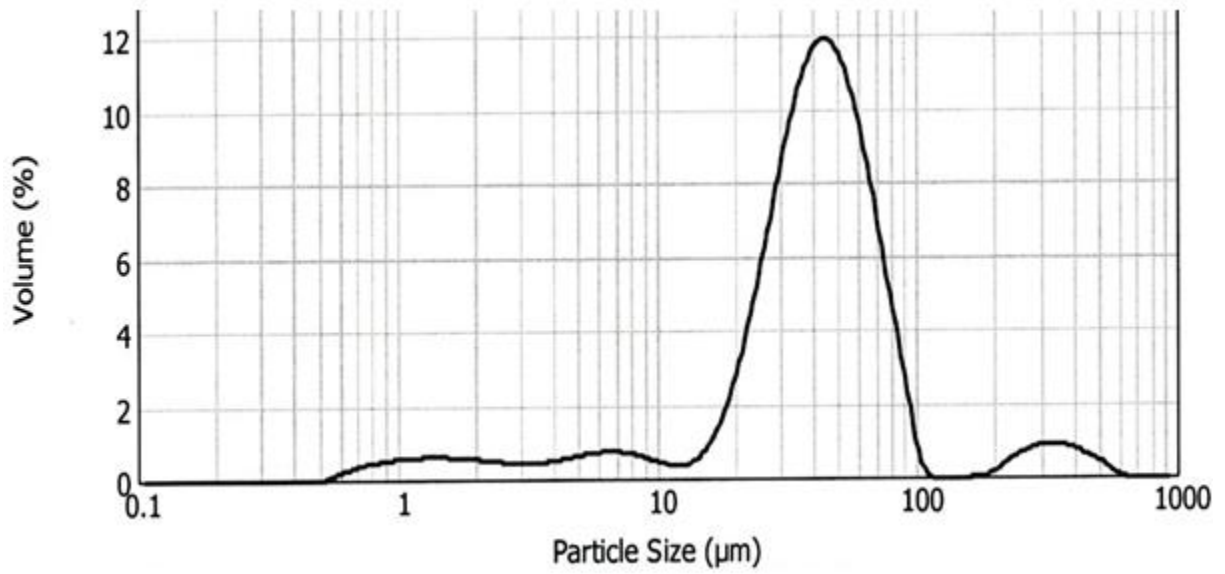
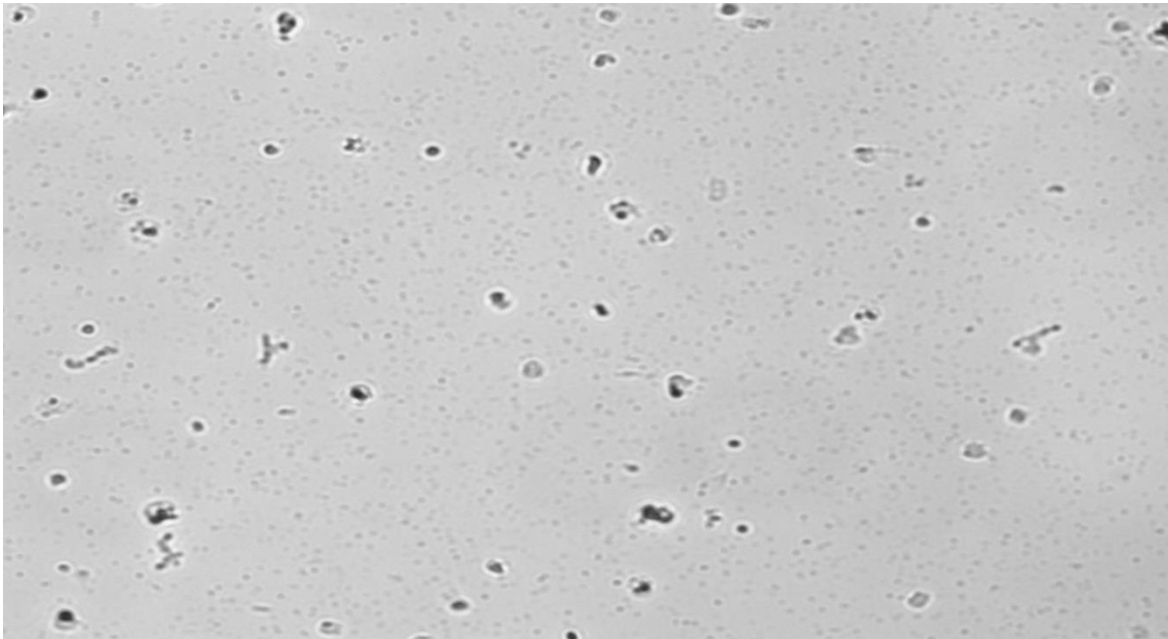


Fig. 27: Microscopic structure (a) and particle size distribution (b) of B100 W/ EPS (10g/L)

(a) Microscopic structure



(b) Particle size distribution

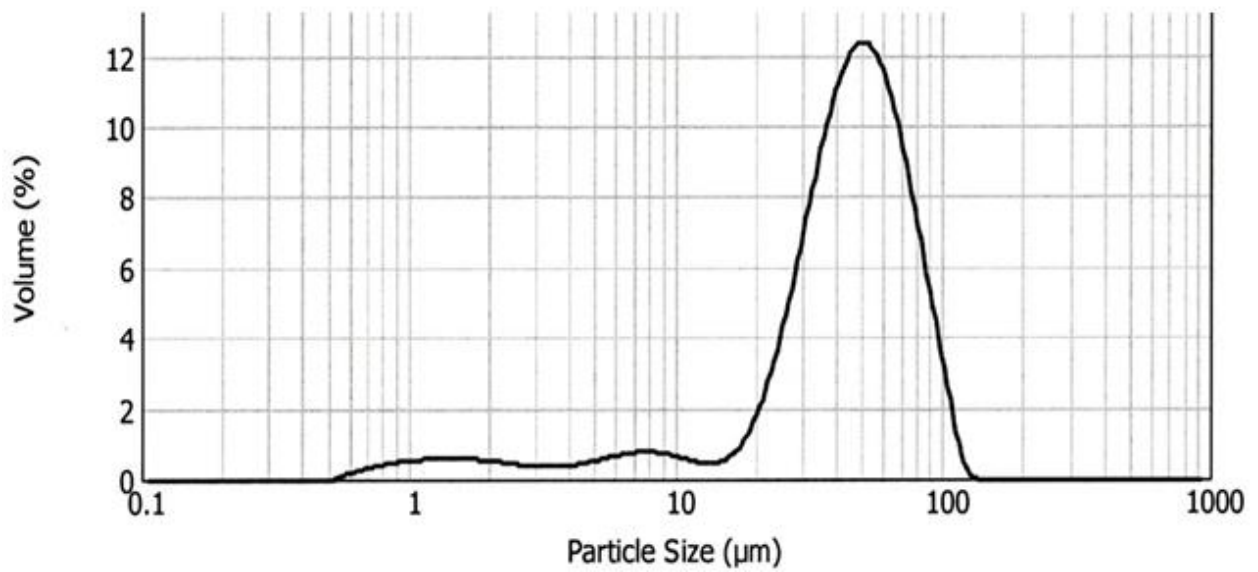
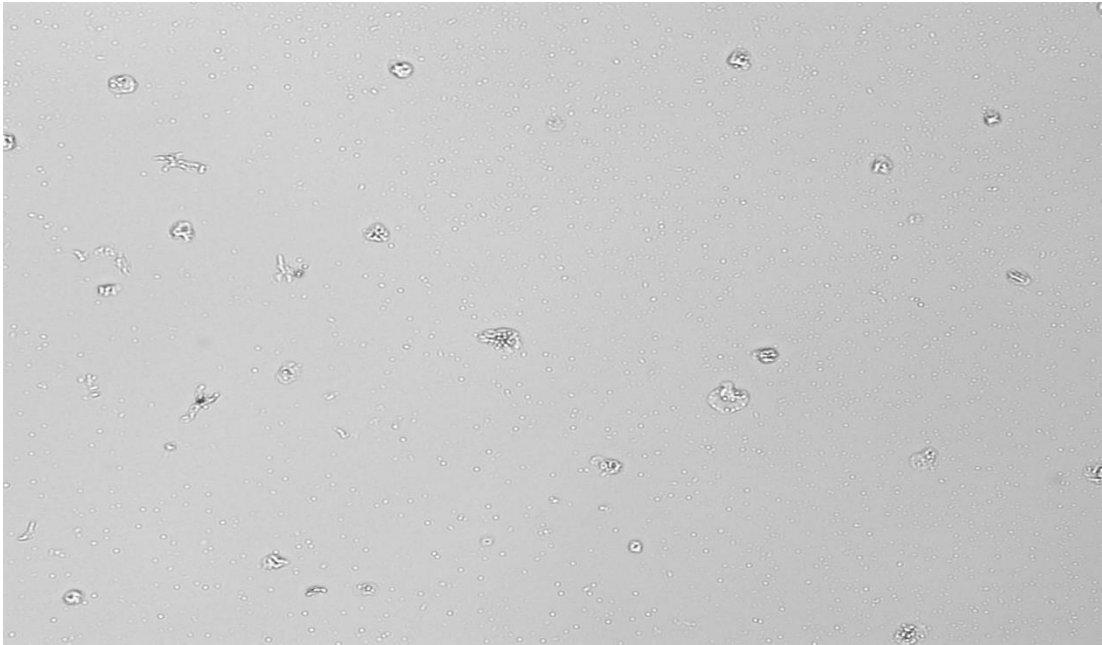


Fig. 28: Microscopic structure (a) and particle size distribution (b) of B100 W/EPS (10g/L) + diethyl ether 10%

(a) Microscopic structure



(b) Particle size distribution

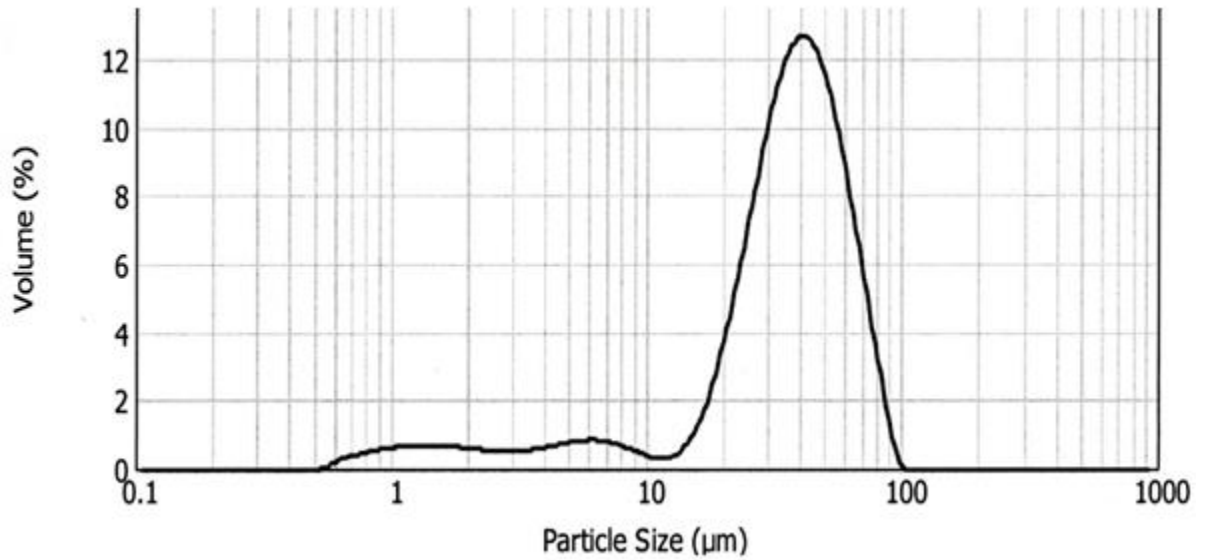
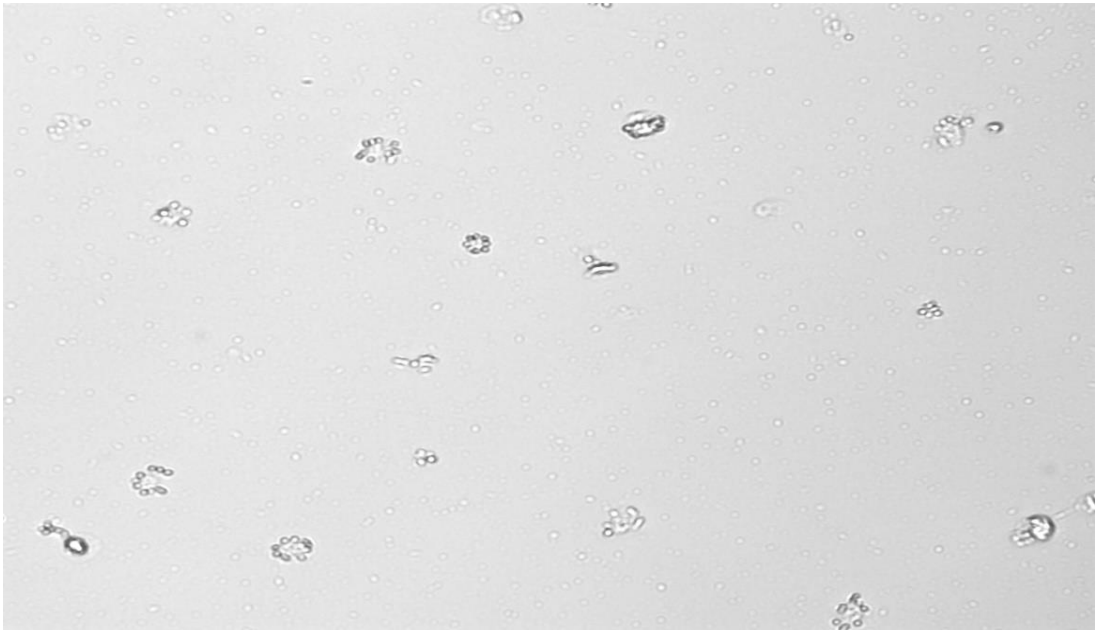


Fig. 29: Microscopic structure (a) and particle size distribution (b) of B100 W/ EPS (10g/L) + Tetrahydrofuran 10%

(a) Microscopic structure



(b) Particle size distribution

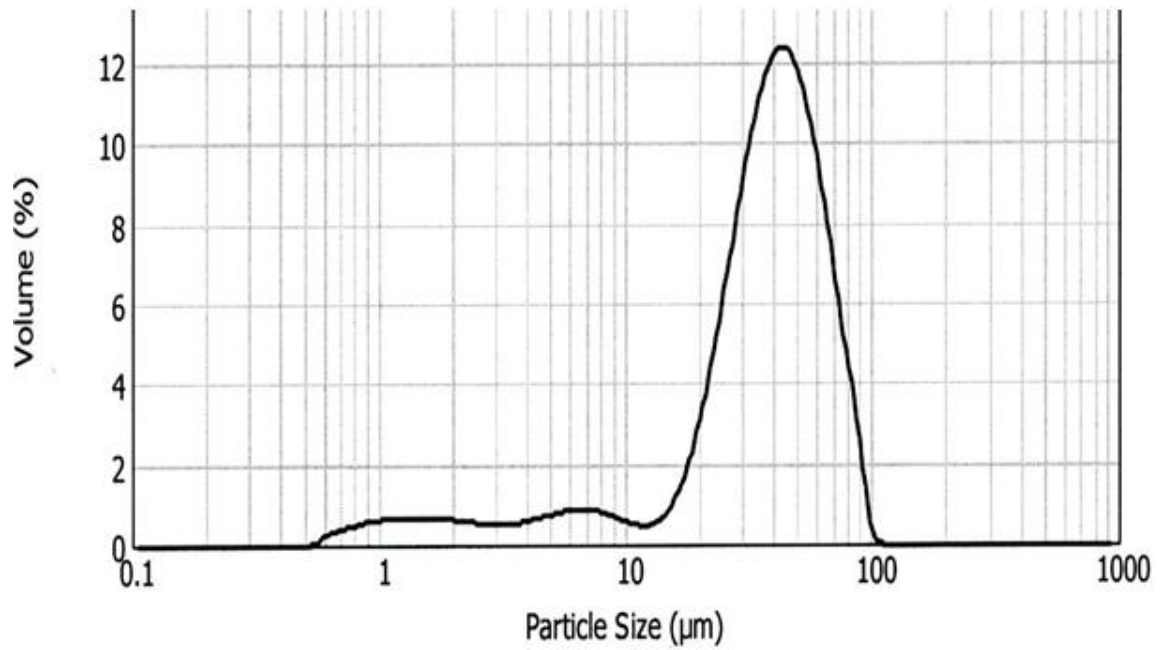
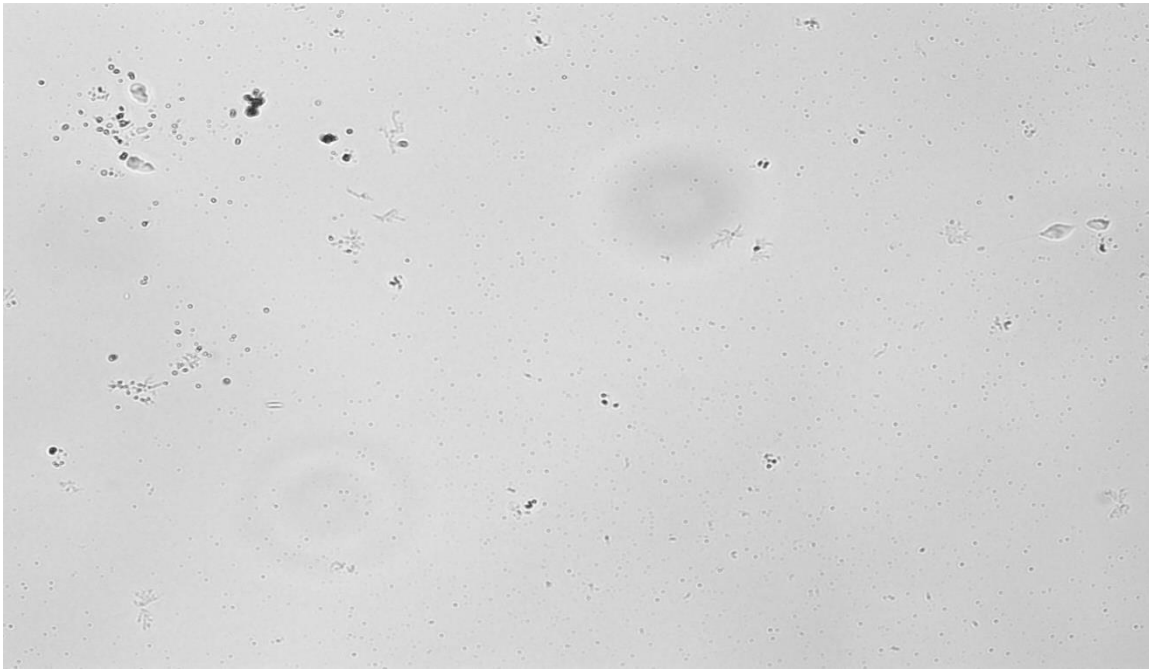


Fig. 30: Microscopic structure (a) and particle size distribution (b) of B100 W/ EPS (10g/L) + Acetone 10%

(a) Microscopic structure



(b) Particle size distribution

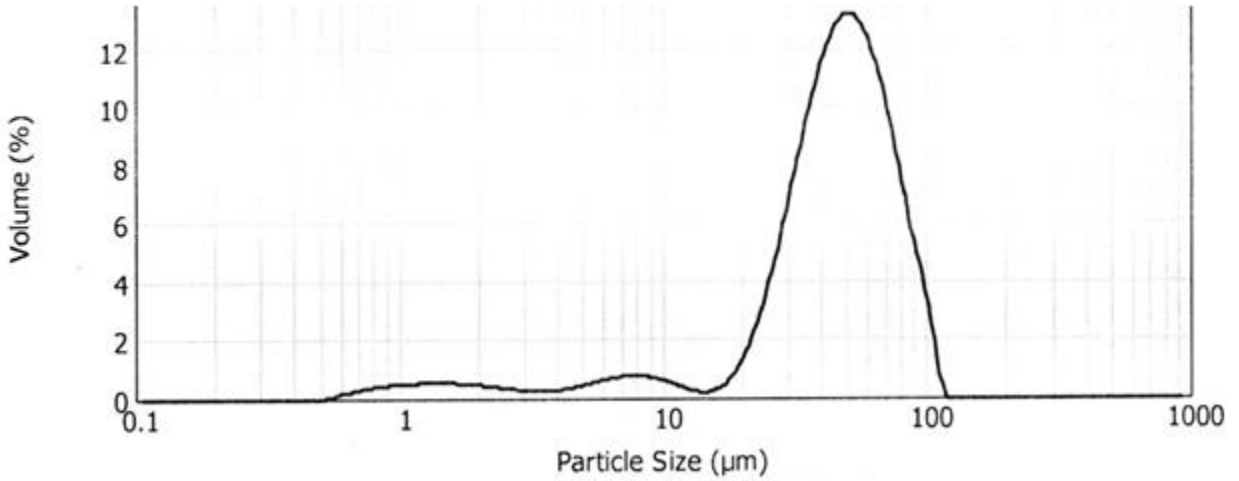


Fig. 31: Microscopic structure (a) and particle size distribution (b) of B100 W/ EPS (10g/L) + Xylene 10%

(a) Microscopic structure



(b) Particle size distribution

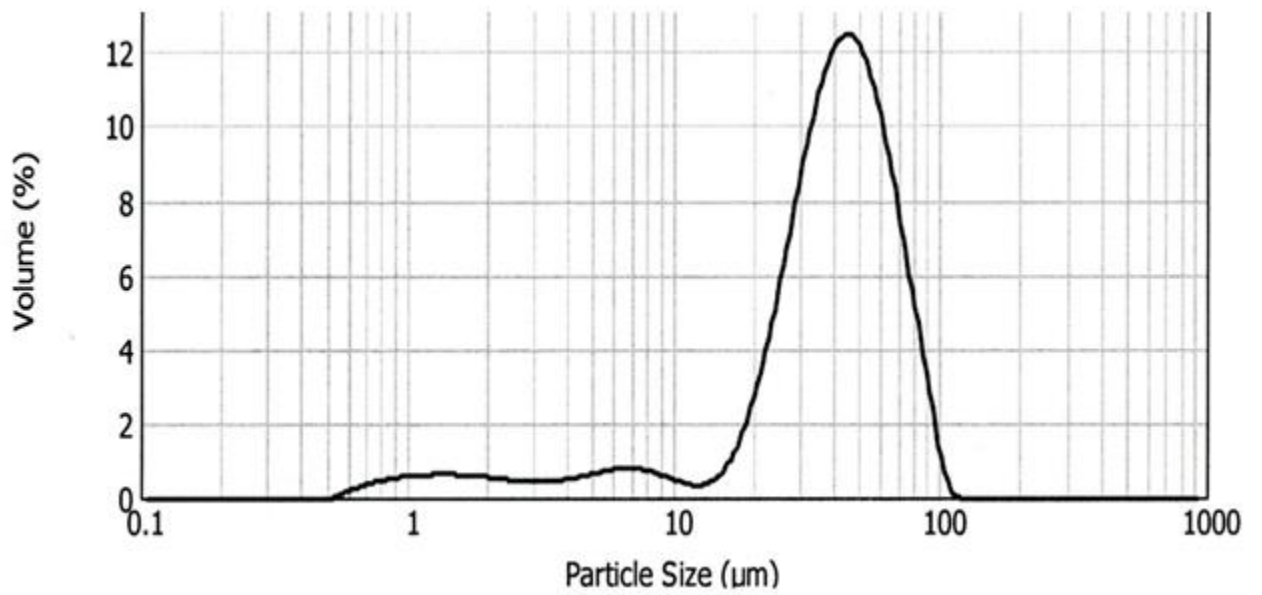


Fig. 32: Microscopic structure (a) and particle size distribution (b) of B100 W/ EPS (10g/L) + Toluene 10%

### **4.3. Light-duty Engine Performance**

#### **4.3.1 Brake thermal efficiency (BTE)**

Brake thermal efficiency can be defined as the measure of how efficiently a system can convert fuel into mechanical output. Fig. 33 shows the variations in BTE with EPS concentrations as well as the improvement with additives. At small EPS concentrations, a low heat release rate during the premixed combustion phase is the reason for lower thermal efficiency at low loads. BTE increased for loads of 2g/L and 6g/L than pure canola oil biodiesel. At low engine speed and low EPS concentrations, BTE increased by a low margin (i.e., 1.4%, 1.29% and 1.18% for low, medium and high load conditions, respectively). At 2100 rpm at a low EPS concentration (2g/L), BTE increased marginally by 4.2%, 2.62%, and 2% for low, medium and high loads, respectively. At high engine speed (3000 rpm), the increase in BTE at lower concentrations of EPS (2g/L) was marginal by 1.9, 1.8, and 1.6 for low, medium and high loads, respectively. At a EPS concentration of 6g/L, at lower engine speeds, BTE increased by 4%, 3%, and 2% for low, medium and high loads, respectively. BTE was maximum at EPS concentration of 6g/L. At 2100 rpm, BTE increased by 6%, 4%, and 3.56% at low, medium and high loads, respectively. At 3000 rpm, BTE increased by 5%, 4.3%, and 4.1% for low, medium and high speeds, respectively. The reason for these increases is the advancement in fuel injection timing caused by the addition of polystyrene. However, higher concentrations tended to reduce BTE, which may be due to poor heating value, poor spray atomization, and deteriorated combustion in highly viscous fuels. At 1000 rpm, BTE for EPS concentration increased thinly by 2.3%, 1.9%, and 1.2% at low, medium and high loads, respectively. At 2100 rpm, BTE dropped further by 4%, 3%, and 2% for low medium and high loads, respectively. At 3000 rpm, BTE narrowly increased to 2.8%, 2.6%, and 2.5% for low,

medium and high loads, respectively. High polystyrene concentrations resulted early injection timings that produced early ignition, which could cause the piston to work against the expanding gas, thus reducing BTE [60]. Adding additives to a high polystyrene concentration may worsen it by reducing the ignition delay further, thereby causing the same above-mentioned problem. Moreover, reduced viscosity of the blend with DEE may be attributed to fuel leakage through the injector nozzle, thereby reducing BTE. At 1000 rpm, with the addition of di ethyl ether, BTE increased by 9%, 8%, and 7% for low, medium and high speeds, respectively. At 2100 rpm, adding di ethyl ether to high concentration of EPS led to a steep increase in BTE (nearly 9%, 7% and 5% for low, medium and high loads compared to pure canola oil biodiesel). At higher engine speeds, the addition of di ethyl ether helped to maintain BTE at 9%, 6.6% and 5.3% for low, medium and high loads, respectively.

BTE improvements of DEE, XYL, TOL, and THF appeared quite similar at 11%, 10%, 10% and 8%, respectively. The high calorific value and volatility may be one of the reasons that promoted combustion efficiency. BTE improvements with the additives are summarized as: di ethyl ether better than xylene almost similar to tetrahydrofuran better than toluene better than acetone.

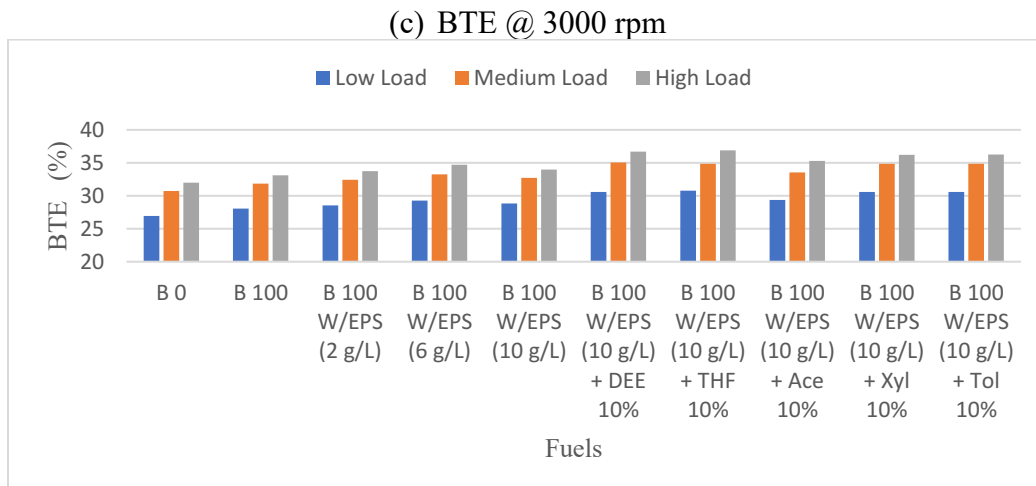
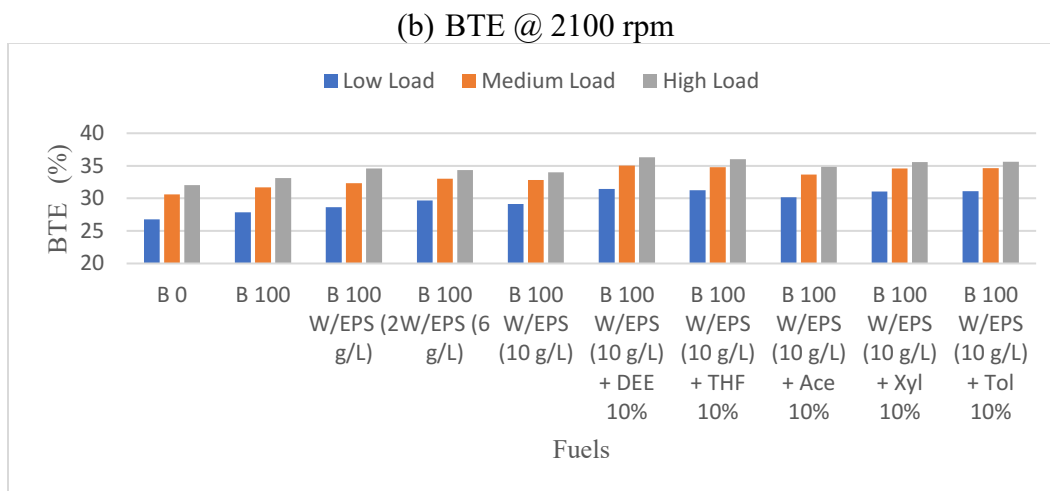
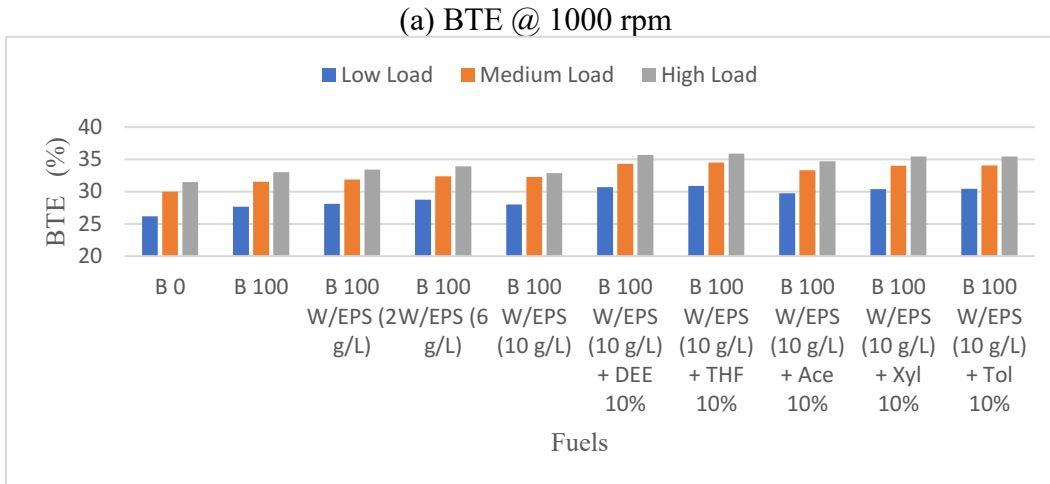


Fig. 33: Brake thermal efficiency (BTE) of fuels at different engine conditions (a) BTE @ 1000 rpm, (b) BTE @ 2100 rpm, (c) BTE @ 3000 rpm

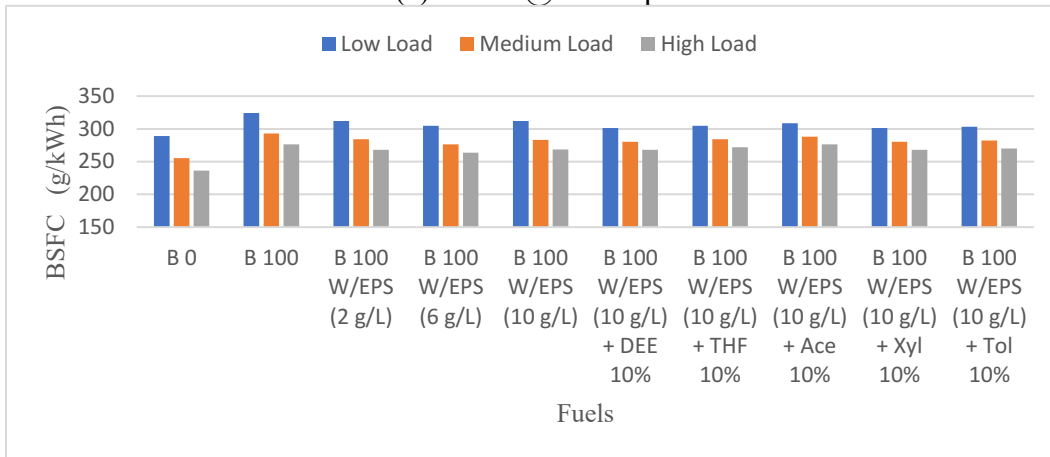
### 4.3.2 Brake-specific fuel consumption (BSFC)

Fig. 34 illustrates the variations on BSFC with EPS concentrations as well as the improvements with additives on EPS infused biodiesel. From the analysis, it was noted that the BSFC values decreased for 2g/L and 6g/L of EPS in canola biodiesel. At 1000 rpm, the BSFC values of 2g/L EPS concentration decreased by 3.7%, 3.1% and 3% compared to pure canola oil biodiesel. For EPS concentration of 2g/L, the BSFC values decreased compared to pure canola biodiesel at low, medium and high load by 7%, 5%, and 3%, respectively, at 2100 rpm. At 3100 rpm, the BSFC values of low EPS concentration (2g/L) reduced by 5%, 4.7%, and 4.3% at low, medium and high loads, respectively. For an EPS concentration of 6g/L, the BSFC values decreased compared to pure canola oil biodiesel for low, medium and high loads by 13%, 8%, and 6%, respectively, at 2100 rpm. At 1000 rpm, at a EPS concentration of 6g/L, the BSFC values decreased by 6.2%, 5.6%, and 4.6% for low, medium and high loads, respectively. At 3000 rpm, the BSFC values at an EPS concentration of 6g/L reduced by 10%, 9%, and 8.3% for low, medium and high loads, respectively, which was due to the increase in viscosity (the injection time advancement took place, thereby reducing the BSFC). Whereas high EPS concentrations (10g/L), led to high viscosity, which in turn led to poor spray atomization and combustion efficiency, thereby increasing BSFC. At 1000 rpm and high EPS concentration (10g/l), the BSFC decrease was slim by 3%, 2.8%, and 2.6 % at low, medium and high loads, respectively. EPS in high concentrations (i.e., 10g/L), at 2100 rpm, marginally decreased the BSFC compared to pure canola biodiesel by only 5%, 3.2%, and 2.8% for low, medium, high loads, respectively. At 3000 rpm, the reduction of BSFC for high polystyrene concentrations was as low as 2%, 1.6%, and nearly 1% for low, medium and high loads, respectively. High EPS concentrations could result in very advanced injection timings, which could in turn produce early ignition and reduced power output

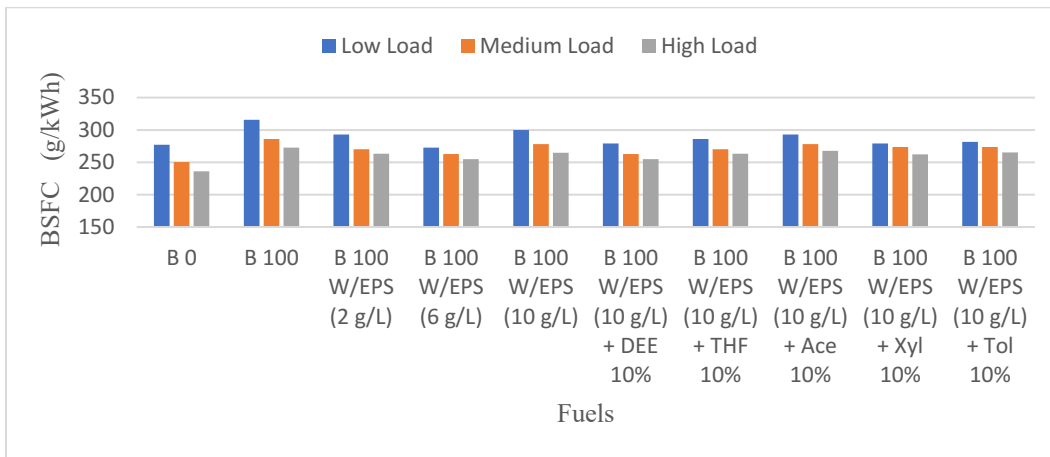
due to the high in-cylinder pressure during piston compression [60,32]. Increasing EPS concentrations beyond 10g/L would exceed the kinematic viscosity limit regulations by ASTM standards. Moreover, exceeded EPS concentration in biodiesel would have serious consequences, such as straining the fuel flow, or rendering the fuel pump incapable of injecting a normal amount of fuel, thus clogging the fuel lines. At high engine speeds, the difference between BSFC values of fuel blends became less due to the short combustion period, regardless of the increased fuel amount. This was due to the excess oxygen content, fast burning of molecules, and combustion temperature increase; these factors favoured better combustion. The high BSFC values of high EPS concentration in biodiesel (10g/L) over the entire load range was due to its high bulk modulus, lower heating value, and high viscosity. Higher bulk modulus will result in more discharge of fuel for the same displacement of the plunger in the injection pump. High EPS concentrations resulted in early injection timings, which could initiate early ignition, which in turn could have caused the piston to work against the expanding gas, thereby increasing BSFC [32,60,61]. The higher or improved heating value of EPS-infused biodiesel with additive (DEE) would lead to a decrease in BSFC values. At 1000 rpm and 10g/L, EPS concentration, the addition of di ethyl ether decreased BSFC values 7%, 4%, and 3% at low, medium and high load conditions, respectively. At 2100 rpm and the same EPS concentration, it reduced the BSFC by 11.6%, 8.1%, and 6.66% at low, medium and high loads, respectively. At 3000 rpm, the addition of di ethyl ether to high EPS concentrations (10g/L) reduced the BSFC values by 10%, 9.1%, and 4.3% at low, medium and high loads, respectively. Among the other additives, xylene and toluene reduced the BSFC values almost like to that of DEE (i.e., 9.8, 8, and 4.1%, respectively.) This may be due to nearly similar calorific value and other fuel properties. High volatility, high oxygen content, and the ability to reduce surface tension may also reduce BSFC values for additives used in EPS-infused biodiesel.

The BSFC values can be summarized as: di ethyl ether better than xylene better than toluene better than tetrahydrofuran better than acetone.

(a) BSFC @ 1000 rpm



(b) BSFC @ 2100 rpm



(c) BSFC @ 3000 rpm

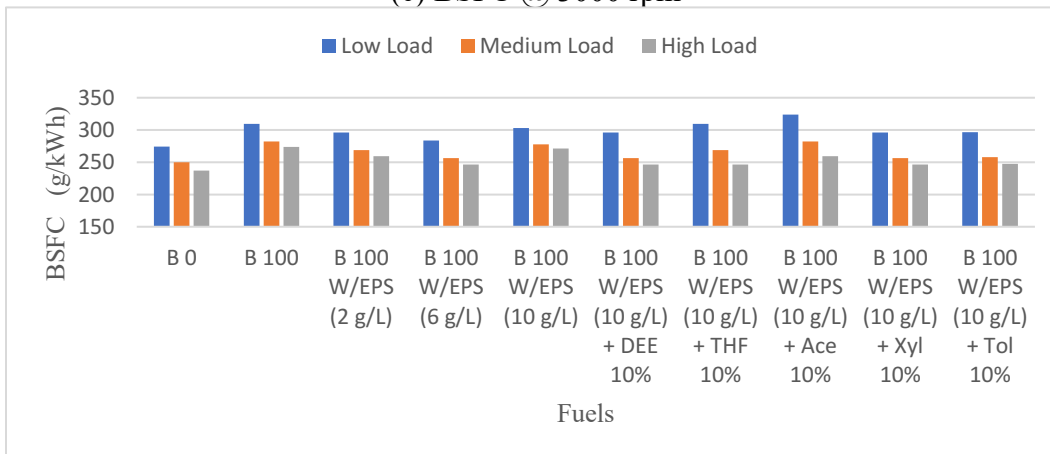


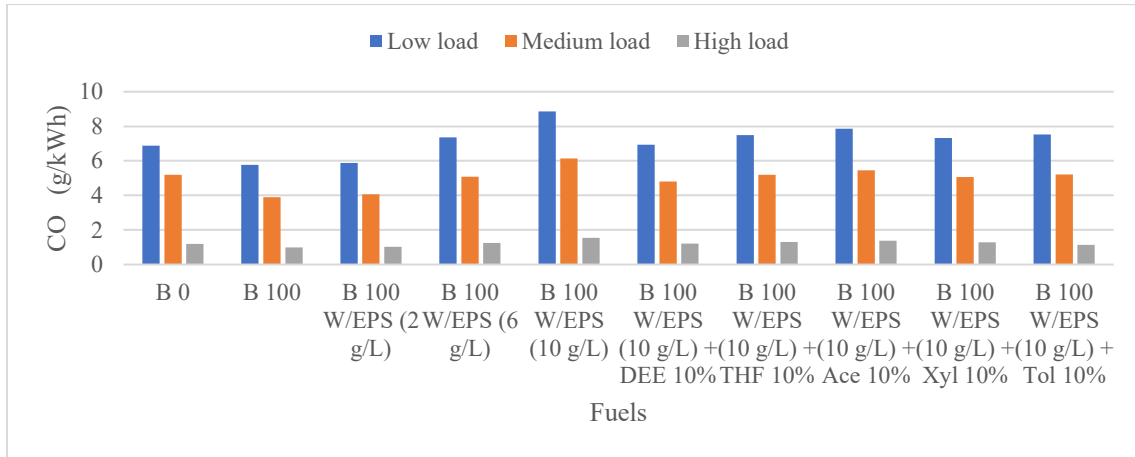
Fig. 34: Brake specific fuel consumption (BSFC) of fuels at different engine conditions (a) BSFC @ 1000 rpm, (b) BSFC @ 2100 rpm, (c) BSFC @ 3000 rpm

## **4.4 Light Duty Engine Emissions**

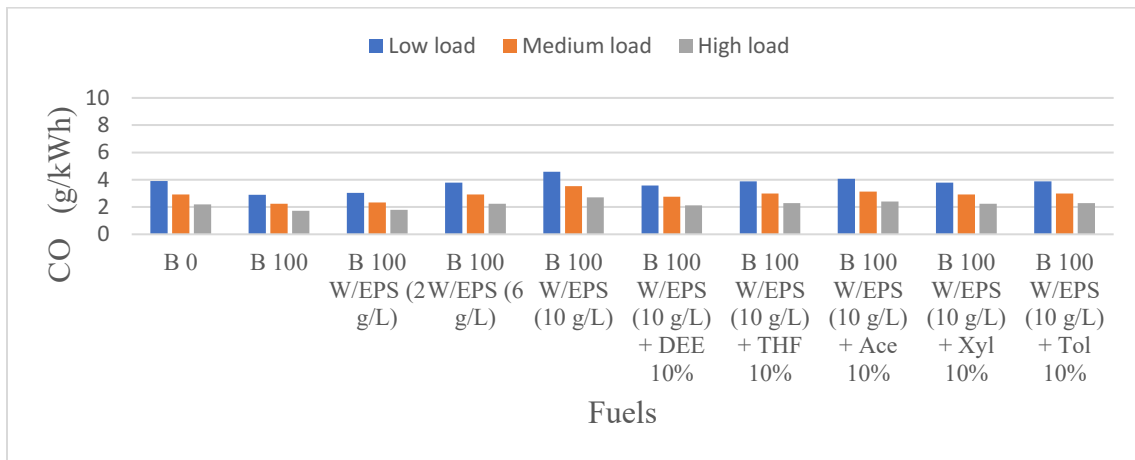
### **4.4.1 Carbon Monoxide (CO) Emissions**

Carbon monoxide is formed by the incomplete combustion, mainly due to lack of oxygen, poor air supply and air-fuel mixture distribution during the combustion process. Fig. 35 shows the variations in CO with different fuels. Carbon monoxide emissions increased aggressively with the EPS content. It increased by 5%, 20%, and 45% with EPS concentrations of 2g/L, 6g/L and 10g/L, at low, medium and high loads, respectively, at 2100 rpm. The presence of a complex polymer structure in the fuel deteriorated combustion. As the EPS concentration increased, it elevated the viscosity, thereby leading to poor spray atomization, thereby resulting in incomplete combustion. Heavier polymer molecules may lower flame temperatures due to incomplete combustion, and may contribute to CO emissions [60,32]. High volatility, high oxygen content, and high latent heat of vaporization reduced CO [73-75]. As EPS increased, injection advancement increased which led to elevated CO emissions [60]. Among the additives, di ethyl ether tended to reduce CO to 10%. The high CN, volatility, high oxygen content, and latent heat of vaporization may result in better fuel atomization, thereby leading to reduced CO emissions [46,16,75-77]. Among the other additives, xylene reduced by 12%, and tetrahydrofuran reduced by 13%, which tended to reduce CO emissions This may be due to their ability to dissolve EPS molecules in the fuels, combined with other factors such as oxygen content and high latent heat of vaporization. All the additives used in the study reduced the fuel's kinematic viscosity, which led to better fuel flow properties, in turn leading to proper atomization. The oxygen content in the additives tended to supply more oxygen, thereby avoiding oxygen-deficient combustion. The CO reduction capability of the additives are summarized as: Di ethyl ether better than xylene better than tetrahydrofuran better than toluene better than acetone.

(a) CO @ 1000 rpm



(b) CO @ 2100 rpm



(c) CO @ 3000 rpm

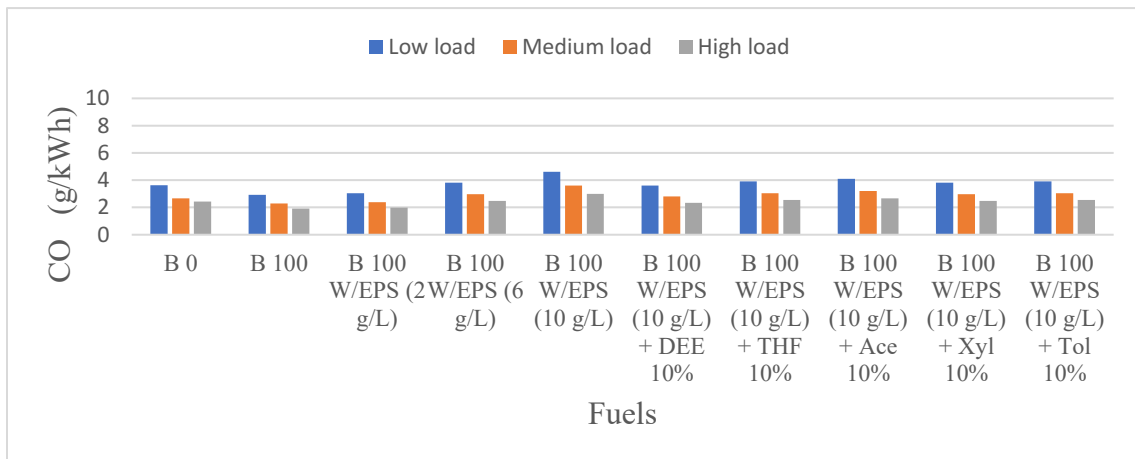


Fig. 35: Carbon Monoxide (CO) emissions of fuels at different engine conditions (a) CO @ 1000 rpm, (b) CO @ 2100 rpm, (c) CO @ 3000 rpm

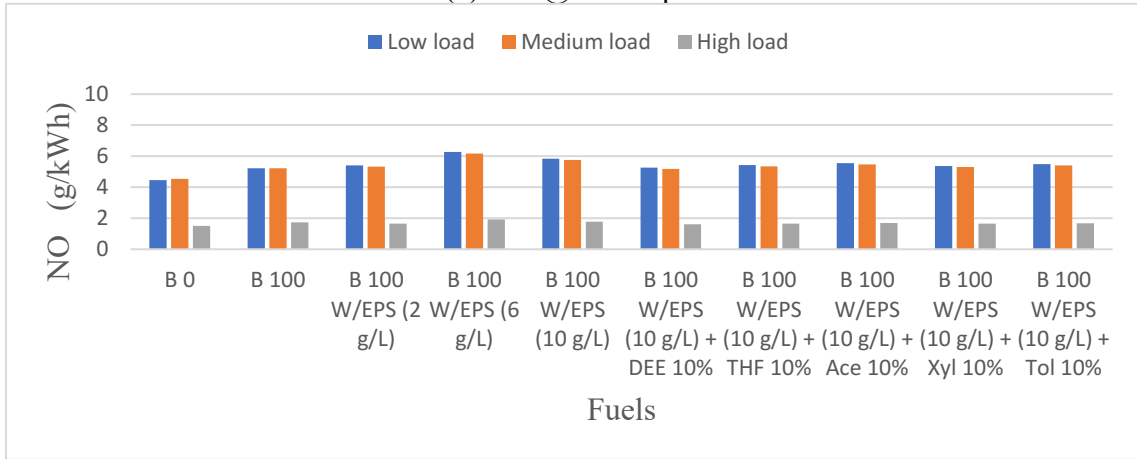
#### 4.4.2. NO<sub>x</sub> Emissions

Fig. 36 depicts the NO emissions of different fuels at different load conditions and engine speeds. Nitric oxide, once released into the atmosphere, was readily oxidized to nitrogen dioxide. NO is generally non-toxic in small quantities; in fact, it has a role in the human body as a regulator. Nitrogen oxides were formed when the engine combustion chamber temperature reached over 1300°C. Therefore, high combustion temperatures caused high nitric oxide emissions. NO emissions increased at low EPS concentrations (< 6 g/L). High EPS concentrations led to a decline in NO emissions. High polystyrene concentrations also reduced the combustion temperature, which also accounts for the reduction in NO emissions. Among the additives used in the study, diethyl ether showed reduced values for NO emissions. This might be due to the increase in cetane number in the blend that was caused by the diethyl ether (diethyl ether has a cetane number of > 125). High latent heat of vaporization also reduced the combustion temperature, which in turn reduced NO emissions.

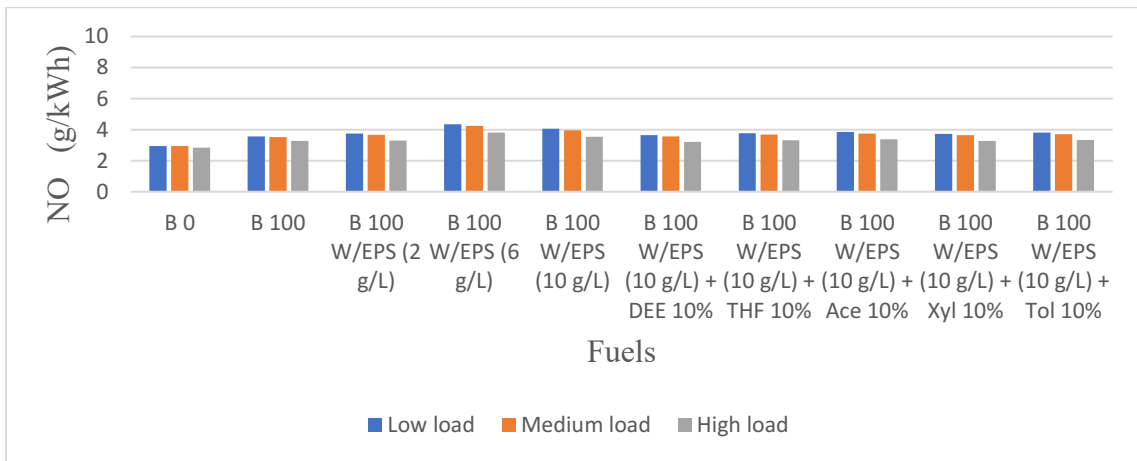
Fig. 37 depicts NO<sub>2</sub> emissions. NO<sub>2</sub> reacts with water to produce nitric acid, which causes irritation to the eyes and respiratory tract. NO<sub>2</sub> also followed a similar trend as NO emissions. It increased with low EPS concentration (< 6 g/L). High EPS concentrations led to decreased NO<sub>2</sub> emissions. High polystyrene concentrations in the fuel led to high viscosity, which caused poor spray atomization, leading to incomplete combustion and thereby reducing the combustion temperature, eventually leading to low NO<sub>2</sub> emissions. Among the additives, diethyl ether showed reduced values of NO<sub>2</sub> emissions, which might be due to the increase in cetane number, which led to cleaner combustion, thereby reducing NO<sub>2</sub> emissions. Other additives such as acetone, tetrahydrofuran, xylene and toluene also considerably reduced NO<sub>2</sub> emissions.

Oxides of nitrogen are formed due to the reaction between nitrogen and oxygen at elevated temperatures. NO is the major component. Since diesel engines combustion takes place in much higher temperature and pressure, it produces more NO<sub>x</sub> emissions. Fig. 38 illustrates NO<sub>x</sub> emissions data for different fuels. NO [fig.36] and NO<sub>2</sub> [Fig. 37] together contributes for NO<sub>x</sub> emissions. The experiment revealed that lower EPS concentrations (2g/L and 6g/L) led to steeper increases in NO<sub>x</sub> (i.e., from 2% for 2g/L, to 20% for 6g/L). This may be due to the advancement in injection timing, resulting in an increase in the premixed burned portion, which could have led to much higher NO<sub>x</sub> emissions [32,60]. At higher EPS concentrations (10g/L) NO<sub>x</sub> reduced to 13% on average. At high polystyrene concentrations, the increase was nominal due to poor spray atomization by high viscous fuel, therefore leading to less vigorous combustion accompanied by reduced combustion temperature due to incomplete combustion [60]. High cetane reduced NO<sub>x</sub> emissions [46,60]. Adding di ethyl ether as an additive reduced NO<sub>x</sub> to 9% on average, which can be associated with the high CN of DEE. Reduction in NO<sub>x</sub> for the DEE blend can be associated with high CN of di ethyl ether. An increase in CN can reduce NO<sub>x</sub> [46]. By adding DEE, heat release decreased at the stage of diffusion-controlled combustion, thereby leading to low NO<sub>x</sub> emissions [75-77]. Additionally, comparatively high latent heat of vaporization and high oxygen content of DEE added the gravity to resist NO<sub>x</sub> formation [16,75-77]. The EPS soluble additives (acetone, THF, xylene, and toluene) also possess high latent heat of vaporization, as discussed in the table of additives [Table 03]. Additives such as acetone, is well known for its ability to reduce NO<sub>x</sub> emissions when mixed in blends [58,72,73]. The reduced ignition delay due to the addition of additives might be a reason for the reduction of NO<sub>x</sub> emissions. The NO<sub>x</sub> reduction capability of additives is summarized as: di ethyl ether better than xylene better than tetrahydrofuran better than toluene better than acetone.

(a) NO @ 1000 rpm



(b) NO @ 2100 rpm



(c) NO @ 3000 rpm.

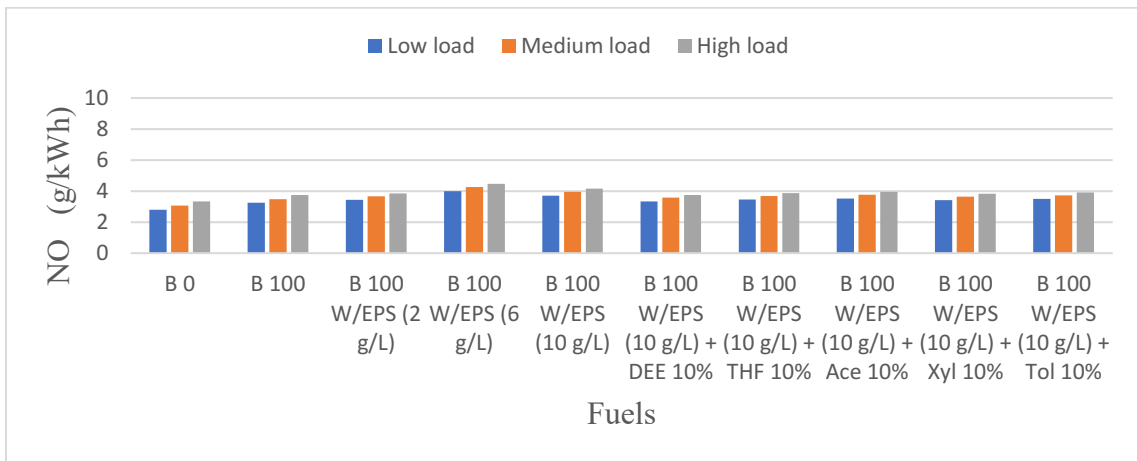
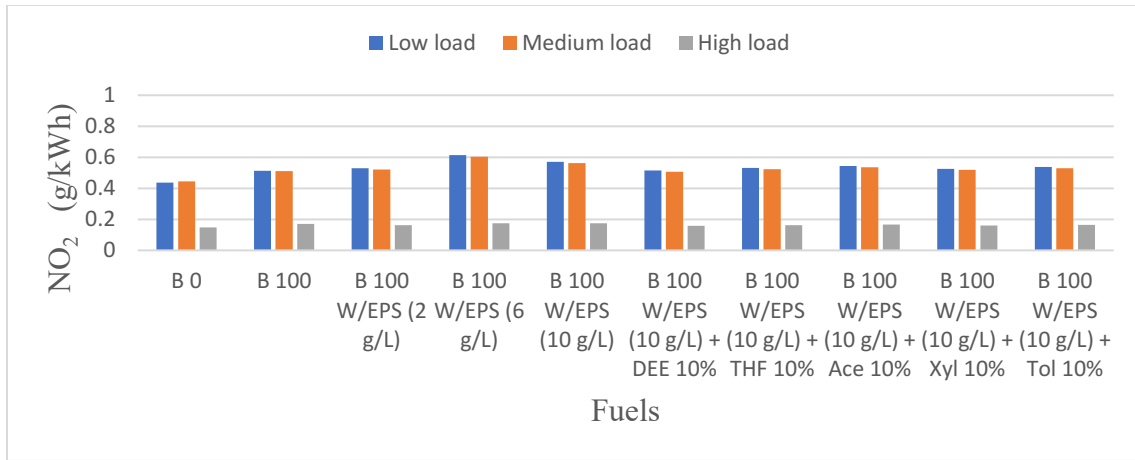
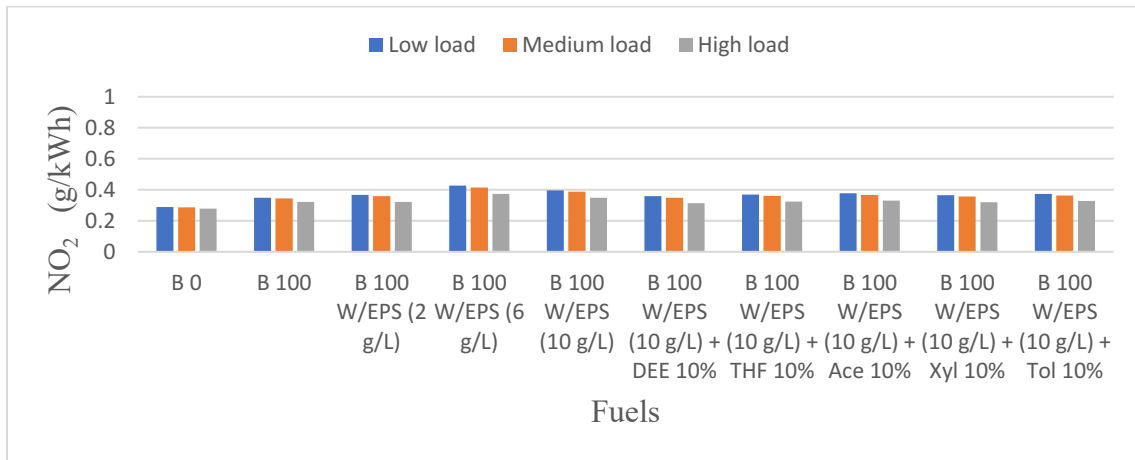


Fig. 36: NO emissions of fuels at different engine conditions (a) NO @ 1000 rpm, (b) NO @ 2100 rpm, (c) NO @ 3000 rpm

(a) NO<sub>2</sub>@ 1000 rpm



(b) NO<sub>2</sub>@ 2100 rpm



(c) NO<sub>2</sub>@ 3000 rpm

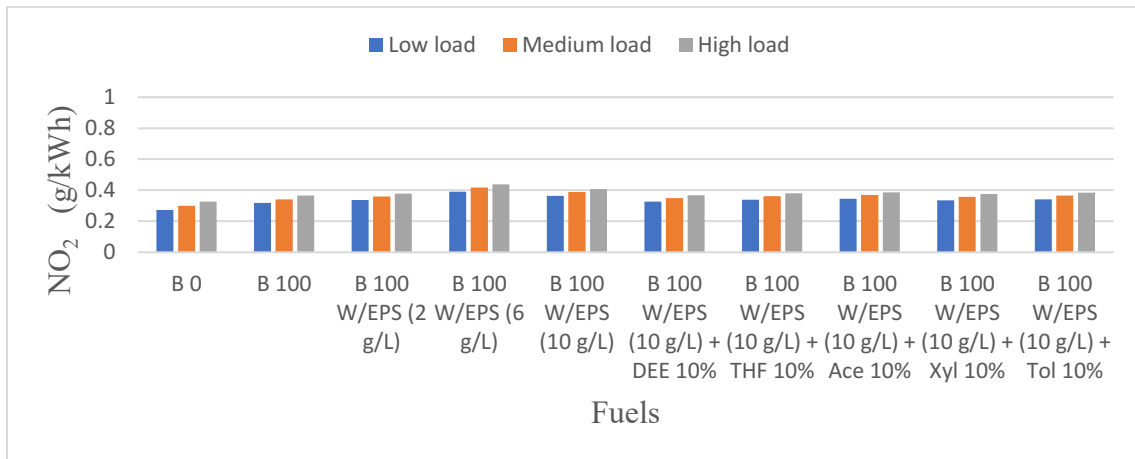
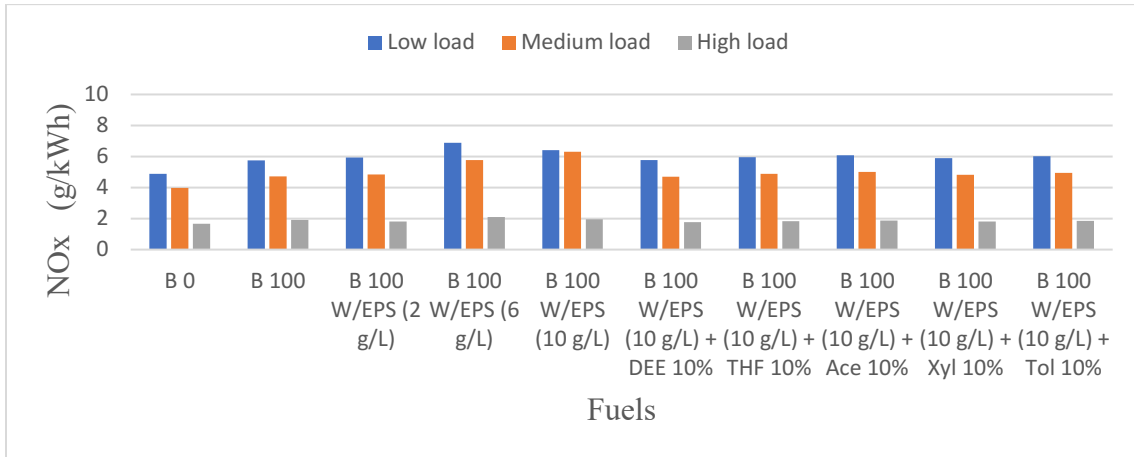
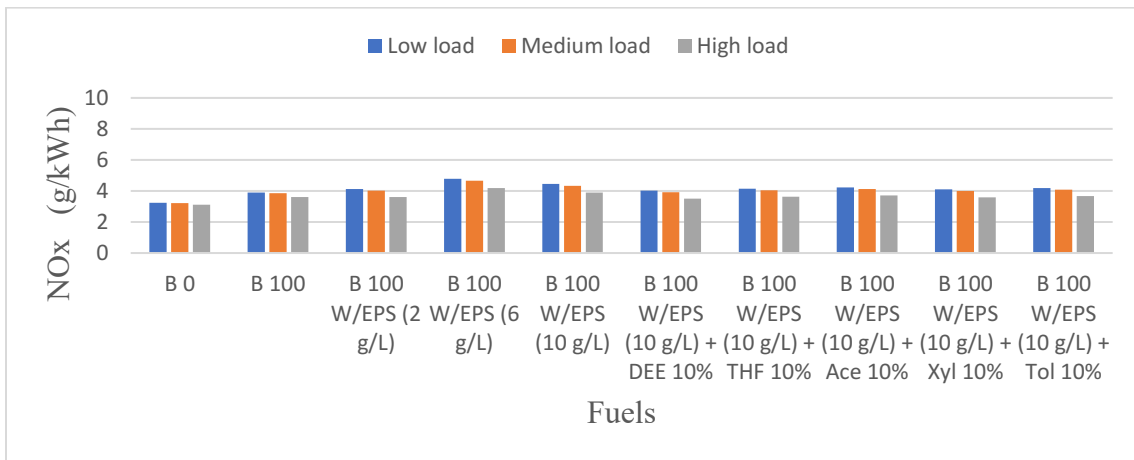


Fig. 37: NO<sub>2</sub> emissions of fuels at different engine conditions (a) NO<sub>2</sub> @ 1000 rpm, (b) NO<sub>2</sub> @ 2100 rpm, (c) NO<sub>2</sub> @ 3000 rpm

(a) NOx @ 1000 rpm



(b) NOx @ 2100 rpm



(c) NOx @ 3000 rpm

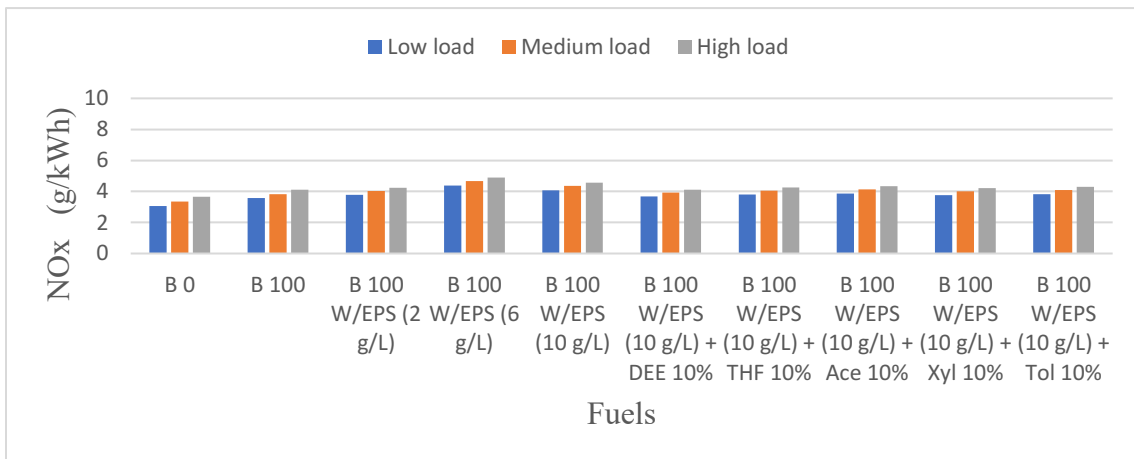


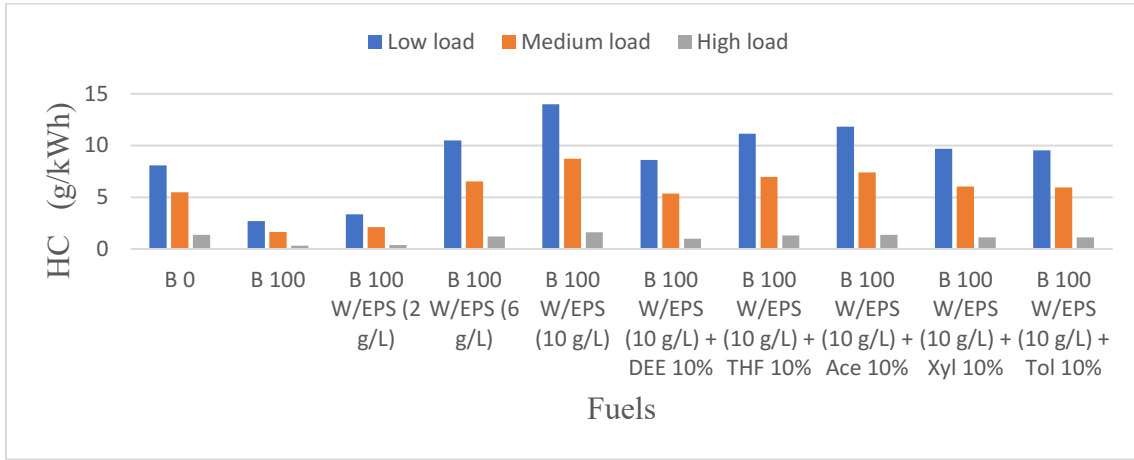
Fig. 38: Nitrogen oxides (NOx) emissions of fuels at different engine conditions (a) NOx @ 1000 rpm, (b) NOx @ 2100 rpm, (c) NOx @ 3000 rpm

#### 4.4.3 HC Emissions

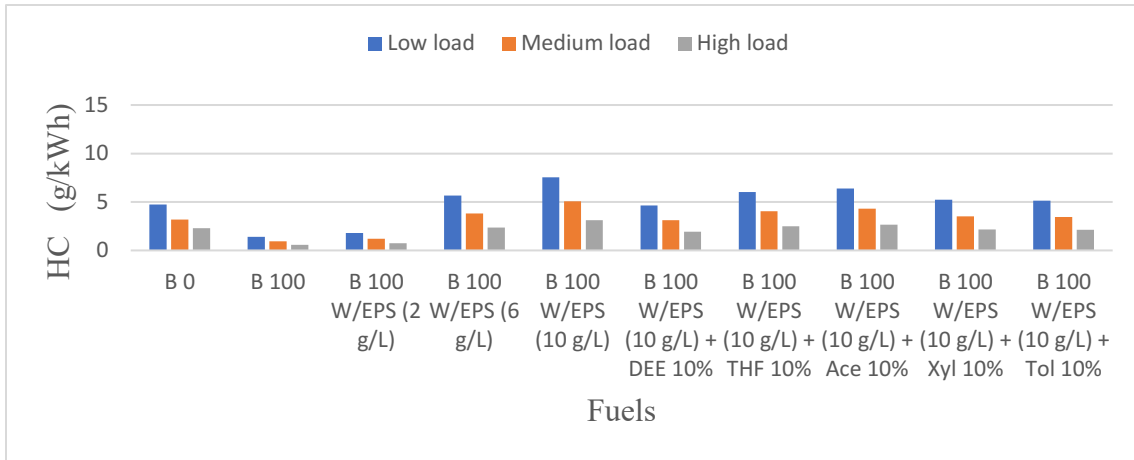
The experiment illustrates that HC increased with the increase in EPS concentrations. HC increased by 10%, 40%, and 70% for 2g/L, 6g/L, and 10g/L at low medium and high speeds, respectively, at 2100 rpm. HC emissions depend on air-fuel mixing and fuel atomization [11,83]. Fig. 39 illustrates the variation of HC emissions with various EPS concentrations as well as with additives. The experiment dictates that unburnt hydrocarbon increased with load and EPS concentration. Combustion of high polystyrene blends might require more time to complete, which resulted in higher HC emissions [32,59]. The increase in unburnt hydrocarbon was due to poor fuel spray atomization, which resulted in incomplete combustion caused by increased fuel viscosity. As the polystyrene content increased, the viscosity increased, which created injection advancement, thereby increasing the premixed burn portion [32,60,59]. The lower CN due to the addition of polymer to biodiesel may have increased the HC emissions, as CN is closely-related to the combustion quality [46]. DEE blends have low charge temperature, which decreased the combustion chamber temperature due to their high latent heat of vaporization [75-77]. Additionally, some DEE additive mixed with air during fuel injection and accumulated in the ring space between the piston and cylinder, resulting in high HC emissions since the combustion flame could not effectively reach those spaces (Crevice HC) [16,75-77]. DEE increased the CN and reduced the kinematic viscosity of the EPS-infused canola biodiesel fuel, which increased the spray atomization and fuel flow properties, thereby improving combustion quality. The EPS soluble additives (acetone, THF, xylene, and toluene) helped to dissolve the complex EPS molecules left in the EPS-infused biodiesel, and reduced the kinematic viscosity of the blend, thereby enhancing fuel atomization, reducing kinematic viscosity, and enhancing flow properties. Xylene and toluene reduced hydrocarbon emissions due to their ability to dissolve EPS molecules,

as well as their higher calorific value [80-83]. The HC reduction capability of can be summarized as: di ethyl ether better than xylene better than toluene tetrahydrofuran better than acetone.

(a) HC @ 1000 rpm



(b) HC @ 2100 rpm



(c) HC @ 3000 rpm

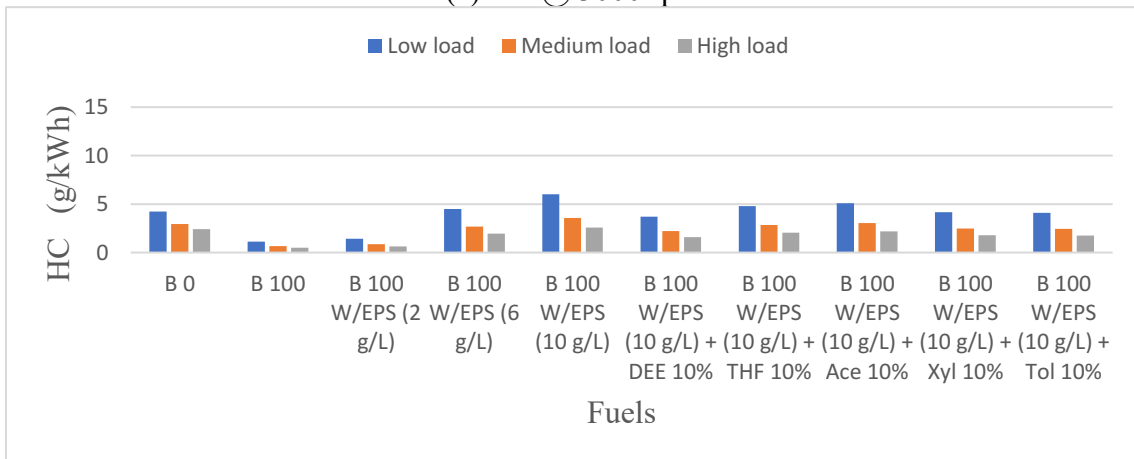


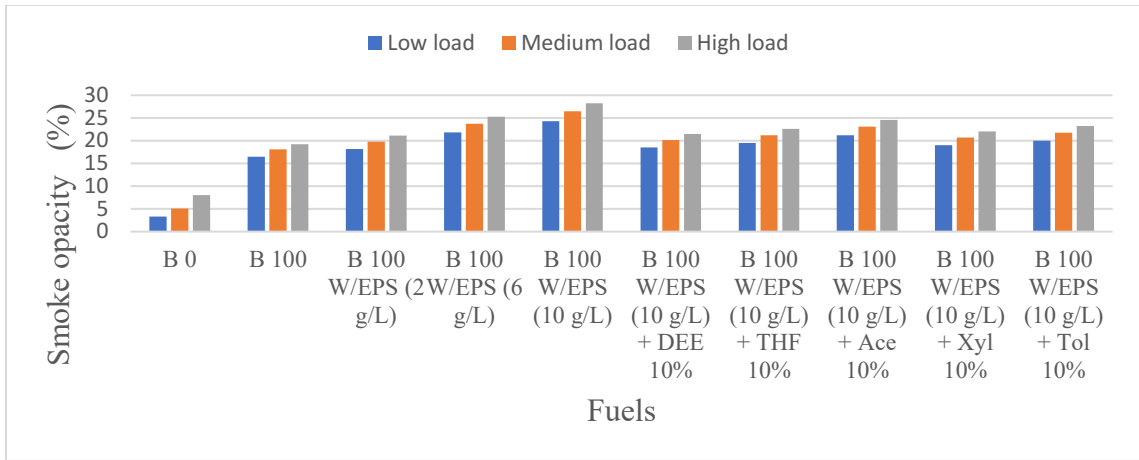
Fig. 39: Hydrocarbon (HC) emissions of fuels at different engine conditions (a) HC @ 1000 rpm, (b) HC @ 2100 rpm, (c) HC @ 3000 rpm

#### 4.4.4 Smoke Opacity

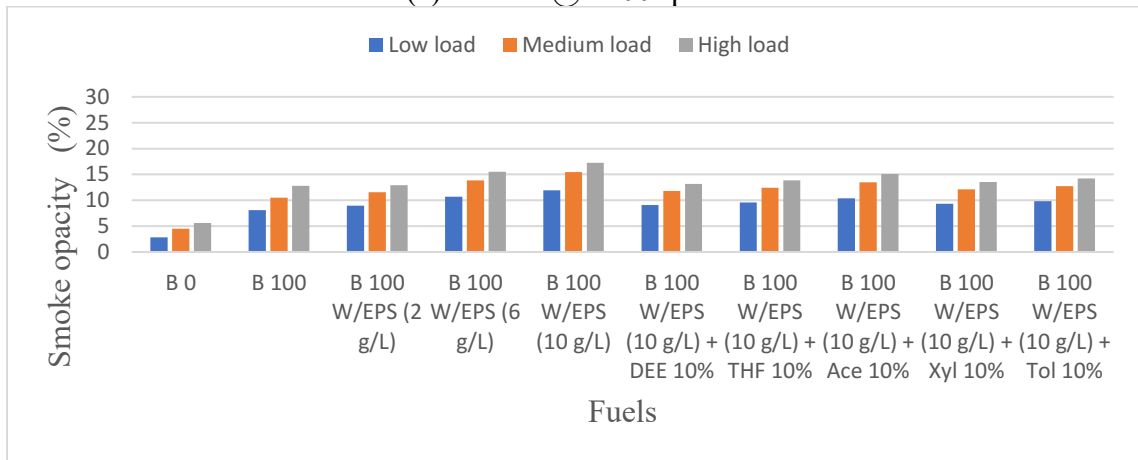
The smoke in IC engine combustion is formed due to incomplete combustion. The following graphs [Fig. 40] represent the smoke emissions at various engine and load conditions. With the increase in EPS concentrations, 2g/L, 6g/L, 10g/L, smoke emissions increased approximately 22%, 40% and 55%, respectively, which illustrates that smoke emissions are proportional to EPS concentration. As EPS concentration increased, the injection time advancement took place, leading to a more premixed combustion phase over and above the presence of heavy polymer molecules in the fuel, which in turn led to poor atomization and further deteriorating combustion [60,32,74]. With the high polystyrene (EPS 10 g/L), the smoke emission was excessive, which may be due to the high viscous fuel, which reduced the fuel flow (did not favor vigorous combustion). The addition of polystyrene reduced the CN due to the bulk structure of the EPS, which is a factor that deteriorates combustion quality. Di ethyl ether was selected as an additive to overcome this drawback. The experiment dictated the expected outcome, as adding a cetane improver (DEE) increased the combustion quality, thereby reducing smoke. The use of additives helped to reduce the smoke, with lowest one being di ethyl ether, which reduced smoke emissions to almost 9% on average at low, medium and high load conditions at 2100 rpm. The high CN and calorific value led to cleaner combustion [16,46,75-77]. Volatility of the additives helped, as it promoted better fuel mixing, as well as improved fuel atomization and vaporization [2,11,83]. The EPS soluble additives (acetone, THF, xylene, and toluene) helped dissolve the bulky EPS molecules left in the EPS-infused biodiesel. It also reduced the kinematic viscosity of the blend, resulting in the additives enhancing cleaner combustion in many ways (i.e., by enhancing dissolution of EPS in biodiesel, increasing the calorific value, and promoting fuel atomization by reducing viscosity). EPS soluble additives (acetone, THF, xylene, toluene) reduced to an average

of 11% to 14% on low, medium and high loads (11% for xylene and 14% for acetone). The smoke reduction capabilities can be summarized as: diethyl ether better than xylene better than tetrahydrofuran better than toluene better than acetone.

(a) Smoke @ 1000 rpm



(a) Smoke @ 2100 rpm



(c) Smoke @ 3000 rpm

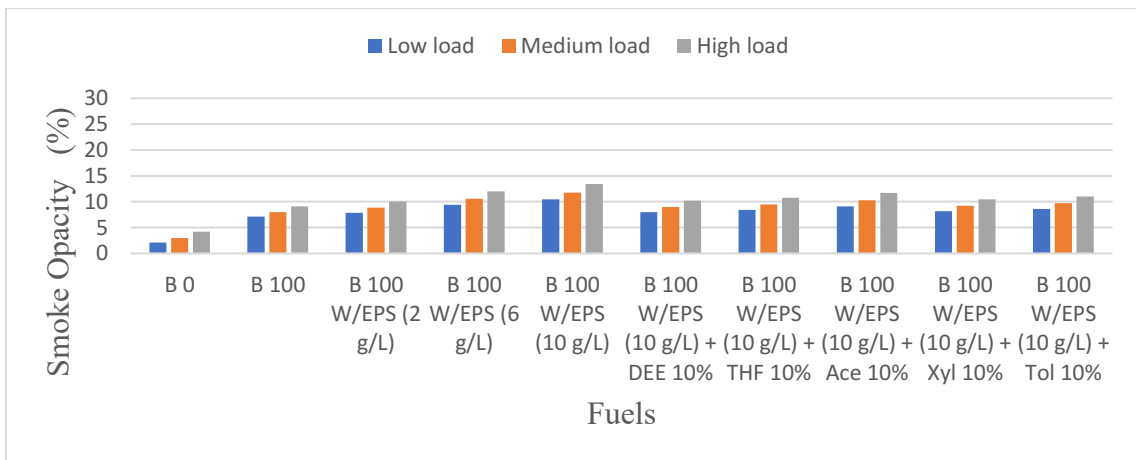
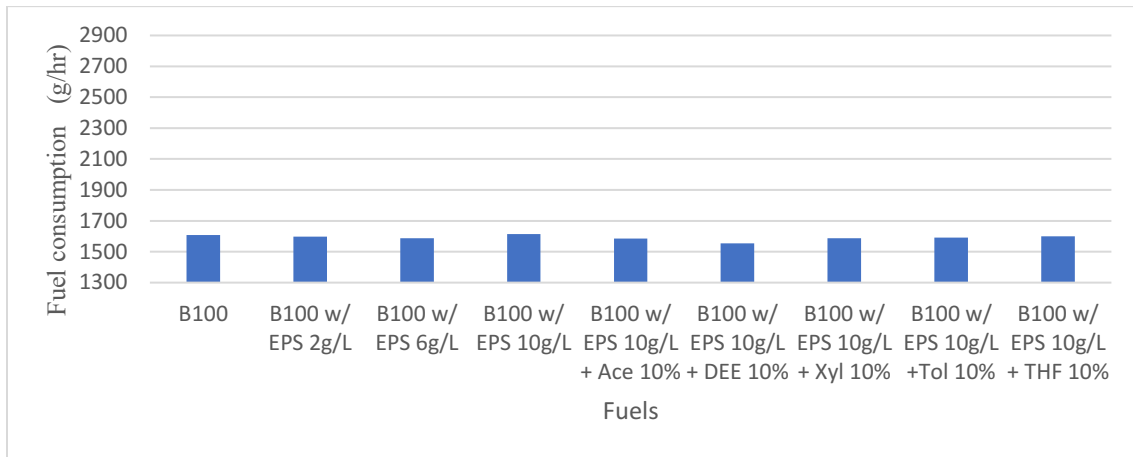


Fig. 40: Smoke opacity emissions of fuels at different engine conditions (a) Smoke @1000 rpm (b) Smoke @ 2100 rpm (c) Smoke @ 3000 rpm

#### 4.5 Heavy-duty Engine Performance

Fig. 41 shows the fuel consumption of fuels at various EPS concentrations, and the improvement with the additives. For the performance point of view, an idling test was performed on the Cummins heavy-duty engine at two engine speeds (700 rpm and 1700 rpm). The fuel consumption for 30 minutes was recorded and, as expected, decreased with an increase in EPS concentration up to 6 g/L, after which point fuel consumption increased abruptly. The initial decrease may have been due to advancement of the fuel injection timing caused by EPS [60]. At high EPS concentrations, the rapid increase in fuel consumption may have been due to very advanced injection timing, which resulted in early ignition, and could have caused the piston to work against the expanding gas. Adding additives reduced the fuel consumption; the best being diethyl ether, which may be a result of its increased cetane number and reduced kinematic viscosity, along with fuel properties such as volatility, heating value, etc. [75-77]. The EPS-soluble additives (acetone, THF, xylene, and toluene) may have helped dissolve the bulky EPS molecules that remained in the EPS-infused biodiesel, thereby avoiding early ignition. Fuel consumption was reduced at levels up to 6 g/L of EPS concentration, and then increased with EPS concentrations beyond 6 g/L. High EPS concentrations led to increased fuel consumption, which might be due to very advanced injection timings, which could in turn produce early ignition and reduced power output. Among the additives used in the EPS-infused canola biodiesel, diethyl reduced the fuel consumption, which might be due to the increased heating value of the blend, as well as other properties such as high volatility, high oxygen content, and its ability to reduce surface tension. The increased oxygen content may have resulted in faster burning of the molecules, resulting in increased burning temperature and complete combustion of the fuel molecules. The capability of the additives to reduce the fuel consumption values can be summarized as follows: Diethyl ether is better than xylene, toluene, tetrahydrofuran, and acetone.

(a) 700 rpm



(b) 1700 rpm

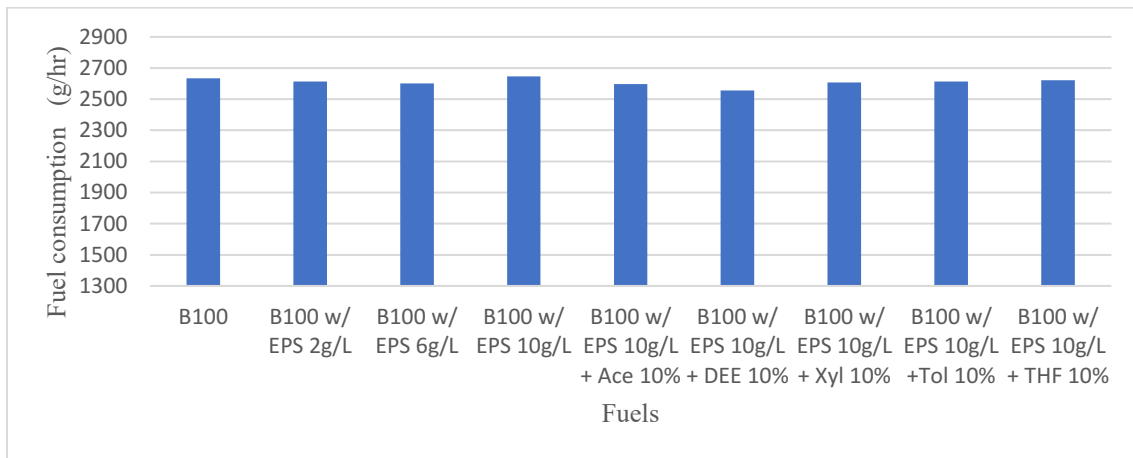


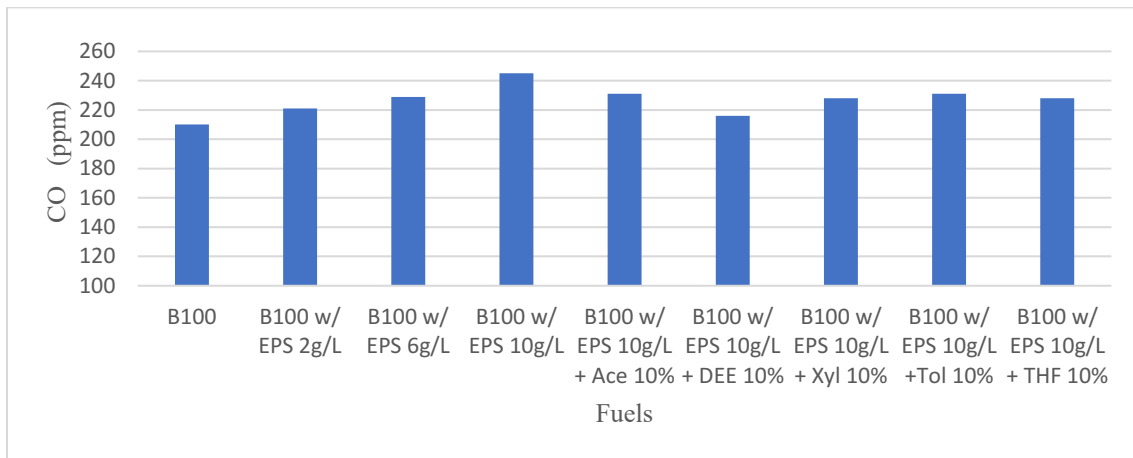
Fig. 41: Fuel consumption of fuels at (a) 700 rpm and (b) 1700 rpm

#### 4.6 Heavy-duty Engine Emissions

The emissions of the heavy-duty engine followed a similar trend to those of the light-duty engine, which is explained in detail in the above sections. Similar emissions trends resulted at both speeds (700 rpm and 1700 rpm). The products of incomplete combustion (CO and HC) increased with EPS concentrations, and the additives reduced them. The best results were obtained from diethyl ether, which improved to a great extent, possibly because of the increase in cetane number from the addition of DEE [46, 16].

Fig. 42 shows CO emissions at various EPS concentrations, and the lower emissions when adding the additives. CO emissions increased with an increase in EPS concentrations. The highest value for CO emissions corresponds to the highest EPS concentrations (10 g/L). As EPS concentration increased, injection advancement took place, resulting in high CO emissions. The additives with the most noticeable improvements of CO emissions was diethyl ether, which reduced kinematic viscosity; the improvements may be due in part to an increased cetane number. Xylene was the second-best additive option.

(a) 700 rpm



(b) 1700 rpm

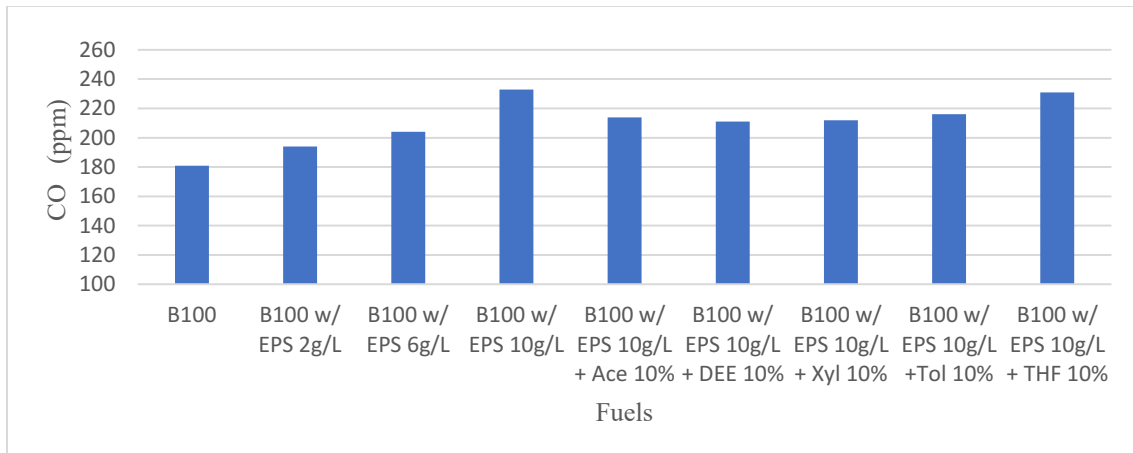
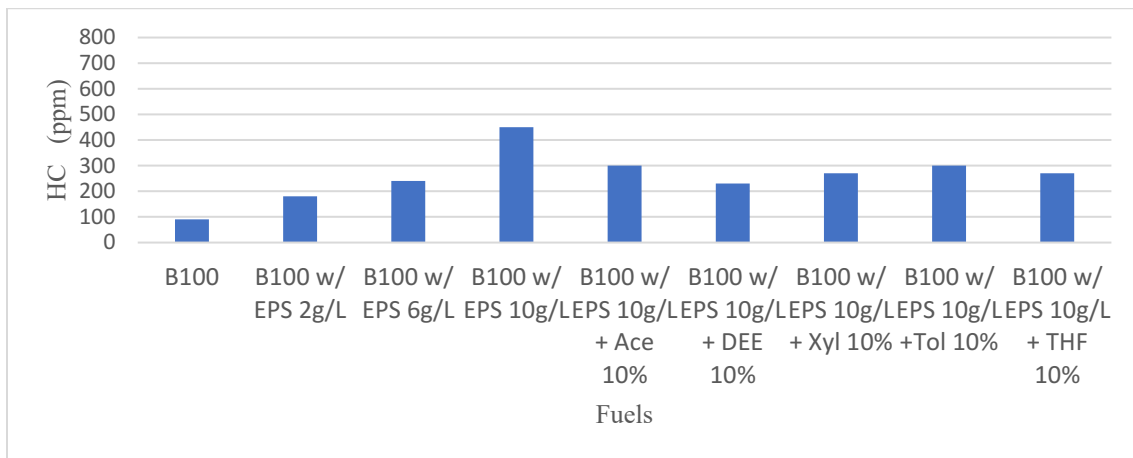


Fig. 42: Carbon monoxide emissions of fuels at (a) 700 rpm and (b) 1700 rpm.

Fig. 43 shows the HC emissions at various EPS concentrations, and the improvements in emissions when adding the additives. HC emissions increased with an increase in EPS concentrations, which could be caused by a high EPS concentration, which might require more time to complete, thus resulting in high HC emissions. The increase in unburnt hydrocarbon was due to poor spray atomization, which resulted in incomplete combustion due to higher fuel viscosity. Among the additives, diethyl ether emitted the lowest HC. This could possibly be because of the increase in cetane number resulting in cleaner combustion, as well as other fuel properties such as oxygen content, high volatility, heating value, etc.

(a) 700 rpm



(b) 1700 rpm

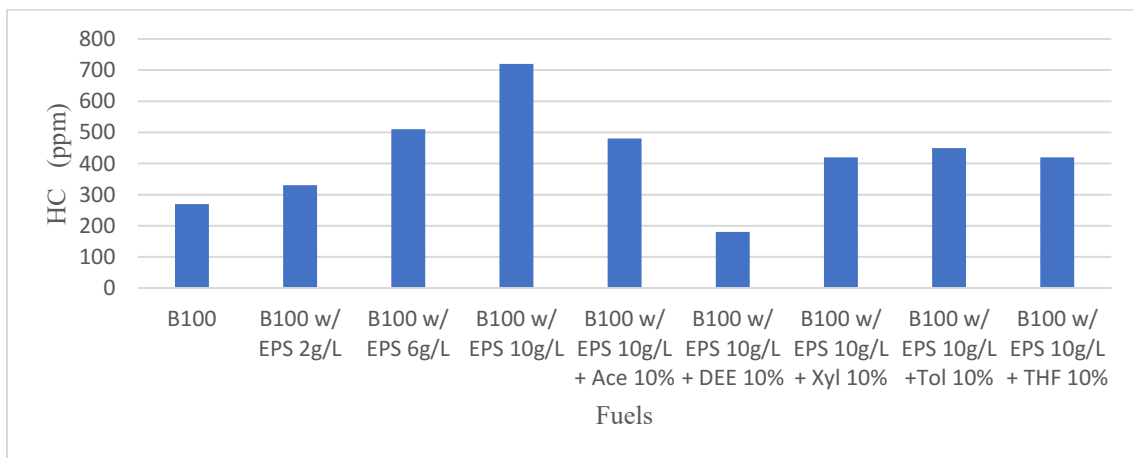
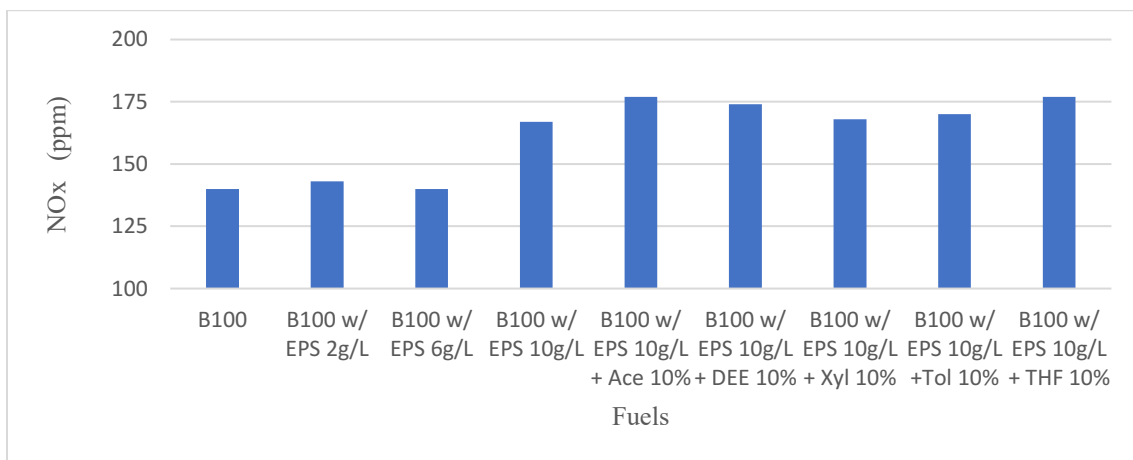


Fig. 43: Hydrocarbon emissions of fuels at (a) 700 rpm and (b) 1700 rpm.

Fig. 44 shows NO<sub>x</sub> emissions at various EPS concentrations, and the improvements in emissions after adding the additives. Low EPS concentrations tended to increase NO<sub>x</sub> emissions, whereas high EPS concentrations were included to reduce NO<sub>x</sub> (possibly due to the reduction in combustion chamber temperature). At high EPS concentrations, poor spray atomization of high viscous fuel took place, leading to less vigorous combustion accompanied by reduced combustion temperature, thereby reducing NO<sub>x</sub> emissions. Among the additives, diethyl ether showed the most improvement in NO<sub>x</sub> emissions, which may have been caused by the increase in cetane number, resulting in cleaner combustion [46] (a) 700 rpm



(b) 1700 rpm

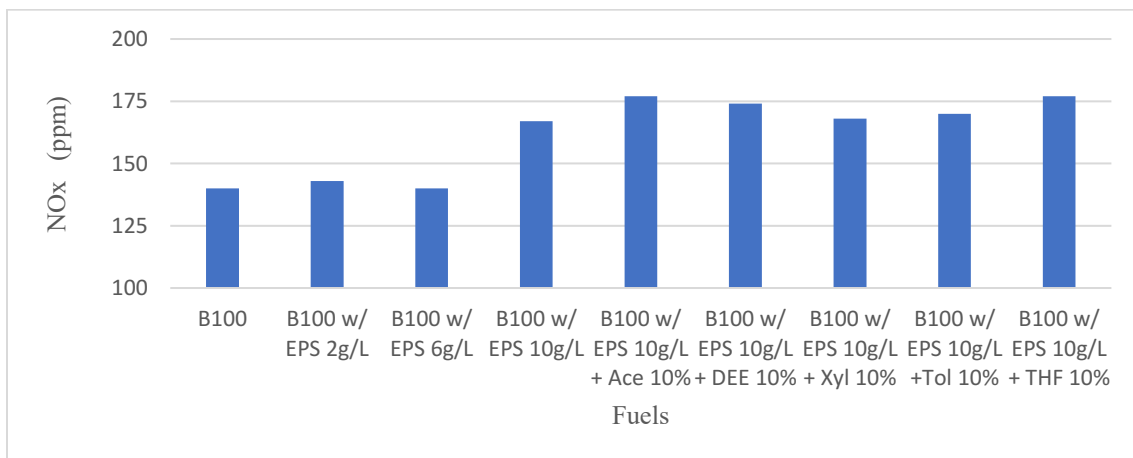


Fig. 44: NO<sub>x</sub> emissions of fuels at (a) 700 rpm and (b) 1700 rpm.

## 5. Conclusions

In light of the experimental investigation conducted to examine performance and emissions of EPS in canola oil with and without additives, the following conclusions were drawn.

1. EPS-infused biodiesel can be used in remote locations where recycling is not an option, and used mainly in stationary power generators or CI engines.
2. Dissolving EPS in biodiesel increases viscosity, whereas density remains almost constant; however, it reduces heating value.
3. The maximum EPS concentration that can be dissolved in canola oil biodiesel within the limits ASTM D445 standards is 10 g/L at 25°C.
4. Dissolving EPS beyond the recommended (10 g/L) limit may be detrimental to the engine, as the highly viscous fuel could clog the fuel lines; engine performance also plummets, and emissions increase.
5. The recommended amount of EPS concentration in canola oil biodiesel for optimum performance and emissions is 6 g/L. Engine power increases with polystyrene concentration up to 6 g/L., but then decreases considerably.
6. Products of incomplete combustion such as CO and HC increase with increases in EPS concentration. The presence of a large number of polymer molecules in the fuel mixture results in poor atomization, resulting in incomplete combustion, thereby triggering an increase of CO & HC.
7. NO<sub>x</sub> is high at a low concentration of EPS, which may be due to ignition time advancement.
8. High EPS concentration results in low NO<sub>x</sub> emissions due to the presence of a large number of polymer molecules in the fuel mixture, resulting in poor atomization.

9. Among the additives used in the study, DEE demonstrated overall low emission and better performance due to its high combustion efficiency, resulting from its elevated CN and heating value.
10. Use of volatile and organic EPS soluble additives (acetone, tetrahydrofuran, xylene and toluene) improved performance and emissions of EPS-infused biodiesel. The use of additives can improve the concentrations of EPS in canola biodiesel.
11. The addition of additives to EPS-infused biodiesel helps in the reduction of drawbacks of EPS in biodiesel by reducing viscosity and increasing combustion efficiency.
12. Adding EPS soluble additives (acetone, xylene, toluene, THF) helps in dissolution of EPS on top of improving combustion by their own properties such as high volatility, calorific value etc.
13. EPS infused canola biodiesel exhibits inferior cold flow properties and the solubility of EPS reduces dramatically below 15°C. The solubility of EPS increases with temperature but on cooling down the formation of gel like structure (reformation of polymer) takes place. This may be detrimental for the engine as it may lead to clogging of fuel lines and injectors.

## **6. Future Work**

The scope of research in the direction of EPS in biodiesel is very vast. Even though this study reached its objective. Some more work can be done in this same direction. Some suggestions are

1. More additives for reducing drawbacks of EPS in biodiesel.
2. Methods to avoid polymer reformation on cooling the EPS dissolved in biodiesel at elevated temperatures.
3. Improve EPS concentration in biodiesel.
4. Dissolving EPS on solvents (e.g. tetrahydrofuran) and blending with petroleum diesel.

## References

- [1.] Saravanan, S., Kumar, B. R., Varadharajan, A., Rana, D., & Sethuramasamyraja, B. (2017). Optimization of DI diesel engine parameters fueled with iso-butanol/diesel blends—response surface methodology approach. *Fuel*, *203*, 658-670.
- [2.] Agarwal, A. K. (2007). Biofuels (alcohols and biodiesel) applications as fuels for internal combustion engines. *Progress in energy and combustion science*, *33*(3), 233-271.
- [3.] Wang, J., Cao, L., & Han, S. (2014). Effect of polymeric cold flow improvers on flow properties of biodiesel from waste cooking oil. *Fuel*, *117*, 876-881.
- [4.] Roy, M. M., Wang, W., & Bujold, J. (2013). Biodiesel production and comparison of emissions of a DI diesel engine fueled by biodiesel–diesel and canola oil–diesel blends at high idling operations. *Applied Energy*, *106*, 198-208.
- [5.] Atabani, A. E., Silitonga, A. S., Badruddin, I. A., Mahlia, T. M. I., Masjuki, H. H., & Mekhilef, S. (2012). A comprehensive review on biodiesel as an alternative energy resource and its characteristics. *Renewable and sustainable energy reviews*, *16*(4), 2070-2093.
- [6.] Khalife, E., Tabatabaei, M., Demirbas, A., & Aghbashlo, M. (2017). Impacts of additives on performance and emission characteristics of diesel engines during steady state operation. *Progress in Energy and Combustion Science*, *59*, 32-78.
- [7.] Sheehan, J., Camobreco, V., Duffield, J., Graboski, M., & Shapouri, H. (1998). Life Cycle Inventory of Biodiesel and Petroleum Diesel for Use in an Urban Bus, NREL/SR-580-24089 UC, (available from [www.nrel.gov](http://www.nrel.gov)).
- [8.] Benson, R. S., & Whitehouse, N. D. (2013). *Internal combustion engines: a detailed introduction to the thermodynamics of spark and compression ignition engines, their design and development* (Vol. 1). Elsevier.
- [9.] Nordin, N. (2005). Introduction to combustion in diesel engines. *PowerPoint PDF File*. Scania.

- [10.] Zhang, W., Chen, Z., Li, W., Shu, G., Xu, B., & Shen, Y. (2013). Influence of EGR and oxygen-enriched air on diesel engine NO–Smoke emission and combustion characteristic. *Applied energy*, 107, 304-314.
- [11.] Yao, M., Chen, Z., Zheng, Z., Zhang, B., & Xing, Y. (2005). *Effect of EGR on HCCI combustion fuelled with dimethyl ether (DME) and methanol dual-fuels* (No. 2005-01-3730). SAE Technical Paper.
- [12.] National Research Council. (2015). *Cost, effectiveness, and deployment of fuel economy technologies for light-duty vehicles*. National Academies Press.
- [13.] Westerholm, R., & Egeback, K. E. (1994). Exhaust emissions from light-and heavy-duty vehicles: chemical composition, impact of exhaust after treatment, and fuel parameters. *Environmental health perspectives*, 102(Suppl 4), 13.
- [14.] Sahoo, B. B., Sahoo, N., & Saha, U. K. (2009). Effect of engine parameters and type of gaseous fuel on the performance of dual-fuel gas diesel engines—A critical review. *Renewable and Sustainable Energy Reviews*, 13(6-7), 1151-1184.
- [15.] Yamamoto, M., Yoneya, S., Matsuguchi, T., & Kumagai, Y. (2002). *Optimization of Heavy Duty Diesel Engine Parameters for Low Exhaust Emissions Using the Design of Experiments*(No. 2002-01-1148). SAE Technical Paper.
- [16.] Clenci, A., Niculescu, R., Danlos, A., Iorga-Simăn, V., & Trică, A. (2016). Impact of biodiesel blends and Di-Ethyl-Ether on the cold starting performance of a compression ignition engine. *Energies*, 9(4), 284.
- [17.] Heywood, J. B. (1988). *Internal combustion engine fundamentals*.
- [18.] Agency, E. P. (2002). A comprehensive analysis of biodiesel impacts on exhaust emissions. *Draft Technical Report EPA420-P-02-001*.
- [19.] Sorda, G., Banse, M., & Kemfert, C. (2010). An overview of biofuel policies across the world. *Energy policy*, 38(11), 6977-6988.
- [20.] Sorda, G., Banse, M., & Kemfert, C. (2010). An overview of biofuel policies across the

world. *Energy policy*, 38(11), 6977-6988.

[21.] Lapuerta, M., Armas, O., & Rodriguez-Fernandez, J. (2008). Effect of biodiesel fuels on diesel engine emissions. *Progress in energy and combustion science*, 34(2), 198-223.

[22.] Ristovski, Z. D., Miljevic, B., Surawski, N. C., Morawska, L., Fong, K. M., Goh, F., & Yang, I. A. (2012). Respiratory health effects of diesel particulate matter. *Respirology*, 17(2), 201-212.

[23.] Bhaskar, K., Nagarajan, G., & Sampath, S. (2013). Optimization of FOME (fish oil methyl esters) blend and EGR (exhaust gas recirculation) for simultaneous control of NO<sub>x</sub> and particulate matter emissions in diesel engines. *Energy*, 62, 224-234.

[24.] Rajasekar, E., Murugesan, A., Subramanian, R., & Nedunchezian, N. (2010). Review of NO<sub>x</sub> reduction technologies in CI engines fuelled with oxygenated biomass fuels. *Renewable and Sustainable Energy Reviews*, 14(7), 2113-2121.

[25.] Pradeep, V., and R. P. Sharma. "Use of HOT EGR for NO<sub>x</sub> control in a compression ignition engine fuelled with bio-diesel from Jatropha oil." *Renewable Energy* 32, no. 7 (2007): 1136-1154.

[26.] Tsolakis, A., & Megaritis, A. (2004). Exhaust gas assisted reforming of rapeseed methyl ester for reduced exhaust emissions of CI engines. *Biomass and Bioenergy*, 27(5), 493-505.

[27.] Agarwal, A. K., Gupta, T., Shukla, P. C., & Dhar, A. (2015). Particulate emissions from biodiesel fuelled CI engines. *Energy Conversion and Management*, 94, 311-330.

[28.] Sundus, F., Fazal, M. A., & Masjuki, H. H. (2017). Tribology with biodiesel: A study on enhancing biodiesel stability and its fuel properties. *Renewable and Sustainable Energy Reviews*, 70, 399-412.

[29.] Knothe, G., & Steidley, K. R. (2005). Kinematic viscosity of biodiesel fuel components and related compounds. Influence of compound structure and comparison to petrodiesel fuel components. *Fuel*, 84(9), 1059-1065.

- [30.] Shahir, V. K., Jawahar, C. P., & Suresh, P. R. (2015). Comparative study of diesel and biodiesel on CI engine with emphasis to emissions—a review. *Renewable and Sustainable Energy Reviews*, 45, 686-697.
- [31.] Gonzalez, Y. M., De Caro, P., Thiebaud-Roux, S., & Lacaze-Dufaure, C. (2007). Fatty acid methyl esters as biosolvents of epoxy resins: a physicochemical study. *Journal of solution chemistry*, 36(4), 437-446.
- [32.] Mohammadi, P., Tabatabaei, M., Nikbakht, A. M., Farhadi, K., & Castaldi, M. J. (2013). Simultaneous energy recovery from waste polymers in biodiesel and improving fuel properties. *Waste and Biomass Valorization*, 4(1), 105-116.
- [33.] Can, Ö., Öztürk, E., & Yücesu, H. S. (2017). Combustion and exhaust emissions of canola biodiesel blends in a single cylinder DI diesel engine. *Renewable Energy*, 109, 73-82.7.
- [34.] Dyer, J. A., Vergé, X. P. C., Desjardins, R. L., Worth, D. E., & McConkey, B. G. (2010). The impact of increased biodiesel production on the greenhouse gas emissions from field crops in Canada. *Energy for Sustainable Development*, 14(2), 73-82.
- [35.] Vaillancourt, K., Alcocer, Y., Bahn, O., Fertel, C., Frenette, E., Garbouj, H., ... & Neji, Y. (2014). A Canadian 2050 energy outlook: Analysis with the multi-regional model TIMES-Canada. *Applied Energy*, 132, 56-65.
- [36.] Sayin, C., Gumus, M., & Canakci, M. (2012). Effect of fuel injection pressure on the injection, combustion and performance characteristics of a DI diesel engine fueled with canola oil methyl esters-diesel fuel blends. *Biomass and Bioenergy*, 46, 435-446.
- [37.] Meher, L. C., Sagar, D. V., & Naik, S. N. (2006). Technical aspects of biodiesel production by transesterification—a review. *Renewable and sustainable energy reviews*, 10(3), 248-268.
- [38.] Ma, F., & Hanna, M. A. (1999). Biodiesel production: a review. *Bioresource technology*, 70(1), 1-15.
- [39.] Sharma, Y. C., & Singh, B. (2009). Development of biodiesel: current scenario. *Renewable and Sustainable Energy Reviews*, 13(6-7), 1646-1651.

- [40.] Balat, M., & Balat, H. (2010). Progress in biodiesel processing. *Applied energy*, 87(6), 1815-1835.
- [41.] Kumara, A. S., Maheswarb, D., & Reddyc, K. V. K. (2009). Comparison of diesel engine performance and emissions from neat and transesterified cotton seed oil. *Jordan Journal of Mechanical and Industrial Engineering*, 3.
- [42.] Ajav, E. A., Singh, B., & Bhattacharya, T. K. (1999). Experimental study of some performance parameters of a constant speed stationary diesel engine using ethanol–diesel blends as fuel. *Biomass and Bioenergy*, 17(4), 357-365.
- [43.] Yadav, S. P. R., Saravanan, C. G., & Kannan, M. (2015). Influence of injection timing on DI diesel engine characteristics fueled with waste transformer oil. *Alexandria Engineering Journal*, 54(4), 881-888.
- [44.] Tangöz, S., Akansu, S. O., Kahraman, N., & Malkoc, Y. (2015). Effects of compression ratio on performance and emissions of a modified diesel engine fueled by HCNG. *international journal of hydrogen energy*, 40(44), 15374-15380.
- [45.] Jindal, S., Nandwana, B. P., Rathore, N. S., & Vashistha, V. (2010). Experimental investigation of the effect of compression ratio and injection pressure in a direct injection diesel engine running on Jatropha methyl ester. *Applied Thermal Engineering*, 30(5), 442-448.
- [46.] Xing-cai, L., Jian-Guang, Y., Wu-Gao, Z., & Zhen, H. (2004). Effect of cetane number improver on heat release rate and emissions of high speed diesel engine fueled with ethanol–diesel blend fuel. *Fuel*, 83(14-15), 2013-2020.
- [47.] Wei, L., Yao, C., Han, G., & Pan, W. (2016). Effects of methanol to diesel ratio and diesel injection timing on combustion, performance and emissions of a methanol port premixed diesel engine. *Energy*, 95, 223-232.
- [48.] Pavlista, A. D., Santra, D. K., Isbell, T. A., Baltensperger, D. D., Hergert, G. W., Krall, J., ... & Berrada, A. (2011). Adaptability of irrigated spring canola oil production to the US High Plains. *Industrial Crops and Products*, 33(1), 165-169.

- [49.] Canakci, M., & Sanli, H. (2008). Biodiesel production from various feedstocks and their effects on the fuel properties. *Journal of industrial microbiology & biotechnology*, 35(5), 431-441.
- [50.] Knothe, G. (2007). Some aspects of biodiesel oxidative stability. *Fuel Processing Technology*, 88(7), 669-677.
- [51.] Jamrozik, A. (2017). The effect of the alcohol content in the fuel mixture on the performance and emissions of a direct injection diesel engine fueled with diesel-methanol and diesel-ethanol blends. *Energy Conversion and Management*, 148, 461-476.
- [52.] Roy, M. M., Calder, J., Wang, W., Mangad, A., & Diniz, F. C. M. (2016). Cold start idle emissions from a modern Tier-4 turbo-charged diesel engine fueled with diesel-biodiesel, diesel-biodiesel-ethanol, and diesel-biodiesel-diethyl ether blends. *Applied Energy*, 180, 52-65.
- [53.] Gürü, M., Koca, A., Can, Ö., Çınar, C., & Şahin, F. (2010). Biodiesel production from waste chicken fat based sources and evaluation with Mg based additive in a diesel engine. *Renewable Energy*, 35(3), 637-643.
- [54.] Karabektas, M., & Hosoz, M. (2009). Performance and emission characteristics of a diesel engine using isobutanol–diesel fuel blends. *Renewable Energy*, 34(6), 1554-1559.
- [56.] Ovejero, G., Perez, P., Romero, M. D., Guzmán, I., & Di, E. (2007). Solubility and Flory Huggins parameters of SBES, poly (styrene-b-butene/ethylene-b-styrene) triblock copolymer, determined by intrinsic viscosity. *European Polymer Journal*, 43(4), 1444-1449.
- [57.] Burke, J. (1984). Solubility parameters: theory and application.
- [58.] Mohammadi, P., Tabatabaei, M., Nikbakht, A. M., & Esmaeili, Z. (2014). Improvement of the cold flow characteristics of biodiesel containing dissolved polymer wastes using acetone. *Biofuel Research Journal*, 1(1), 26-29.
- [59.] Vera Morales, J. M., & López Ordáz, S. (2017). Quality values of a blend of expanded polystyrene dissolved in biodiesel for potential use as an alternative fuel. *Energy Sources, Part A: Recovery, Utilization, and Environmental Effects*, 39(6), 618-622.

- [60.] Kuzhiyil, N., & Kong, S. C. (2009). Energy recovery from waste plastics by using blends of biodiesel and polystyrene in diesel engines. *Energy & Fuels*, 23(6), 3246-3253.
- [61.] Belmares, M., Blanco, M., Goddard lii, W. A., Ross, R. B., Caldwell, G., Chou, S. H., ... & Thomas, C. (2004). Hildebrand and Hansen solubility parameters from molecular dynamics with applications to electronic nose polymer sensors. *Journal of computational chemistry*, 25(15), 1814-1826.
- [62.] Issariyakul, T., Kulkarni, M. G., Meher, L. C., Dalai, A. K., & Bakhshi, N. N. (2008). Biodiesel production from mixtures of canola oil and used cooking oil. *Chemical Engineering Journal*, 140(1-3), 77-85.
- [63.] Dessureaul, D. (2016). Biofuels Annual-Canada.
- [64.] Sukjit, E., Herreros, J. M., Dearn, K. D., Tsolakis, A., & Theinnoi, K. (2013). Effect of hydrogen on butanol–biodiesel blends in compression ignition engines. *international journal of hydrogen energy*, 38(3), 1624-1635.
- [65.] Pavlista, A. D., Santra, D. K., Isbell, T. A., Baltensperger, D. D., Hergert, G. W., Krall, J., ... & Berrada, A. (2011). Adaptability of irrigated spring canola oil production to the US High Plains. *Industrial crops and products*, 33(1), 165-169.
- [66.] Pullen, J., & Saeed, K. (2012). An overview of biodiesel oxidation stability. *Renewable and Sustainable Energy Reviews*, 16(8), 5924-5950.
- [67.] Tesfa, B., Gu, F., Mishra, R., & Ball, A. D. (2013). LHV predication models and LHV effect on the performance of CI engine running with biodiesel blends. *Energy conversion and management*, 71, 217-226.
- [68.] Usta, N. (2005). Use of tobacco seed oil methyl ester in a turbocharged indirect injection diesel engine. *Biomass and bioenergy*, 28(1), 77-86.
- [69.] Lang, X., Dalai, A. K., Reaney, M. J., & Hertz, P. B. (2001). Biodiesel esters as lubricity

additives: effects of process variables and evaluation of low-temperature properties. *Fuels Int*, 1, 207-227

[70.] Issariyakul, T., Kulkarni, M. G., Meher, L. C., Dalai, A. K., & Bakhshi, N. N. (2008).

Biodiesel production from mixtures of canola oil and used cooking oil. *Chemical Engineering Journal*, 140(1-3), 77-85.

[71.] Sharma, R. V., Somidi, A. K., & Dalai, A. K. (2015). Preparation and properties evaluation of biolubricants derived from canola oil and canola biodiesel. *Journal of agricultural and food chemistry*, 63(12), 3235-3242.

[72.] Aghbashlo, M., Tabatabaei, M., Hosseinpour, S., Rastegari, H., & Ghaziaskar, H. S. (2018). Multi-objective exergy-based optimization of continuous glycerol ketalization to synthesize solketal as a biodiesel additive in subcritical acetone. *Energy Conversion and Management*, 160, 251-261.

[73.] Shantharaman, P. P., Pushparaj, T., & Prabhakar, M. (2017). Performance And Emission Studies On Cashewnut Shell Liquid Bio-Oil Fuelled Diesel Engine With Acetone As Additive. *Advances in Natural and Applied Sciences*, 11(12), 56-63.

[74.] Zhang, Y., Mallapragada, S. K., & Narasimhan, B. (2010). Dissolution of waste plastics in biodiesel. *Polymer Engineering & Science*, 50(5), 863-870.

[75.] Rakopoulos, D. C., Rakopoulos, C. D., Giakoumis, E. G., & Dimaratos, A. M. (2012). Characteristics of performance and emissions in high-speed direct injection diesel engine fueled with diethyl ether/diesel fuel blends. *Energy*, 43(1), 214-224.

[76.] Bailey, B., Eberhardt, J., Goguen, S., & Erwin, J. (1997). *Diethyl ether (DEE) as a renewable diesel fuel* (No. 972978). SAE technical paper.

[77.] Sivalakshmi, S., & Balusamy, T. (2013). Effect of biodiesel and its blends with diethyl ether on the combustion, performance and emissions from a diesel engine. *Fuel*, 106, 106-110.

- [78.] Tran, L. S., Verdicchio, M., Monge, F., Martin, R. C., Bounaceeur, R., Sirjean, B., ... & Battin-Leclerc, F. (2015). An experimental and modeling study of the combustion of tetrahydrofuran. *Combustion and Flame*, 162(5), 1899-1918.
- [79.] Yang, M., Jing, W., Zhao, J., Ling, Z., & Song, Y. (2016). Promotion of hydrate-based CO<sub>2</sub> capture from flue gas by additive mixtures (THF (tetrahydrofuran)+ TBAB (tetra-n-butyl ammonium bromide)). *Energy*, 106, 546-553
- [80.] Bierkandt, T., Hemberger, P., Oßwald, P., Köhler, M., & Kasper, T. (2017). Insights in m-xylene decomposition under fuel-rich conditions by imaging photoelectron photoion coincidence spectroscopy. *Proceedings of the Combustion Institute*, 36(1), 1223-1232.
- [81.] Han, D., Deng, S., Liang, W., Zhao, P., Wu, F., Huang, Z., & Law, C. K. (2017). Laminar flame propagation and nonpremixed stagnation ignition of toluene and xylenes. *Proceedings of the Combustion Institute*, 36(1), 479-489.
- [82.] Papurello, D., Lanzini, A., Leone, P., & Santarelli, M. (2016). The effect of heavy tars (toluene and naphthalene) on the electrochemical performance of an anode-supported SOFC running on bio-syngas. *Renewable Energy*, 99, 747-753.
- [83.] Liu, X., Wang, H., Wei, L., Liu, J., Reitz, R. D., & Yao, M. (2016). Development of a reduced toluene reference fuel (TRF)-2, 5-dimethylfuran-polycyclic aromatic hydrocarbon (PAH) mechanism for engine applications. *Combustion and Flame*, 165, 453-465.
- [80.] Beatrice, C., Di Blasio, G., Guido, C., Cannilla, C., Bonura, G., & Frusteri, F. (2014). Mixture of glycerol ethers as diesel bio-derivable oxy-fuel: Impact on combustion and emissions of an automotive engine combustion system. *Applied energy*, 132, 236-247.
- [81.] Leng, L., Yuan, X., Zeng, G., Chen, X., Wang, H., Li, H., ... & Lai, C. (2015). Rhamnolipid based glycerol-in-diesel microemulsion fuel: formation and characterization. *Fuel*, 147, 76-81.

[82.] Bozkurt, Ö. D., Tunc, F. M., Bağlar, N., Celebi, S., Günbaş, İ. D., & Uzun, A. (2015). Alternative fuel additives from glycerol by etherification with isobutene: Structure–performance relationships in solid catalysts. *Fuel Processing Technology*, *138*, 780-804.

[83.] Chen, Z., Liu, J., Wu, Z., & Lee, C. (2013). Effects of port fuel injection (PFI) of n-butanol and EGR on combustion and emissions of a direct injection diesel engine. *Energy conversion and management*, *76*, 725-731.

# Appendices

## I. Sample Calculations

### Brake Specific Fuel Consumption

$$\text{BSFC} = \frac{\text{Fuel Consumption}}{\text{Power Produced}} = \left( \frac{\text{g or kg}}{\text{h}} \right) / \text{kW}$$

Where BSFC is brake specific fuel consumption in grams per kilowatt hour or kilograms per kilowatt- hour. Fuel consumption per grams is used in this study.

$$\text{Brake power (kW)} = (2 \cdot 3.14 \cdot N \cdot T) / 60000$$

$$1 \text{ kW} = 1.34 \text{ hp}$$

### Brake thermal Efficiency

$$\text{BTE (\%)} = \frac{3600 \cdot \text{Power (kW)}}{\text{Fuel consumption} \left( \frac{\text{kg}}{\text{h}} \right) \cdot \text{Higher Calorific Value} \left( \frac{\text{kJ}}{\text{kg}} \right)} * 100$$

Where BTE is the brake thermal efficiency. To get the value in percentage, we multiply by 100.

### Emissions (ppm to g/kWh Conversion.)

1. Carbon monoxide (CO) emissions.

$$\text{CO (ppm)} * 1.25 = \text{CO mg/m}^3$$

$$(\text{CO (mg/m}^3) * \text{mass flow rate of (air + fuel (m}^3/\text{hr}))) / (1000 * \text{BP (kW)}) = \text{CO g/kWh}$$

2. Nitrous oxide (NO<sub>x</sub>) emissions.

$$\text{NO (ppm)} * 1.34 = \text{NO mg/m}^3$$

$$\text{NO}_2 (\text{ppm}) * 2.056 = \text{NO}_2 \text{ mg/m}^3$$

$$\text{NO}_x = \text{NO} + \text{NO}_2 \text{ mg/m}^3$$

$$(\text{NO}_x (\text{mg/m}^3) * \text{mass flow rate of (air + fuel(m}^3/\text{hr))}) / (1000 * \text{BP (kW)}) = \text{NO}_x \text{ g/kWh}$$

3. Hydrocarbon (HC) emissions.

$$\text{HC (ppm)} * 1.965 = \text{HC mg/m}^3$$

$$(\text{HC (mg/m}^3) * \text{mass flow rate of (air + fuel (m}^3/\text{hr))}) / (1000 * \text{BP (kW)}) = \text{HC g/kWh}$$

### **Mass Flow Rate of Fuel & Air**

1. Mass flow rate of fuel:

Density of fuel in ( $\text{g/cm}^3$ ) given or found.

Fuel Consumption in ( $\text{ml/min}$ ) was noted.

$$\text{F.C in (g/min)} = (\text{ml/ min}) * \text{density (g/cm}^3\text{)}.$$

$$\text{i.e. } 1 \text{ ml} = 1 \text{ cm}^3$$

Fuel consumption in ( $\text{g/hr}$ ) = ( $\text{g/min}$ ) \* 60 was found.

2. Mass flow rate of air:

$$\text{Area of the pipe (a)} = \frac{\pi}{4} d^2 = \frac{\pi}{4} (.04599996521^2)$$

$$\text{Area of the pipe (a)} = 0.0016619 (\text{m}^2)$$

$$\text{Acceleration due to gravity (g)} = 9.81 (\text{m/s}^2)$$

$$\text{Density of air @ } 25 \text{ }^\circ\text{C} (\rho_a) = 1.184 (\text{kg/m}^3)$$

Density of liquid used in manometer ( $\rho_l$ ) = 1000 (kg/m<sup>3</sup>)

$$\rho = \rho_l / \rho_a$$

1. Deflection in the manometer reading due to intake air was calculated and noted to be  $\Delta h$  in m.

2. For calculating the velocity of the intake air, the formula used was  $v = \sqrt{(2 * g * \rho * \Delta h)}$  in m/s.

3. Then, volumetric flow rate,  $Q = \text{area} * \text{velocity}$  in m<sup>3</sup> /s.

4.  $\dot{m}$  of intake air (kg/s) =  $Q * \rho$ .

5.  $\dot{m}$  of intake air (m<sup>3</sup>/hr) = ( $\dot{m}$  of air (kg/s)/ density ( $\rho$ )) \*3600

6. The total  $\dot{m}$  was calculated ( $\dot{m}$  of intake air +  $\dot{m}$  of fuel) in (m<sup>3</sup>/hr)

$h$  in flowing fluid (air) height  $h = H * (\rho_l / \rho_a)$

Where  $H$  is height of manometric fluid.

### **Brake Specific Fuel consumption**

$$\text{BSFC (g/kWh)} = \frac{10 * 3600}{81 * 1.4235} = 312.2194903 \text{ g/kWh}$$

### **Brake Thermal Efficiency**

$$\text{BTE (\%)} = \frac{3600 * 1.4235 * 10^4}{40.196 * 461.5385} * 100 = 27.6228\%$$

### **Mass flow rate of fuel**

$$\text{Density of fuel} = 883.61 \text{ kg/m}^3 = \frac{883.61 * 1000}{100^3} \left( \frac{\text{g}}{\text{cm}^3} \right)$$

$$\text{Fuel consumption noted} = \frac{10}{78} \left( \frac{\text{ml}}{\text{s}} \right)$$

$$\text{Fuel consumption (g/s)} = \frac{883.61 \cdot 1000}{100^3} \cdot \frac{10}{78} \text{ (g/s)}$$

### **Mass flow rate of air**

$$\text{Area of the pipe} = 0.0016619 \text{ m}^2$$

$$\text{Acceleration due to gravity} = 9.81 \text{ m/s}^2$$

$$\text{Density of air @ 25 }^\circ\text{C } (\rho_a) = 1.184 \text{ kg/m}^3$$

$$\text{Density of liquid used in manometer } (\rho_l) = 1000 \text{ kg/m}^3$$

$$\text{Relative density} = \rho_l / \rho_a = \frac{1000}{1.184} = 844.59459$$

$$V = \sqrt{(2 * g * \rho * \Delta h)} = \sqrt{(2 * 9.81 * 0.0017 * 844.59459)} = 5.307599 \text{ m/s}$$

$$Q = A * V = 0.0016619 * 5.307599 = 8.8206989 * 10^{-3} \text{ m}^3/\text{s}$$

### **Fuel consumption**

$$\text{Fuel consumption} = 910 \text{ ml/ 30min}$$

$$\text{Density of the fuel } (\rho) = 883.6 \text{ kg/m}^3$$

(g/ 30 min to g/hr)

$$910 \text{ ml/ 30 min} = 910 * 60 / 30 * 0.8836 \text{ g/h} = 1608.152 \text{ g/h}$$

## Emissions

The values used in the sample calculations are taken from Hatz 1500 light duty engine results for different fuels.

CO: 243 ppm

$$\text{CO: } \frac{243 \cdot 1.25 \cdot [(4.61538 \cdot 10^{-4}) + (8.8206989 \cdot 10^{-3} \cdot 3600)]}{1.4235 \cdot 1000} = 6.9283 \text{ g/kWh}$$

HC: 90 ppm

$$\text{HC: } \frac{90 \cdot 1.965 \cdot [(4.61538 \cdot 10^{-4}) + (8.8206989 \cdot 10^{-3} \cdot 3600)]}{1.4235 \cdot 1000} = 4.033810283 \text{ g/kWh}$$

NO: 67 ppm

$$\text{NO: } \frac{90 \cdot 1.34 \cdot [(4.61538 \cdot 10^{-4}) + (8.8206989 \cdot 10^{-3} \cdot 3600)]}{1.4235 \cdot 1000} = 2.04781163 \text{ g/kWh}$$

NO<sub>2</sub>: 57 ppm

$$\text{NO}_2: \frac{90 \cdot 2.056 \cdot [(4.61538 \cdot 10^{-4}) + (8.8206989 \cdot 10^{-3} \cdot 3600)]}{1.4235 \cdot 1000} = 2.673057928 \text{ g/kWh}$$

NO<sub>x</sub>: 2.04781163 g/kWh + 2.673057928 g/kWh = 4.720869561 g/kWh.

## Heating Value

$$H_g = \frac{\Delta t \cdot W - (L \cdot 2.3)}{m} \left( \frac{\text{cal}}{\text{g}} \right)$$

H<sub>g</sub> = heat of combustion in calories per gram.

W = energy equivalent of the calorimeters in calories per cm

L = length of burned ignition wire.

2.3 = calorie per com of nickel-chromium wire

m= mass of hydrocarbon tested.

Initial temp = 21.636 °C

final temp = 24.3173 °C

$\Delta t = 24.3173 - 21.636 = 2.6813$  °C

m = .6400 gms

Length of wire burned = 8 cm.

1 cal = 4.184 Joules

$$H_g = \frac{2.6813 * 2402 - (8 * 2.3)}{.6400} = 10034.504 \text{ cal/g} = 10.034504 \text{ kcal/g} = 41984.364 \text{ kJ/kg}$$

### **Kinematic viscosity**

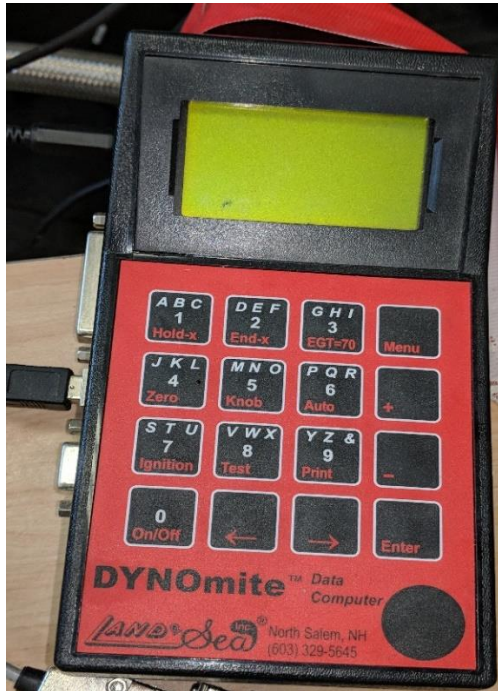
Mass of 10 ml of fuel = 8.57 gm

$$\text{Density} = \frac{\text{mass}}{\text{volume}} \frac{(g)}{(cm^3)} = \frac{8.57}{10} = 0.857 \text{ g/cm}^3$$

Kinematic viscosity =  $\frac{\text{viscosity of water} * \text{density of test liquid} * \text{time required for test liquid}}{\text{density of water} * \text{time required for water}}$

$$= \frac{.658 * .857 * 522}{1 * 56} = 5.2564095 \text{ cSt}$$

## II. Photographs of Equipment Used



1. Data Acquisition System



2. Digital Thermometer



3. Novagas Analyzer



4. Land & Sea dynamometer



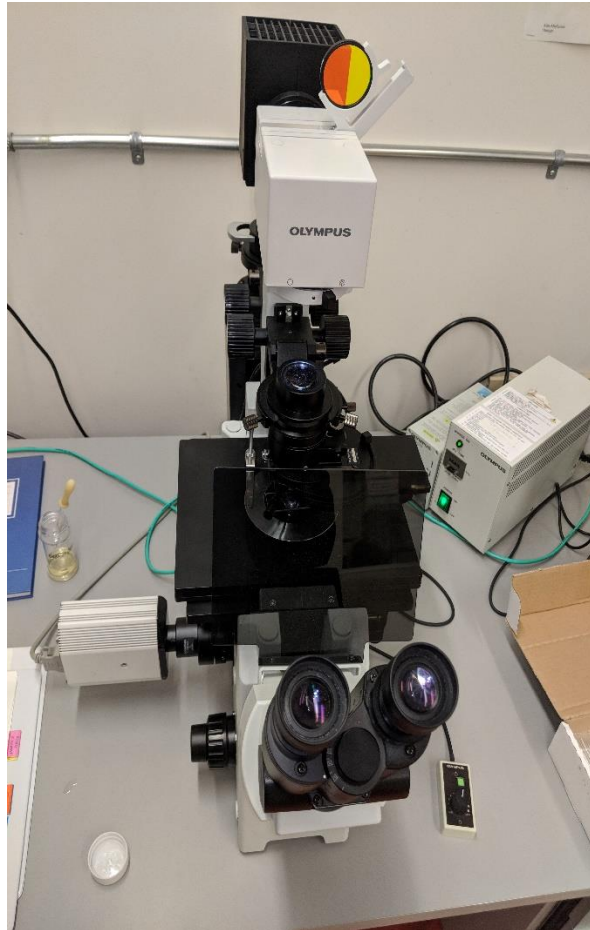
5. Smart 2000 Smoke Opacity Meter



6. Bomb calorimeter setup



7. Dwyer 1205 CO analyzer



8. Polaris Microscope



9. Particle size measuring system.

### III. Tables

Data points for Brake specific fuel consumption (BSFC) values @ various engine conditions

Engine Speed: 1000 rpm	BSFC (g/kWh)		
Fuel	Low Load	Medium Load	High Load
B 0	289.227932	255.241	236.497579
B 100	324.2279322	292.9910014	276.4976959
B 100 W/EPS (2 g/L)	312.2194903	284.1231958	267.8571429
B 100 W/EPS (6 g/L)	304.6961291	276.4441905	263.7362637
B 100 W/EPS (10 g/L)	312.2194903	283.2410014	268.755762
B 100 W/EPS (10 g/L) + DEE 10%	301.0687942	280.2310972	267.8572483
B 100 W/EPS (10 g/L) + THF 10%	304.6961291	284.1231958	272.1088435
B 100 W/EPS (10 g/L) + Ace 10%	308.4119355	288.124931	276.4976959
B 100 W/EPS (10 g/L) + Xyl 10%	301.0687942	280.2310972	267.8571429
B 100 W/EPS (10 g/L) + Tol 10%	303.0487942	282.1023972	269.9857143

Engine Speed: 2100 rpm	BSFC (g/kWh)		
Fuel	Low Load	Medium Load	High Load
B 0	276.9147932	250.177574	235.914599
B 100	315.8947719	286.0757401	272.905902
B 100 W/EPS (2 g/L)	292.7805203	270.1826435	263.4953537
B 100 W/EPS (6 g/L)	272.8182121	262.8804099	254.7121752
B 100 W/EPS (10 g/L)	300.1000333	277.9021476	264.7187249
B 100 W/EPS (10 g/L) + DEE 10%	279.1628217	262.8804099	254.7121752
B 100 W/EPS (10 g/L) + THF 10%	285.8095556	270.1826435	263.4953537
B 100 W/EPS (10 g/L) + Ace 10%	292.7805203	277.9021476	267.905902
B 100 W/EPS (10 g/L) + Xyl 10%	279.1628217	273.8804099	262.4953537
B 100 W/EPS (10 g/L) + Tol 10%	281.6282172	273.483041	265.289537

Engine Speed: 3000 rpm	BSFC (g/kWh)		
Fuel	Low Load	Medium Load	High Load
B 0	274.31396	250.02999	236.89381
B 100	309.31396	282.02999	273.89381
B 100 W/EPS (2 g/L)	295.8655258	268.5999897	259.4783476
B 100 W/EPS (6 g/L)	283.5377956	256.3908993	246.5044302
B 100 W/EPS (10 g/L)	303.126	277.5051	271.4277657
B 100 W/EPS (10 g/L) + DEE 10%	295.8655258	256.3908993	246.5044302
B 100 W/EPS (10 g/L) + THF 10%	309.3139588	268.5999897	246.5044302
B 100 W/EPS (10 g/L) + Ace 10%	324.043195	282.0299892	259.4783476
B 100 W/EPS (10 g/L) + Xyl 10%	295.8655258	256.3908993	246.5044302
B 100 W/EPS (10 g/L) + Tol 10%	296.6285258	257.6905993	247.4045302

### Data points for Brake thermal efficiency (BTE) values @ different engine conditions

Engine Speed: 1000 rpm	BTE (%)		
	Fuel	Low Load	Medium Load
B 0	26.1730272	30.0128703	31.4975785
B 100	27.6730272	31.5128703	32.9975785
B 100 W/EPS (2 g/L)	28.09051985	31.8905729	33.43046714
B 100 W/EPS (6 g/L)	28.76347543	32.36257342	33.89566233
B 100 W/EPS (10 g/L)	27.99182085	32.26692542	32.89466597
B 100 W/EPS (10 g/L) + DEE 10%	30.70730162	34.31606169	35.71414555
B 100 W/EPS (10 g/L) + THF 10%	30.90730162	34.51606169	35.91414555
B 100 W/EPS (10 g/L) + Ace 10%	29.74538874	33.32595023	34.69709762
B 100 W/EPS (10 g/L) + Xyl 10%	30.41434383	34.02143606	35.42664217
B 100 W/EPS (10 g/L) + Tol 10%	30.43764292	34.05018559	35.45902962

Engine Speed: 2100 rpm	BTE (%)		
	Fuel	Low Load	Medium Load
B 0	26.775	30.5963324	32.0159983
B 100	27.87543813	31.69633242	33.11599828
B 100 W/EPS (2 g/L)	28.6276846	32.34929777	34.58657506
B 100 W/EPS (6 g/L)	29.65251078	33.01740957	34.33865276
B 100 W/EPS (10 g/L)	29.11738596	32.84565199	34.02590201
B 100 W/EPS (10 g/L) + DEE 10%	31.47046245	35.02607922	36.33156619
B 100 W/EPS (10 g/L) + THF 10%	31.26277245	34.78116422	36.02178817
B 100 W/EPS (10 g/L) + Ace 10%	30.18560619	33.65061766	34.81814329
B 100 W/EPS (10 g/L) + Xyl 10%	31.05500182	34.60037021	35.57854837
B 100 W/EPS (10 g/L) + Tol 10%	31.0840527	34.63431738	35.61229963

Engine Speed: 3000 rpm	BTE (%)		
	Fuel	Low Load	Medium Load
B 0	<b>26.94299212</b>	<b>30.72108225</b>	<b>31.98311772</b>
B 100	28.04299212	31.82108225	33.08311772
B 100 W/EPS (2 g/L)	28.53772327	32.40438601	33.73498563
B 100 W/EPS (6 g/L)	29.28758273	33.27096025	34.68289414
B 100 W/EPS (10 g/L)	28.84579488	32.70154926	33.98973952
B 100 W/EPS (10 g/L) + DEE 10%	30.58170193	35.03702945	36.6918863
B 100 W/EPS (10 g/L) + THF 10%	30.78170193	34.83702945	36.8918863
B 100 W/EPS (10 g/L) + Ace 10%	29.34764605	33.51668758	35.30034104
B 100 W/EPS (10 g/L) + Xyl 10%	30.55792687	34.83703745	36.22154148
B 100 W/EPS (10 g/L) + Tol 10%	30.58251504	34.87310941	36.2610655

**Data points for Carbon Monoxide emissions (CO) in ppm @ different engine conditions**

<b>Engine Speed: 1000 rpm</b>	<b>Carbon Monoxide (ppm)</b>		
<b>Fuel</b>	<b>Low Load</b>	<b>Medium Load</b>	<b>High Load</b>
B 0	241	224	185
B 100	202	168	152
B 100 W/EPS (2 g/L)	206	171	155
B 100 W/EPS (6 g/L)	258	214	194
B 100 W/EPS (10 g/L)	311	258	234
B 100 W/EPS (10 g/L) + DEE 10%	243	202	182
B 100 W/EPS (10 g/L) + THF 10%	263	218	197
B 100 W/EPS (10 g/L) + Ace 10%	276	229	207
B 100 W/EPS (10 g/L) + Xyl 10%	257	213	193
B 100 W/EPS (10 g/L) + Tol 10%	264	219	198

<b>Carbon Monoxide Emissions (ppm)</b>			
<b>Engine Speed: 2100 rpm</b>	<b>Carbon Monoxide (ppm)</b>		
<b>Fuel</b>	<b>Low Load</b>	<b>Medium Load</b>	<b>High Load</b>
B 0	195	173	158
B 100	145	133	124
B 100 W/EPS (2 g/L)	147	135	126
B 100 W/EPS (6 g/L)	185	169	158
B 100 W/EPS (10 g/L)	223	204	190
B 100 W/EPS (10 g/L) + DEE 10%	174	159	149
B 100 W/EPS (10 g/L) + THF 10%	188	173	161
B 100 W/EPS (10 g/L) + Ace 10%	198	181	169
B 100 W/EPS (10 g/L) + Xyl 10%	184	169	157
B 100 W/EPS (10 g/L) + Tol 10%	189	173	162

<b>Engine Speed: 3000 rpm</b>	<b>Carbon Monoxide (ppm)</b>		
<b>Fuel</b>	<b>Low Load</b>	<b>Medium Load</b>	<b>High Load</b>
B 0	182	150	141
B 100	147	128	111
B 100 W/EPS (2 g/L)	149	130	113
B 100 W/EPS (6 g/L)	187	163	141
B 100 W/EPS (10 g/L)	226	197	170
B 100 W/EPS (10 g/L) + DEE 10%	176	153	133
B 100 W/EPS (10 g/L) + THF 10%	191	166	144
B 100 W/EPS (10 g/L) + Ace 10%	200	174	151
B 100 W/EPS (10 g/L) + Xyl 10%	187	162	141
B 100 W/EPS (10 g/L) + Tol 10%	192	167	145

**Data points for Carbon Monoxide emissions (CO) in g/kWh @ different engine conditions**

<b>Engine Speed: 1000 rpm</b>	<b>Carbon Monoxide (g/kWh)</b>		
<b>Fuel</b>	<b>Low Load</b>	<b>Medium Load</b>	<b>High Load</b>
B 0	6.8712734	5.1989819	1.1994456
B 100	5.759327658	3.899241258	0.985492886
B 100 W/EPS (2 g/L)	5.87337	4.06586	1.0278
B 100 W/EPS (6 g/L)	7.355967	5.092178	1.246996
B 100 W/EPS (10 g/L)	8.86708	6.13825	1.55138
B 100 W/EPS (10 g/L) + DEE 10%	6.92829	4.79613	1.21217
B 100 W/EPS (10 g/L) + THF 10%	7.49852	5.19088	1.31194
B 100 W/EPS (10 g/L) + Ace 10%	7.86917	5.44747	1.37679
B 100 W/EPS (10 g/L) + Xyl 10%	7.32745	5.07246	1.28201
B 100 W/EPS (10 g/L) + Tol 10%	7.527034446	5.21060042	1.13169219

<b>Engine Speed: 2100 rpm</b>	<b>Carbon Monoxide (g/kWh)</b>		
<b>Fuel</b>	<b>Low Load</b>	<b>Medium Load</b>	<b>High Load</b>
B 0	3.9092121	2.9162684	2.1897993
B 100	2.90685551	2.241991679	1.71854142
B 100 W/EPS (2 g/L)	3.03106	2.3378	1.79201
B 100 W/EPS (6 g/L)	3.796178	2.927904	2.244366
B 100 W/EPS (10 g/L)	4.57603	3.52938	2.70543
B 100 W/EPS (10 g/L) + DEE 10%	3.57548	2.75768	2.11388
B 100 W/EPS (10 g/L) + THF 10%	3.86975	2.98465	2.28787
B 100 W/EPS (10 g/L) + Ace 10%	4.06104	3.12178	2.40096
B 100 W/EPS (10 g/L) + Xyl 10%	3.78146	2.91656	2.23567
B 100 W/EPS (10 g/L) + Tol 10%	3.884464521	2.996003863	2.296560433

<b>Engine Speed: 3000 rpm</b>	<b>Carbon Monoxide (g/kWh)</b>		
<b>Fuel</b>	<b>Low Load</b>	<b>Medium Load</b>	<b>High Load</b>
B 0	3.6280992	2.6771738	2.4237957
B 100	2.930401523	2.284527563	1.908092233
B 100 W/EPS (2 g/L)	3.05562	2.38215	1.98692
B 100 W/EPS (6 g/L)	3.826923	2.983456	2.491851
B 100 W/EPS (10 g/L)	4.6131	3.59634	3.00375
B 100 W/EPS (10 g/L) + DEE 10%	3.60445	2.81	2.34699
B 100 W/EPS (10 g/L) + THF 10%	3.9011	3.04127	2.54015
B 100 W/EPS (10 g/L) + Ace 10%	4.09393	3.20986	2.6657
B 100 W/EPS (10 g/L) + Xyl 10%	3.81211	2.97189	2.4822
B 100 W/EPS (10 g/L) + Tol 10%	3.915937709	3.05283884	2.549800315

## Data points for Hydrocarbon emissions (HC) in ppm @ different engine conditions

<b>Engine speed: 1000 rpm</b>	<b>Hydrocarbon Emission (ppm)</b>		
<b>Fuel</b>	<b>Low Load</b>	<b>Medium Load</b>	<b>High Load</b>
B 0	180	150	135
B 100	60	45	30
B 100 W/EPS (2 g/L)	75	56	37.5
B 100 W/EPS (6 g/L)	234	175	117
B 100 W/EPS (10 g/L)	312	234	156
B 100 W/EPS (10 g/L) + DEE 10%	192	144	96
B 100 W/EPS (10 g/L) + THF 10%	249	186	124
B 100 W/EPS (10 g/L) + Ace 10%	264	198	132
B 100 W/EPS (10 g/L) + Xyl 10%	216	162	108
B 100 W/EPS (10 g/L) + Tol 10%	213	159	106

<b>Engine speed: 2100 rpm</b>	<b>Hydrocarbon Emission (ppm)</b>		
<b>Fuel</b>	<b>Low Load</b>	<b>Medium Load</b>	<b>High Load</b>
B 0	150	120	105
B 100	45	36	27
B 100 W/EPS (2 g/L)	56	45	33
B 100 W/EPS (6 g/L)	175	140	105
B 100 W/EPS (10 g/L)	234	187	140
B 100 W/EPS (10 g/L) + DEE 10%	144	115	86
B 100 W/EPS (10 g/L) + THF 10%	186	149	112
B 100 W/EPS (10 g/L) + Ace 10%	198	158	118
B 100 W/EPS (10 g/L) + Xyl 10%	162	129	97
B 100 W/EPS (10 g/L) + Tol 10%	159	127	95

<b>Engine speed: 3000 rpm</b>	<b>Hydrocarbon Emission (ppm)</b>		
<b>Fuel</b>	<b>Low Load</b>	<b>Medium Load</b>	<b>High Load</b>
B 0	135	105	90
B 100	36	24	18
B 100 W/EPS (2 g/L)	45	30	22
B 100 W/EPS (6 g/L)	140	93	70
B 100 W/EPS (10 g/L)	187	124	93
B 100 W/EPS (10 g/L) + DEE 10%	115	76	57
B 100 W/EPS (10 g/L) + THF 10%	149	99	74
B 100 W/EPS (10 g/L) + Ace 10%	158	105	79
B 100 W/EPS (10 g/L) + Xyl 10%	129	86	64
B 100 W/EPS (10 g/L) + Tol 10%	127	85	63

**Data points for Hydrocarbon emissions (HC) in g/kWh @ different engine conditions**

<b>Engine speed: 1000 rpm</b>	<b>Hydrocarbon Emission (g/kWh)</b>		
<b>Fuel</b>	<b>Low Load</b>	<b>Medium Load</b>	<b>High Load</b>
B 0	8.067616318	5.472856822	1.375926222
B 100	2.689206855	1.641859087	0.305762135
B 100 W/EPS (2 g/L)	3.361506799	2.098465155	0.390794734
B 100 W/EPS (6 g/L)	10.48789775	6.547208634	1.219278622
B 100 W/EPS (10 g/L)	13.98386828	8.729618775	1.625708741
B 100 W/EPS (10 g/L) + DEE 10%	8.605453199	5.372069694	1.000434519
B 100 W/EPS (10 g/L) + THF 10%	11.16019889	6.966904313	1.297439556
B 100 W/EPS (10 g/L) + Ace 10%	11.83250196	7.386598901	1.375599704
B 100 W/EPS (10 g/L) + Xyl 10%	9.681134849	6.043578406	1.125488833
B 100 W/EPS (10 g/L) + Tol 10%	9.546674642	5.959639817	1.109857044

<b>Engine speed: 2100 rpm</b>	<b>Hydrocarbon Emission (g/kWh)</b>		
<b>Fuel</b>	<b>Low Load</b>	<b>Medium Load</b>	<b>High Load</b>
B 0	4.727139611	3.179912525	2.287647309
B 100	1.418144544	0.953975888	0.58825472
B 100 W/EPS (2 g/L)	1.81253297	1.219278489	0.75184972
B 100 W/EPS (6 g/L)	5.655095983	3.804146871	2.34576931
B 100 W/EPS (10 g/L)	7.540140522	5.072201354	3.127697432
B 100 W/EPS (10 g/L) + DEE 10%	4.640080551	3.121351279	1.924733792
B 100 W/EPS (10 g/L) + THF 10%	6.017606903	4.048004583	2.496141071
B 100 W/EPS (10 g/L) + Ace 10%	6.380116056	4.291862684	2.646513212
B 100 W/EPS (10 g/L) + Xyl 10%	5.22009062	3.511520189	2.165327194
B 100 W/EPS (10 g/L) + Tol 10%	5.147589361	3.462749075	2.135253205

<b>Engine speed: 3000 rpm</b>	<b>Hydrocarbon Emission (g/kWh)</b>		
<b>Fuel</b>	<b>Low Load</b>	<b>Medium Load</b>	<b>High Load</b>
B 0	4.230523128	2.945962095	2.432046896
B 100	1.128144782	0.673364499	0.486408809
B 100 W/EPS (2 g/L)	1.441884632	0.86062874	0.621680168
B 100 W/EPS (6 g/L)	4.49867665	2.685159425	1.939640336
B 100 W/EPS (10 g/L)	5.998245015	3.580218854	2.586192152
B 100 W/EPS (10 g/L) + DEE 10%	3.691224657	2.203207733	1.591499763
B 100 W/EPS (10 g/L) + THF 10%	4.787060925	2.857287418	2.063976255
B 100 W/EPS (10 g/L) + Ace 10%	5.075442674	3.029415953	2.188314193
B 100 W/EPS (10 g/L) + Xyl 10%	4.152627739	2.4786087	1.790437233
B 100 W/EPS (10 g/L) + Tol 10%	4.094952354	2.444183579	1.765570049

**Data points for Nitrous oxides Emissions (NOx) in ppm @ different engine conditions**

<b>Engine Speed: 1000 rpm</b>	<b>Nitrous oxides (Nox) Emissions (ppm)</b>		
<b>Fuel</b>	<b>Low Load</b>	<b>Medium Load</b>	<b>High Load</b>
B 0	155	194	232
B 100	182	223	266
B 100 W/EPS (2 g/L)	188	222	247
B 100 W/EPS (6 g/L)	218	258	286
B 100 W/EPS (10 g/L)	203	240	267
B 100 W/EPS (10 g/L) + DEE 10%	183	216	240
B 100 W/EPS (10 g/L) + THF 10%	189	223	248
B 100 W/EPS (10 g/L) + Ace 10%	193	228	253
B 100 W/EPS (10 g/L) + Xyl 10%	187	221	246
B 100 W/EPS (10 g/L) + Tol 10%	191	226	251

<b>Engine Speed: 2100 rpm</b>	<b>Nitrous oxides (Nox) Emissions (ppm)</b>		
<b>Fuel</b>	<b>Low Load</b>	<b>Medium Load</b>	<b>High Load</b>
B 0	146	173	203
B 100	176	207	235
B 100 W/EPS (2 g/L)	181	210	230.4
B 100 W/EPS (6 g/L)	210	244	267
B 100 W/EPS (10 g/L)	196	227	248
B 100 W/EPS (10 g/L) + DEE 10%	176	205	224
B 100 W/EPS (10 g/L) + THF 10%	182	211	231
B 100 W/EPS (10 g/L) + Ace 10%	186	216	236
B 100 W/EPS (10 g/L) + Xyl 10%	180	209	229
B 100 W/EPS (10 g/L) + Tol 10%	184	214	234

<b>Engine Speed: 3000 rpm</b>	<b>Nitrous oxides (Nox) Emissions (ppm)</b>		
<b>Fuel</b>	<b>Low Load</b>	<b>Medium Load</b>	<b>High Load</b>
B 0	139	170	192
B 100	162	194	216
B 100 W/EPS (2 g/L)	167	199	217
B 100 W/EPS (6 g/L)	194	231	252
B 100 W/EPS (10 g/L)	180	215	234
B 100 W/EPS (10 g/L) + DEE 10%	162	194	211
B 100 W/EPS (10 g/L) + THF 10%	168	200	218
B 100 W/EPS (10 g/L) + Ace 10%	171	204	223
B 100 W/EPS (10 g/L) + Xyl 10%	166	198	216
B 100 W/EPS (10 g/L) + Tol 10%	170	202	221

**Data points for Nitrous oxides Emissions (NOx) in g/kWh @ different engine conditions**

<b>Engine Speed: 1000 rpm</b>	<b>Nitrous oxides (Nox) Emissions (g/kWh)</b>		
<b>Fuel</b>	<b>Low Load</b>	<b>Medium Load</b>	<b>High Load</b>
B 0	4.453223847	4.537270324	1.515721675
B 100	5.228949464	5.215528554	1.737857576
B 100 W/EPS (2 g/L)	5.401329569	5.322384472	1.652463202
B 100 W/EPS (6 g/L)	6.263241796	6.171698565	1.916152622
B 100 W/EPS (10 g/L)	5.832286716	5.747045351	1.784311564
B 100 W/EPS (10 g/L) + DEE 10%	5.257674617	5.180830772	1.608514717
B 100 W/EPS (10 g/L) + THF 10%	5.430058255	5.350695152	1.661254216
B 100 W/EPS (10 g/L) + Ace 10%	5.544981026	5.463938516	1.696414451
B 100 W/EPS (10 g/L) + Xyl 10%	5.372596466	5.294072961	1.643673448
B 100 W/EPS (10 g/L) + Tol 10%	5.487518316	5.407315149	1.67883225

<b>Engine Speed: 2100 rpm</b>	<b>Nitrous oxides (Nox) Emissions (g/kWh)</b>		
<b>Fuel</b>	<b>Low Load</b>	<b>Medium Load</b>	<b>High Load</b>
B 0	2.949375871	2.938665319	2.835083833
B 100	3.555418678	3.516214332	3.282007855
B 100 W/EPS (2 g/L)	3.755196134	3.659620019	3.290105599
B 100 W/EPS (6 g/L)	4.354424252	4.243599544	3.815119494
B 100 W/EPS (10 g/L)	4.054814543	3.951613025	3.552616973
B 100 W/EPS (10 g/L) + DEE 10%	3.655320752	3.562287683	3.202600309
B 100 W/EPS (10 g/L) + THF 10%	3.775168954	3.679085961	3.307606161
B 100 W/EPS (10 g/L) + Ace 10%	3.85506826	3.756952387	3.377611211
B 100 W/EPS (10 g/L) + Xyl 10%	3.735218387	3.640151965	3.272605037
B 100 W/EPS (10 g/L) + Tol 10%	3.815116241	3.718016061	3.342607284

<b>Engine Speed: 3000 rpm</b>	<b>Nitrous oxides (Nox) Emissions (g/kWh)</b>		
<b>Fuel</b>	<b>Low Load</b>	<b>Medium Load</b>	<b>High Load</b>
B 0	2.792191513	3.057432474	3.325835476
B 100	3.254224049	3.489078989	3.741560527
B 100 W/EPS (2 g/L)	3.437079463	3.671030714	3.853884597
B 100 W/EPS (6 g/L)	3.985547255	4.256829942	4.468862071
B 100 W/EPS (10 g/L)	3.711317599	3.963935852	4.161379568
B 100 W/EPS (10 g/L) + DEE 10%	3.345667698	3.57339396	3.751384109
B 100 W/EPS (10 g/L) + THF 10%	3.455364578	3.690557584	3.874380353
B 100 W/EPS (10 g/L) + Ace 10%	3.528497325	3.768668142	3.956381436
B 100 W/EPS (10 g/L) + Xyl 10%	3.418797197	3.651500985	3.833381542
B 100 W/EPS (10 g/L) + Tol 10%	3.491926478	3.72960801	3.915379163

## Data points for Smoke Opacity emissions in % @ different engine conditions

<b>Engine Speed: 1000 rpm</b>	<b>Smoke Opacity Emissions (%)</b>		
<b>Fuel</b>	<b>Low Load</b>	<b>Medium Load</b>	<b>High Load</b>
B 0	3.3	5.1	8
B 100	16.5	18.1	19.2
B 100 W/EPS (2 g/L)	18.2	19.808	21.123
B 100 W/EPS (6 g/L)	21.8	23.727	25.301
B 100 W/EPS (10 g/L)	24.3	26.448	28.203
B 100 W/EPS (10 g/L) + DEE 10%	18.5	20.135	21.471
B 100 W/EPS (10 g/L) + THF 10%	19.5	21.223	22.632
B 100 W/EPS (10 g/L) + Ace 10%	21.2	23.074	24.605
B 100 W/EPS (10 g/L) + Xyl 10%	19	20.679	22.051
B 100 W/EPS (10 g/L) + Tol 10%	20	21.767	23.212

<b>Engine Speed: 2100 rpm</b>	<b>Smoke Opacity Emissions (%)</b>		
<b>Fuel</b>	<b>Low Load</b>	<b>Medium Load</b>	<b>High Load</b>
B 0	2.8	4.5	5.6
B 100	8.1	10.5	12.8
B 100 W/EPS (2 g/L)	8.934	11.581	12.939
B 100 W/EPS (6 g/L)	10.701	13.872	15.498
B 100 W/EPS (10 g/L)	11.929	15.463	17.275
B 100 W/EPS (10 g/L) + DEE 10%	9.081	11.772	13.152
B 100 W/EPS (10 g/L) + THF 10%	9.572	12.409	13.863
B 100 W/EPS (10 g/L) + Ace 10%	10.407	13.49	15.071
B 100 W/EPS (10 g/L) + Xyl 10%	9.327	12.09	13.507
B 100 W/EPS (10 g/L) + Tol 10%	9.818	12.727	14.218

<b>Engine Speed: 3000 rpm</b>	<b>Smoke Opacity Emissions (%)</b>		
<b>Fuel</b>	<b>Low Load</b>	<b>Medium Load</b>	<b>High Load</b>
B 0	2.1	3	4.2
B 100	7.1	8	9.1
B 100 W/EPS (2 g/L)	7.831	8.824	10.037
B 100 W/EPS (6 g/L)	9.38	10.569	12.023
B 100 W/EPS (10 g/L)	10.456	11.781	13.401
B 100 W/EPS (10 g/L) + DEE 10%	7.96	8.969	10.203
B 100 W/EPS (10 g/L) + THF 10%	8.39	9.454	10.754
B 100 W/EPS (10 g/L) + Ace 10%	9.122	10.278	11.692
B 100 W/EPS (10 g/L) + Xyl 10%	8.175	9.212	10.478
B 100 W/EPS (10 g/L) + Tol 10%	8.606	9.696	11.03

**Data points of performance and emissions of fuels for heavy-duty engine @ idling.**

**1. Fuel: Biodiesel (B100)**

Kinematic viscosity: 4.74 cSt		Calorific Value: 40.196 MJ/kg			Density: 883.61 kg/m <sup>3</sup>		
Atmospheric Temperature: 14 °C		Fuel consumed: 910 ml/30mins			Speed: 700 rpm		
Sl no.	Time	O <sub>2</sub>	CO	CO <sub>2</sub>	HC	NO <sub>x</sub>	T
Units	(s)	(%)	(ppm)	(%)	(ppm)	(ppm)	(°C)
1	60	18	152	2.2	30	222	30
2	120	18.1	191	2.3	30	221	39.6
3	240	18.2	202	2.3	60	212	53
4	360	18.4	210	2.4	90	187	55
5	480	18.5	245	2.4	90	176	57
6	600	18.5	304	2.4	90	171	59
7	900	18.6	311	2.5	120	171	61
8	1200	18.6	322	2.5	150	163	62
9	1500	18.7	324	2.4	180	167	63
10	1800	18.8	351	2.5	180	132	64
Atmospheric Temperature: 14 °C		Fuel consumed: 1490 ml/30 mins			Speed: 1700 rpm		
Sl no.	Time	O <sub>2</sub>	CO	CO <sub>2</sub>	HC	NO <sub>x</sub>	T
Units	(s)	(%)	(ppm)	(%)	(ppm)	(ppm)	(°C)
1	60	17.2	184	2.7	30	169	48
2	120	17.3	213	2.7	30	198	76
3	240	17.6	226	2.8	90	178	84
4	360	17.9	209	2.8	150	153	96
5	480	18.1	192	2.8	210	140	99
6	600	18.1	181	3	270	145	101
7	900	18.1	154	3	270	142	104
8	1200	18.1	143	3	330	145	107
9	1500	18.1	138	3.1	330	151	109
10	1800	18.1	128	3.2	330	156	113

**2. Fuel: Biodiesel + Styrofoam 2 g/L (B 100 W/EPS (2 g/L))**

Kinematic viscosity: 4.92 cSt		Calorific Value: 39.588 MJ/kg				Density: 883 kg/m <sup>3</sup>	
Atmospheric Temp: 15 °C		Fuel consumed: 905 ml/30 mins				Speed: 700 rpm	
Sl no.	Time	O <sub>2</sub>	CO	CO <sub>2</sub>	HC	NO <sub>x</sub>	T
Units	(s)	(%)	(ppm)	(%)	(ppm)	(ppm)	(°C)
1	60	18	164	2.1	90	220	29
2	120	18	198	2.2	120	215	35
3	240	18.1	213	2.3	120	207	48
4	360	18.3	221	2.3	120	183	52
5	480	18.4	254	2.4	180	177	59
6	600	18.4	310	2.4	210	173	65
7	900	18.4	318	2.5	270	172	69
8	1200	18.5	331	2.5	270	169	72
9	1500	18.6	328	2.5	330	167	74
10	1800	18.6	358	2.5	390	163	79
Atmospheric Temp: 14 °C		Fuel consumed: 1485 ml/30 mins				Speed: 1700 rpm	
Sl no.	Time	O <sub>2</sub>	CO	CO <sub>2</sub>	HC	NO <sub>x</sub>	T
Units	(s)	(%)	(ppm)	(%)	(ppm)	(ppm)	(°C)
1	60	17.2	191	2.4	90	165	44
2	120	17.3	221	2.5	120	187	66
3	240	17.4	234	2.7	120	168	81
4	360	17.6	219	2.7	210	151	94
5	480	17.9	203	2.8	270	140	97
6	600	18	194	2.9	330	143	104
7	900	18.1	162	3	360	144	108
8	1200	18.1	154	3	420	146	110
9	1500	18.1	147	3.1	390	149	115
10	1800	18.2	133	3.1	420	147	120

### 3. Fuel: Biodiesel + Styrofoam 6g/L (B 100 W/EPS (6 g/L))

Kinematic viscosity: 5.34 cSt		Calorific Value: 37.974 MJ/kg			Density: 882 kg/m <sup>3</sup>		
Atmospheric Temp: 7° C		Fuel consumed: 900 ml/30 mins			Speed: 700 rpm		
Sl no.	Time	O <sub>2</sub>	CO	CO <sub>2</sub>	HC	NO <sub>x</sub>	T
Units	(s)	(%)	(ppm)	(%)	(ppm)	(ppm)	(°C)
1	60	17.3	177	1.9	180	213	27
2	120	17.4	210	1.9	180	205	34
3	240	17.5	220	1.9	210	197	49
4	360	17.7	229	1.9	210	180	50
5	480	17.9	259	2	240	175	58
6	600	18.1	321	2.1	270	171	66
7	900	18.2	328	2.1	330	165	69
8	1200	18.3	340	2.2	420	168	76
9	1500	18.3	343	2.2	480	167	83
10	1800	18.4	360	2.3	570	166	88
Atmospheric Temp: 9° C		Fuel consumed: 1475 ml/30 mins			Speed: 1700 rpm		
Sl no.	Time	O <sub>2</sub>	CO	CO <sub>2</sub>	HC	NO <sub>x</sub>	T
Units	(s)	(%)	(ppm)	(%)	(ppm)	(ppm)	(°C)
1	60	17.1	208	2.3	210	162	41
2	120	17.2	229	2.3	210	175	59
3	240	17.3	241	2.4	270	162	63
4	360	17.5	228	2.5	390	150	78
5	480	17.8	213	2.5	450	137	82
6	600	17.9	204	2.7	510	140	94
7	900	18	190	2.8	540	141	97
8	1200	18.1	162	2.8	480	141	103
9	1500	18.1	157	2.9	450	143	108
10	1800	18.1	141	3	510	145	115

**4. Fuel: Biodiesel + Styrofoam 10 g/L (B 100 W/EPS (10 g/L))**

Kinematic viscosity: 5.81 cSt			Calorific Value: 36.548 MJ/kg			Density: 882 kg/m <sup>3</sup>	
Atmospheric Temp: 7 °C			Fuel consumed: 915 ml/30 mins			Speed: 700 rpm	
Sl no.	Time	O <sub>2</sub>	CO	CO <sub>2</sub>	HC	NO <sub>x</sub>	T
Units	(s)	(%)	(ppm)	(%)	(ppm)	(ppm)	(°C)
1	60	18	202	1.9	270	207	25
2	120	18.1	224	1.9	330	201	32
3	240	18.2	236	1.9	390	189	40
4	360	18.3	245	2	390	174	51
5	480	18.3	267	2.1	450	174	59
6	600	18.3	335	2.1	480	163	63
7	900	18.4	349	2.2	510	163	69
8	1200	18.5	363	2.2	570	165	74
9	1500	18.5	369	2.2	660	161	81
10	1800	18.5	382	2.3	690	158	92
Atmospheric Temp: 6 °C			Fuel consumed: 1500 ml/30 mins			Speed: 1700 rpm	
Sl no.	Time	O <sub>2</sub>	CO	CO <sub>2</sub>	HC	NO <sub>x</sub>	T
Units	(s)	(%)	(ppm)	(%)	(ppm)	(ppm)	(°C)
1	60	17.1	224	2.1	330	180	33
2	120	17.1	245	2.2	390	197	48
3	240	17.2	271	2.2	420	188	53
4	360	17.4	253	2.3	570	180	61
5	480	17.5	241	2.4	660	171	69
6	600	17.8	233	2.5	720	167	77
7	900	18	218	2.7	630	163	84
8	1200	18.1	211	2.8	600	163	88
9	1500	18.1	193	2.8	690	163	93
10	1800	18.1	182	2.9	720	159	102

**5. Fuel: Biodiesel + Styrofoam 10 g/L + Acetone 10% (B 100 W/EPS (10 g/L))**

Kinematic viscosity: 5.255 cSt			Calorific Value: 39.324 MJ/kg			Density: 871.47 kg/m <sup>3</sup>	
Atmospheric Temp: 4°C			Fuel consumed: 910 ml/30 mins			Speed: 700 rpm	
Sl no.	Time	O <sub>2</sub>	CO	CO <sub>2</sub>	HC	NO <sub>x</sub>	T
Units	(s)	(%)	(ppm)	(%)	(ppm)	(ppm)	(°C)
1	60	17.5	188	2	150	241	22.5
2	120	17.6	208	2.1	180	234	26.7
3	240	17.8	223	2.1	180	222	34.9
4	360	17.9	231	2.2	240	212	49.4
5	480	18.1	252	2.2	300	209	54.2
6	600	18.3	315	2.3	330	205	57.7
7	900	18.4	334	2.3	390	198	59.3
8	1200	18.6	351	2.4	450	202	61
9	1500	18.6	355	2.7	480	196	63
10	1800	18.6	368	2.7	510	192	74
Atmospheric Temp: 6°C			Fuel consumed: 1500 ml/30 mins			Speed: 1700 rpm	
Sl no.	Time	O <sub>2</sub>	CO	CO <sub>2</sub>	HC	NO <sub>x</sub>	T
Units	(s)	(%)	(ppm)	(%)	(ppm)	(ppm)	(°C)
1	60	17.1	210	2.3	210	189	33
2	120	17.3	229	2.4	270	205	48
3	240	17.6	258	2.4	300	196	53
4	360	17.9	239	2.5	360	191	61
5	480	18	221	2.5	390	192	69
6	600	18.1	214	2.6	480	177	77
7	900	18.1	203	2.5	480	172	84
8	1200	18.1	185	2.4	450	172	88
9	1500	18.1	172	2.5	450	167	93
10	1800	18.1	164	2.5	390	167	108

**6. Biodiesel + Styrofoam 10 g/L + Di ethyl ether 10 % (B 100 W/EPS (10g/L))**

Kinematic viscosity: 5.252 cSt			Calorific Value: 39.9326 MJ/kg			Density: 863.3 kg/m <sup>3</sup>	
Atmospheric Temp: 3 °C			Fuel consumed: 905 ml/ 30mins			Speed: 700 rpm	
Sl no.	Time	O <sub>2</sub>	CO	CO <sub>2</sub>	HC	NO <sub>x</sub>	T
Units	(s)	(%)	(ppm)	(%)	(ppm)	(ppm)	(°C)
1	60	17.4	179	2.3	90	194	26.7
2	120	17.7	195	2.3	120	188	34.9
3	240	17.9	202	2.4	150	181	49.4
4	360	18	216	2.5	150	170	54.2
5	480	18.1	234	2.6	180	167	57.7
6	600	18.2	253	2.6	180	163	58.5
7	900	18.3	282	2.7	210	161	59.3
8	1200	18.3	305	2.9	210	158	61.8
9	1500	18.3	313	3	270	155	64.6
10	1800	18.3	323	3.1	330	151	66
Atmospheric Temp: 3 °C			Fuel consumed: 1500 ml/ 30mins			Speed: 1700 rpm	
Sl no.	Time	O <sub>2</sub>	CO	CO <sub>2</sub>	HC	NO <sub>x</sub>	T
Units	(s)	(%)	(ppm)	(%)	(ppm)	(ppm)	(°C)
1	60	17.4	194	2.3	60	189	33
2	120	17.7	217	2.4	60	194	48
3	240	17.9	241	2.4	60	183	53
4	360	18.1	236	2.5	120	179	61
5	480	18.2	225	2.7	150	179	69
6	600	18.2	211	2.8	180	174	77
7	900	18.3	191	2.8	210	164	84
8	1200	18.3	182	3	210	162	88
9	1500	18.3	164	3	240	158	93
10	1800	18.3	149	3.1	270	157	108

**7. Fuel: Biodiesel + Styrofoam 10 g/L + Tetrahydrofuran 10% (B 100 W/ EPS (10g/L) +THF 10%))**

Kinematic viscosity:5.281 cSt			Calorific Value: 39.037 MJ/kg			Density:881.3 kg/m <sup>3</sup>	
Atmospheric Temp 8 °C			Fuel consumed: 907 ml/30 mins			Speed: 700 rpm	
Sl no.	Time	O <sub>2</sub>	CO	CO <sub>2</sub>	HC	NO <sub>x</sub>	T
Units	(s)	(%)	(ppm)	(%)	(ppm)	(ppm)	(°C)
1	60	17.9	184	2	120	209	31.2
2	120	18	206	2.1	150	198	44.2
3	240	18.2	220	2.1	150	191	58.3
4	360	18.4	228	2.1	210	181	61.6
5	480	18.4	233	2.2	270	173	61.3
6	600	18.5	244	2.3	270	168	60.2
7	900	18.5	308	2.3	300	171	61.2
8	1200	18.5	331	2.3	270	170	59.5
9	1500	18.5	343	2.4	390	167	60.6
10	1800	18.6	358	2.6	420	163	63
Atmospheric Temp 8 °C			Fuel consumed: 1490 ml/30 mins			Speed: 1700 rpm	
Sl no.	Time	O <sub>2</sub>	CO	CO <sub>2</sub>	HC	NO <sub>x</sub>	T
Units	(s)	(%)	(ppm)	(%)	(ppm)	(ppm)	(°C)
1	60	17.4	207	2.3	180	186	51
2	120	17.3	214	2.3	240	190	59
3	240	17.7	226	2.4	270	180	63
4	360	17.9	237	2.4	360	178	71
5	480	17.9	243	2.5	360	177	79
6	600	18.1	231	2.6	420	177	86
7	900	18.1	204	2.5	390	171	95
8	1200	18.2	186	2.4	390	170	101
9	1500	18.2	170	2.4	390	165	109
10	1800	18.2	158	2.5	360	162	110.4

**8. Fuel: Biodiesel + Styrofoam 10 g/L + Toluene 10% (B 100 W/ EPS (10 g/L) + Tol 10%) )**

Kinematic viscosity: 5.265 cSt		Calorific Value: 40.321 MJ/kg				Density: 879.7 kg/m <sup>3</sup>	
Atmospheric Temp: 9 °C		Fuel consumed: 903 ml/30 mins				Speed: 700 rpm	
Sl no.	Time	O <sub>2</sub>	CO	CO <sub>2</sub>	HC	NO <sub>x</sub>	T
Units	(s)	(%)	(ppm)	(%)	(ppm)	(ppm)	(°C)
1	60	17.3	186	2.2	120	208	27
2	120	17.4	213	2.3	120	200	31
3	240	17.5	223	2.4	180	193	33
4	360	17.8	231	2.4	180	187	37
5	480	17.9	264	2.5	300	174	41
6	600	18	263	2.7	360	170	47
7	900	18.3	338	2.6	480	176	53.3
8	1200	18.4	344	2.6	420	177	57
9	1500	18.4	356	2.5	360	167	61
10	1800	18.4	365	2.5	390	163	63.8
Atmospheric Temp: 9 °C		Fuel consumed: 1483 ml/30 mins				Speed: 1700 rpm	
Sl no.	Time	O <sub>2</sub>	CO	CO <sub>2</sub>	HC	NO <sub>x</sub>	T
Units	(s)	(%)	(ppm)	(%)	(ppm)	(ppm)	(°C)
1	60	17.2	209	2.1	210	186	53
2	120	17.3	224	2.3	180	199	61
3	240	17.7	253	2.3	270	196	69
4	360	17.8	251	2.4	330	186	72
5	480	17.9	229	2.5	390	180	77
6	600	18.1	216	2.6	450	170	85
7	900	18.1	210	2.5	420	168	96
8	1200	18.2	195	2.6	390	165	99
9	1500	18.3	176	2.6	360	159	102
10	1800	18.1	167	2.5	360	156	108

**9. Fuel: Biodiesel + Styrofoam 10 g/L + Xylene 10% (B 100 W/ EPS (10 g/L) + Xyl 10%)**

Kinematic viscosity: 5.291 cSt		Calorific Value: 40.683 MJ/kg			Density: 879.3 kg/m <sup>3</sup>		
Atmospheric Temp: 11 °C		Fuel consumed: 900 ml/30 mins			Speed: 700 rpm		
Sl no.	Time	O <sub>2</sub>	CO	CO <sub>2</sub>	HC	NO <sub>x</sub>	T
Units	(s)	(%)	(ppm)	(%)	(ppm)	(ppm)	(°C)
1	60	17.2	184	2.1	90	206	34
2	120	17.3	204	2.3	150	196	39
3	240	17.6	220	2.3	150	188	18
4	360	17.8	228	2.4	180	182	51
5	480	17.9	261	2.5	270	169	53
6	600	18.1	292	2.6	300	167	55
7	900	18.1	336	2.5	330	170	61
8	1200	18.1	341	2.4	420	171	68
9	1500	18.1	352	2.5	390	165	72
10	1800	18.1	361	2.5	420	160	79
Atmospheric Temp: 11 °C		Fuel consumed: 1480 ml/30 mins			Speed: 1700 rpm		
Sl no.	Time	O <sub>2</sub>	CO	CO <sub>2</sub>	HC	NO <sub>x</sub>	T
Units	(s)	(%)	(ppm)	(%)	(ppm)	(ppm)	(°C)
1	60	17.2	205	2.2	210	184	55
2	120	17.3	220	2.3	210	196	62
3	240	17.6	250	2.3	300	190	70
4	360	17.8	241	2.4	330	184	83
5	480	17.9	225	2.5	360	175	91
6	600	18.1	212	2.6	420	168	93
7	900	18.1	206	2.5	420	165	97
8	1200	18.1	189	2.4	390	161	99
9	1500	18.1	171	2.5	360	156	102
10	1800	18.1	162	2.5	330	153	108